A SYNTHESIS OF HYDROCARBON MATURATION DATA FOR THE EAST NEWFOUNDLAND BASIN

A report

Submitted to

Atlantic Geoscience Centre
Geological Survey of Canada
Dartmouth, N.S.

by

Warren B. Ervine, Ph.D., P.Eng.
GeoTech Surveys Limited
Lower Sackville, N.S.

August, 1984

CONTENTS

ILLUSTRATIONS

TABLES

I. INTRODUCTION

Petroleum geologists generally agree that oil and gas are generated from sedimentary organic matter by a gradual increase in temperature over a long period of time. The factors of time and temperature act in the same direction to develop or mature any buried organic material so that a fluid fraction is produced. Other factors, such as pressure, type and quantity of organic matter, and tectonic history also play a role in the overall maturation process, but their relative value has only recently been reported (e.g. Powell and Snowdon, 1983).

Measuring the degree of maturity has been a prime objective in petroleum exploration for many years. A number of methods have been tried with quite a wide range of success. Thermal maturity of organic material has been measured, for example, by vitrinite reflectance (R_o), thermal alteration index (TAI), carbon preference index (CPI), kerogen hydrogen/carbon (H/C) ratio, bitumen/organic carbon ratio (Bit/C_{org}), per cent expandable clays, and gravity (API). All these methods involve considerable subjectivity in deriving values for maturation.

Only recently was it possible to provide an almost completely objective evaluation of maturity. Pioneer work by Lopatin (1969, 1971) and subsequent efforts by Waples (1980), and Issler (1982, 1984) have developed a mathematical model which uses depth and temperature measurements from well logs and age determinations from biostratigraphy to calculate a theoretical value for the maturity of any strata intersected by drilling. This value, called the time-temperature index (TTI), is a calculated value of maturity and must be calibrated against other data for each basin in which it is used.

This report attempts, first of all, to calculate TTI values using a schematic model modified after the one proposed by Lopatin (1971) and secondly, to calibrate these values by comparing them with vitrinite reflectance data, thermal alteration indices and with other geochemical information. Thirdly, this information on maturity is correlated with hydrocarbon occurrences, type and quantity of organic material and with geology to create a hydrocarbon generation model for the East Newfoundland Basin. All information for the model has been gathered from the 23 wells listed in Table 1 shown with their location coordinates and total depths. Their geographic locations and those of other drilled wells not used in this study are shown on a general map of the area (Figure 1).

Data for this report has been drawn from many sources, mostly at the Atlantic Geoscience Centre, Dartmouth, N.S. Particularly useful paleontological and geochemical reports have been written by Piero Ascoli, M. Sedley Barss, Jonathan P. Bujak, Edward H. Davies, P. Doeven, F. M. Gradstein, Peter A. Hacquebard, and Graham L. Williams. Some general information has been drawn from well history reports written by staff workers at Mobil Oil, Chevron Oil, and Imperial Oil. The well logs run by Schlumberger and by Dresser Atlas also provided considerable data. All published information is referenced (See References).

The writer would like to thank K. Donald McAlpine, Atlantic Geoscience Centre, for his assistance in providing relevant data and information on the geology and petroleum occurrences for this area and for his constructive criticism of the manuscript. Carolyn J. Ervine, Research Associate, GeoTech Surveys Limited, is responsible for the calculations and graphic displays in this report.

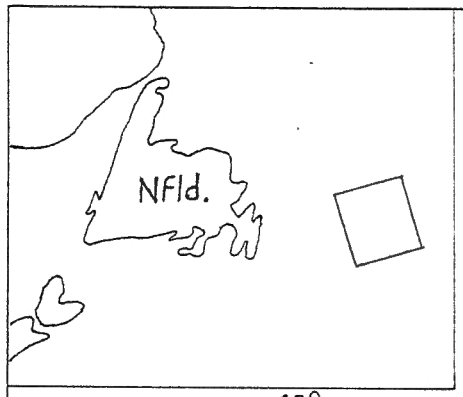

48°

49°

47°

46°

Bonanza M-71

Dominion O-23

North Dana I-43

South Tempest G-88

Flying Foam I-13

West L-23

Adolphus K-41 2K-41

D-50

Trave E-87

Nautilus C-92

Whiterose N-22

K-18

B-27

B-08

Hibernia

I-46

G-55

P-15

O-35

J-34

K-14

South Mara C-13

Archer K-18

Rankin M-36

Ben Nevis I-45

Hebron I-13

Terra Nova K-08

Voyager J-18

N-46

Egret K-36

Port Au Port J-97

Murre G-67

Cormorant N 83

Bonnition H-32

Spoonbill C-30

Skua E-41

FIGURE 1

Well Location in the
East Newfoundland Basin
Scale 1:1,000,000

● Wells used in this study

o Other wells

TABLE 1

Wells in the East Newfoundland Basin
Used in this Study

Well Name	Latitude	Longitude	Total Depth*
Adolphus D-50	46° 59' 03.06" N	48° 22' 28.86" W	3656 m
Adolphus 2K-41	47° 00' 40.56" N	48° 22' 06.47" W	3626 m
Ben Nevis I-45	46° 34' 39.74" N	48° 21' 09.84" W	4905 m
Bonnition H-32	45° 51' 26.79" N	48° 19' 31.76" W	3017 m
Cormorant N-83	46° 02' 45.43" N	48° 58' 02.07" W	3131 m
Dominion O-23	47° 22' 49.14" N	48° 18' 27.90" W	3968 m
Egret K-36	46° 25' 37.88" N	48° 50' 22.38" W	3323 m
Egret N-46	46° 25' 56.14" N	48° 51' 42.35" W	2713 m
Flying Foam I-13	47° 02' 41.96" N	48° 46' 30.98" W	3652 m
Hebron I-13	46° 32' 33.95" N	48° 31' 45.47" W	4696 m
Hibernia B-08	46° 47' 06.36" N	48° 45' 29.87" W	4408 m
Hibernia G-55	46° 44' 17.07" N	48° 53' 10.75" W	3430 m
Hibernia I-46	46° 45' 39.00" N	48° 51' 18.64" W	3403 m
Hibernia J-34	46° 43' 33.84" N	48° 50' 13.00" W	3683 m
Hibernia K-18	46° 47' 34.69" N	48° 47' 17.05" W	5009 m
Hibernia O-35	46° 44' 54.92" N	48° 49' 53.74" W	4764 m
Hibernia P-15	46° 44' 58.98" N	48° 46' 51.18" W	4395 m
Murre G-67	46° 06' 20.40" N	49° 09' 38.20" W	3307 m
Nautilus C-92	46° 51' 03.55" N	48° 44' 20.64" W	5090 m
Skua E-41	45° 20' 23.23" N	48° 52' 26.26" W	3209 m
South Tempest G-88	47° 07' 19.92" N	47° 57' 30.48" W	4647 m
Spoonbill C-30	45° 49' 06.47" N	49° 04' 06.18" W	2727 m
West Flying Foam L-23	47° 02' 43.70" N	48° 49' 17.20" W	4527 m

*Below Mean Sea Level

II. SUBSURFACE TEMPERATURES

A. Geothermal Gradients

In order to obtain some understanding of the subsurface thermal regime now present in the East Newfoundland Basin, a graphic representation of the geothermal gradient has been drawn for each well for which there was adequate depth and temperature information recorded on their respective well log headings. This information includes: date of log, elevation of rotary table, water depth, depth (to temperature measurement), temperature, time drilling stopped, time circulation stopped, time of temperature measurement, and time since circulation. (See the Appendix for details on each of these parameters.) Unfortunately, much of the data is missing, incorrect, confusing and even contradictory. It appears that in the past little importance was given to recording accurate times and temperatures on well log headings.

The raw depth and temperature information, as it appears on the headings, had to be adjusted or "corrected" to make it useful for drawing the gradients. The depth data was corrected to a sea-floor datum and, where necessary, converted to the metric system. The temperature data was corrected by two methods described in the Appendix and converted, where necessary, to degrees Celsius. These corrected data were then used to construct temperature-depth graphs for the 23 wells used in this study. The graphic results are in the Appendix.

Three kinds of bottomhole temperatures were used to construct the graphs. Corrected temperatures derived by the CT projection (i.e. where circulation times were recorded) are indicated by a "."; those derived by the TSC projection (i.e. where no circulation times were recorded) are indicated by

an "x". Where only one temperature was recorded for a given depth, it was impossible to make any sort of projection or correction. This lone temperature is therefore only a minimum value and so was plotted on the graphs by an arrow pointing to the right (i.e. toward higher temperatures). In most cases a straight line was simply drawn between points to represent the most obvious trend in values. Most inflection points therefore coincide with data points, although other interpretations are possible. In drawing the straight lines, the points derived by the projections were given equal value, but the arrows were not considered.

The geothermal gradients for the wells in the East Newfoundland Basin appear to be of two types: straight and doglegged. Eight of the wells (Bonnition, Dominion, Egret K-36, Egret N-46, Murre, West Flying Foam, Skua and South Tempest) have reasonably straight lines passing through $0^{\circ}C$ at the sea floor and extending to a depth of 4000 to 5000 metres. These wells have approximately the same gradient ($3.0 \pm 0.2^{\circ}C/100m$) and are generally at some considerable distance from the Hibernia field.

On the other hand, as many as eleven wells (including the 7 Hibernias, Flying Foam, Ben Nevis, Hebron and probably Nautilus) have gradients reasonably similar to each other and to the "straight" variety to a depth of about 2600 metres. However, from that point these geothermal gradients suddenly steepen (or decrease in value) for 600 to 900 m, below which they continue the initial gradient to create a "dogleg" shape. These gradients are reasonably similar to each other in shape, depth and temperature characteristics. All are relatively close to the Hibernia field.

There may be a possible explanation for the dogleg shape. Heat flow is the product of the geothermal gradient and the thermal conductivity of the rocks through which the heat passes. So, if the heat flow is assumed to be

uniform, then changes in the gradient must be reflected in corresponding changes in the thermal conductivity of the rocks, i.e. higher gradients are produced by rocks of lower conductivity. Therefore, the low gradient below 2600 m resulting in the dogleg effect might be caused by a thick section of strata (say, up to 1000 m) of high conductivity in or near the Hibernia field.

However, the stratigraphy of this area does not support the possibility that there could be strata of these characteristics at a common depth of 2600 m. It is more likely that pore fluids under pressures greater than hydrostatic are responsible for the unusual shape. Because pore fluids have lower thermal conductivity which therefore create higher gradients, a rock tending towards increased porosity through restricted compaction should show higher gradients. It is interesting to note that in most of the wells with the dogleg gradient, the top of the overpressure zone occurs at close to the same depth as the Verrill Canyon shales and both features fall near the base of the crooked part of the dogleg gradient. Perhaps the Verrill Canyon shales act as an effective barrier to fluids contained in the Jurassic rocks below. This will then produce overpressures which will tend to increase the geothermal gradient beneath the shales and, if leakage has occurred, decrease the gradient above the shales.

A few wells closely associated with piercement salt diapirs, salt pillows, or salt beds (i.e. Cormorant, Adolphus D-50, Adolphus 2K-41, Spoonbill, and perhaps Hibernia I-46) have gradients which, at different depths, tend to increase for several hundred metres (i.e. the slope of the curve flattens) and then abruptly to decrease to nearly vertical (i.e. the gradient diminishes to nearly zero). The vertical part is undoubtedly due to the high thermal conductivity of salt. The gentler slope above could be a combination of the higher thermal gradients (i.e. low conductivity) associated with caprocks and the effect of a lag in thermal equilibrium for rocks overlying a rapidly rising diapir.

FIGURE 2

Average Geothermal Gradient
for the East Newfoundland Basin

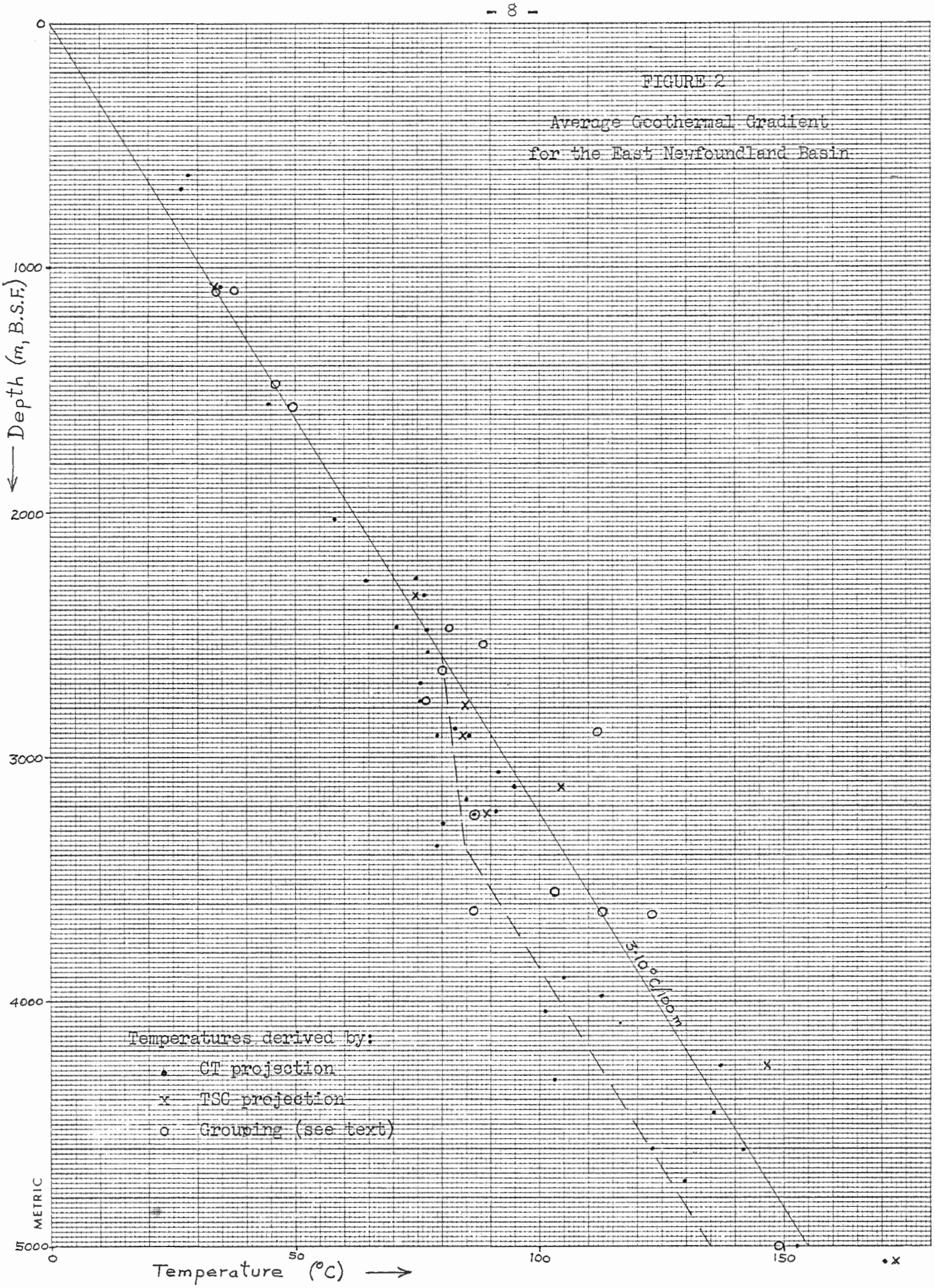

To show how consistent all the gradients are, a composite graph has been drawn using all available data (Figure 2). The gradients for closely spaced wells were averaged first as a group so that the resulting composite gradient could be based on a more even distribution of information. Specifically, average gradients were made for the Hibernias (B-08, G-55, I-46, J-34, K-18, O-35, P-15), Adolphuses (D-50, 2K-41), Egrets (K-36, N-46) and Flying Foams (I-13, L-23). Average values from each of these groups were then used for the composite gradient to represent their respective locations. A "best-fit" straight line was easily drawn through the data points, resulting in a composite geothermal gradient of 3.10°C/100m. It is interesting to note that the line passes through 0°C at the sea floor, a temperature probably not much different from actual sea-floor values (Hyndman et al, 1979; John A. Wade, pers. comm.).

B. Heat Distribution Maps

From the geothermal gradients a series of heat distribution maps has been drawn to show different subsurface temperatures on a regional basis. Temperatures have been selected for depths of 1000, 2000, 3000, 4000, and 5000 metres below sea floor (Table 2, Figures 3 to 7). An attempt has been made to show mutual relationships by adding contouring, although much of this was difficult, especially where the temperature values of two closely spaced wells differ more than those of many widely spaced wells.

The maps reveal some interesting patterns.

1. There are at least 3 areas showing above-average temperatures:
   (a) A zone around the Adolphuses has a temperature contrast with the surrounding areas which increases with depth. The high temperatures in this zone probably reflect the increasing influence of salt diapirs with depth.
   (b) A zone around Cormorant has a temperature contrast which decreases

TABLE 2

Temperatures for Specified Depths (B.S.F.)*

Well Name	Temperatures (°C) 1000 m	2000 m	3000 m	4000 m	5000 m
Adolphus D-50	36.5	73.0	113.5	(136.5)	(167.5)
Adolphus 2K-41	31.0	68.0	112.0	(113.5)	(115.0)
Ben Nevis I-45	28.5	60.0	79.0	107.5	137.5
Bonnition H-32	29.5	58.5	(87.5)	(119.0)	(150.0)
Cormorant N-83	36.5	66.5	(84.5)	—	—
Dominion O-23	31.5	62.0	92.5	(123.5)	(155.0)
Egret K-36	28.5	56.0	80.5	(110.5)	(141.5)
Egret N-46	31.5	61.5	(91.0)	(121.5)	(152.5)
Flying Foam I-13	34.5	67.0	92.5	(117.5)	(149.5)
Hebron I-13	29.0	57.5	78.0	99.5	(135.0)
Hibernia B-08	30.0	57.0	80.0	112.0	(145.0)
Hibernia G-55	32.0	60.5	74.0	(96.5)	(127.0)
Hibernia I-46	32.5	58.5	79.0	(107.0)	(138.0)
Hibernia J-34	33.5	55.0	70.5	(92.5)	(123.0)
Hibernia K-18	28.5	56.5	81.5	103.5	(146.5)
Hibernia O-35	27.0	56.5	82.5	(95.5)	(126.0)
Hibernia P-15	26.0	52.0	76.0	97.5	(137.5)
Murre G-67	36.5	58.0	83.5	(113.5)	(144.5)
Nautilus C-92	30.0	60.0	89.5	113.5	152.5
Skua E-41	32.5	64.5	96.0	(127.5)	(158.5)
South Tempest G-88	28.5	57.0	81.0	(111.0)	(142.0)
Spoonbill C-30	29.0	57.5	(87.0)	(117.5)	(148.5)
West Flying Foam L-23	29.5	58.5	87.5	(117.5)	(149.0)

*Below Sea Floor
( ) Projected value

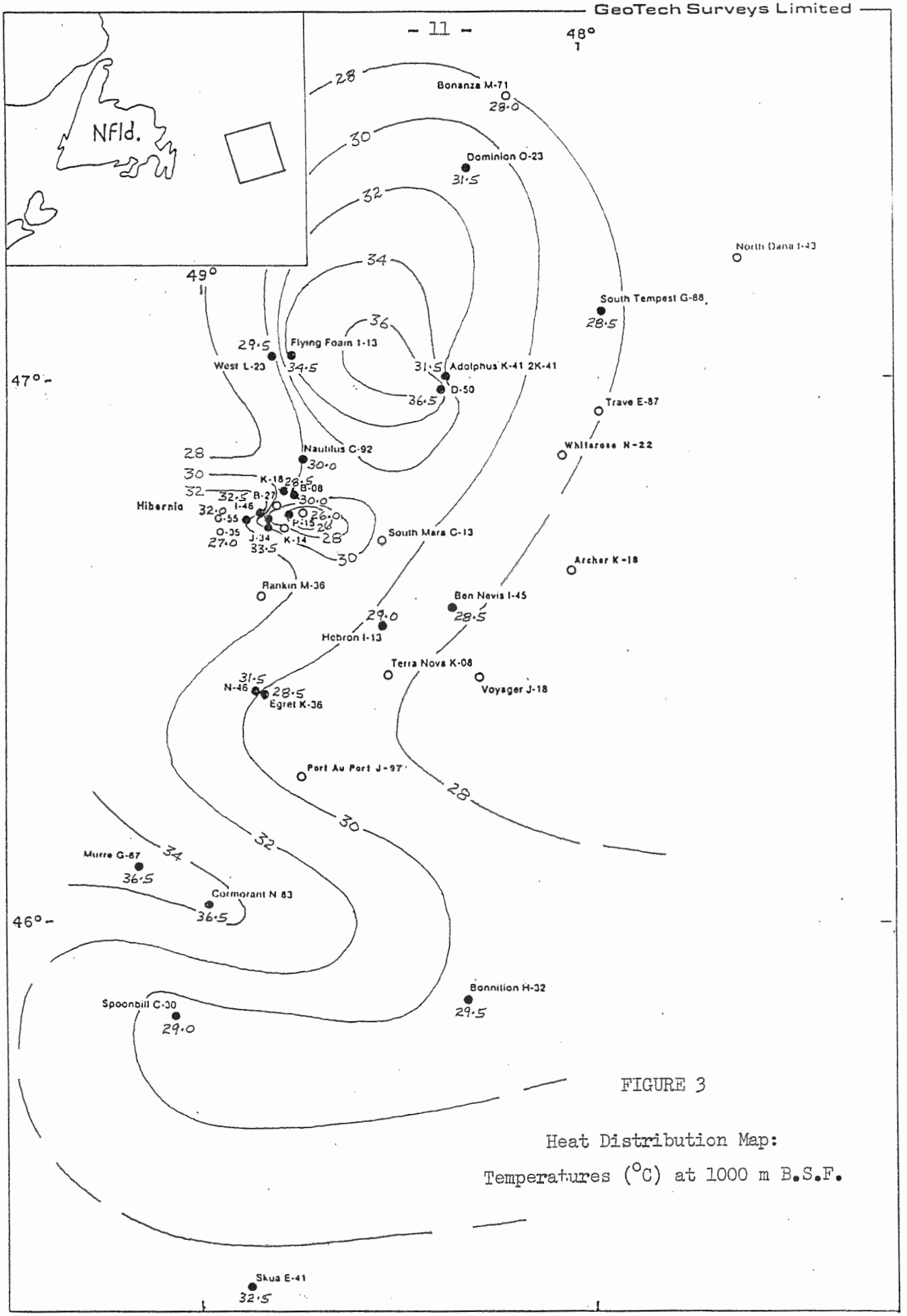

FIGURE 3

Heat Distribution Map:

Temperatures (°C) at 1000 m B.S.F.

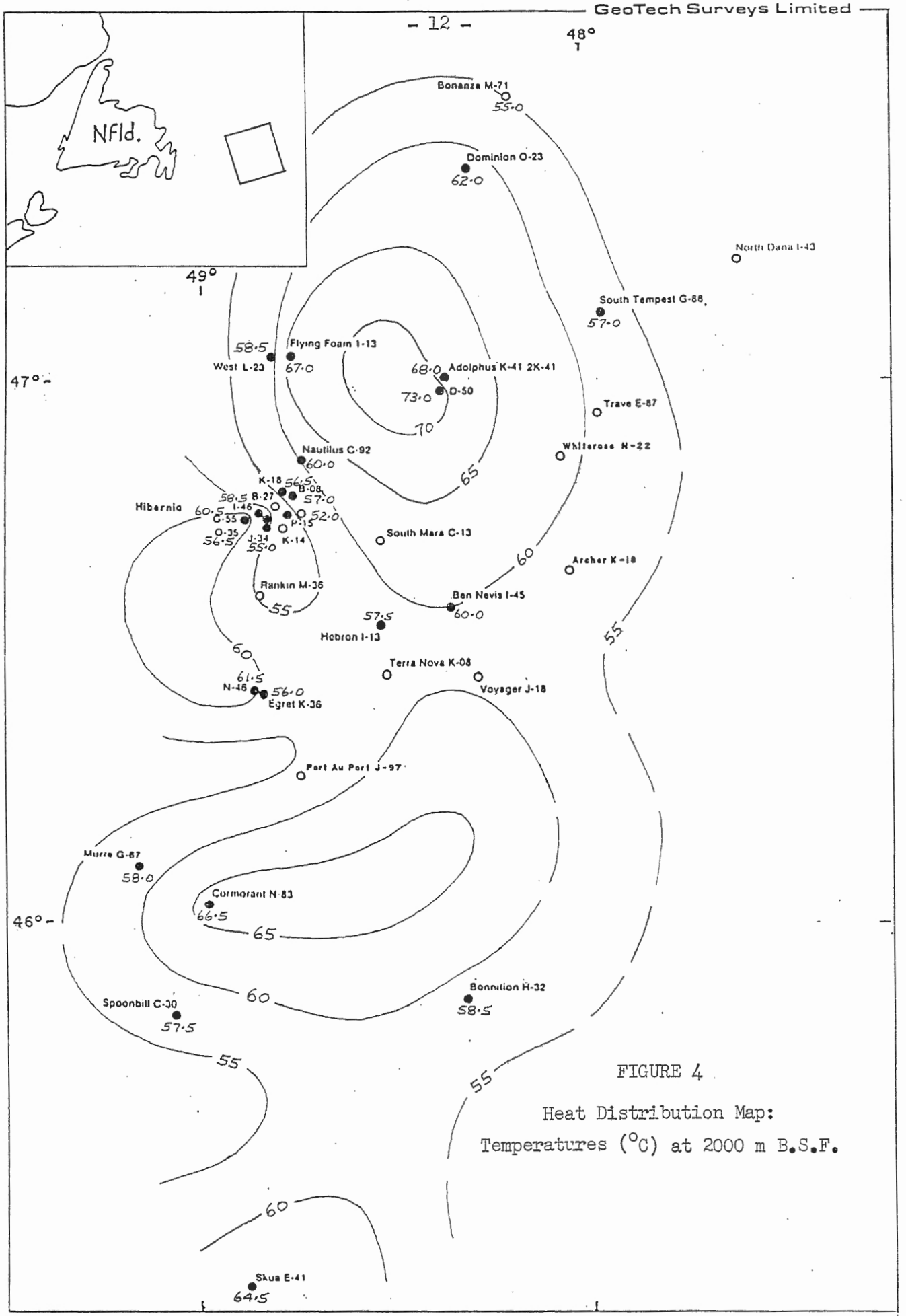

FIGURE 4

Heat Distribution Map:

Temperatures (^{o}C) at 2000 m B.S.F.

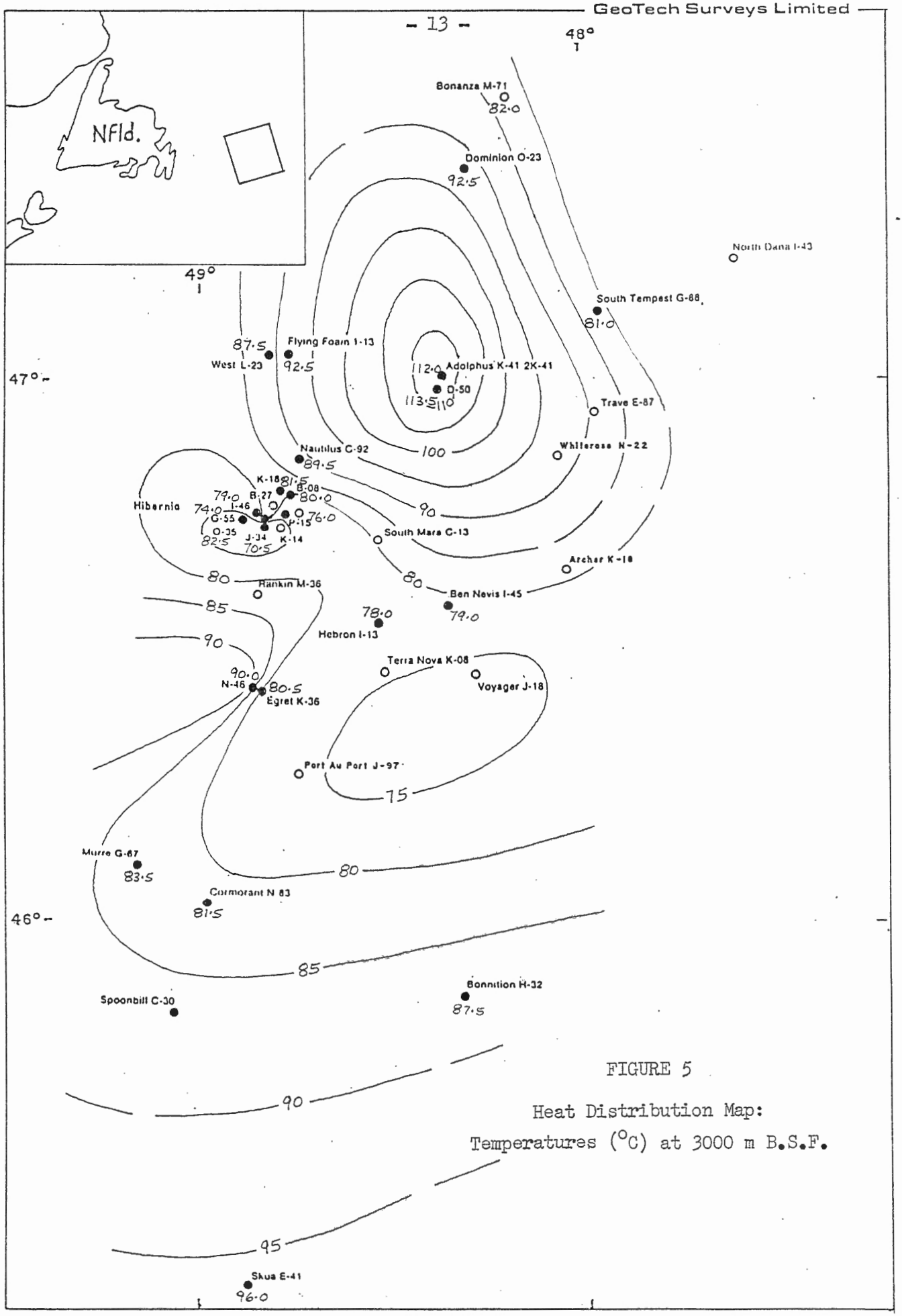

FIGURE 5

Heat Distribution Map:

Temperatures (°C) at 3000 m B.S.F.

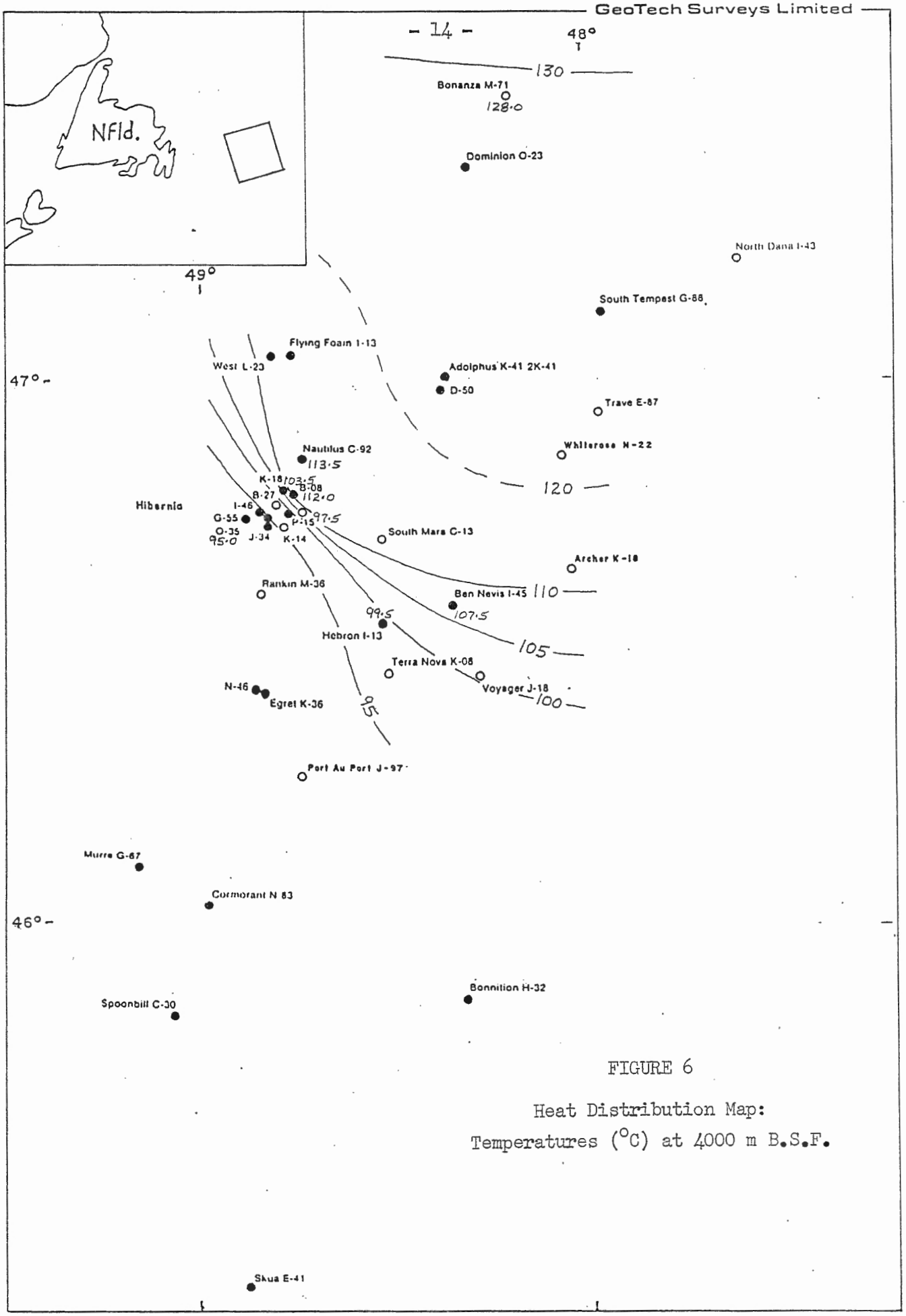

FIGURE 6

Heat Distribution Map:
Temperatures (°C) at 4000 m B.S.F.

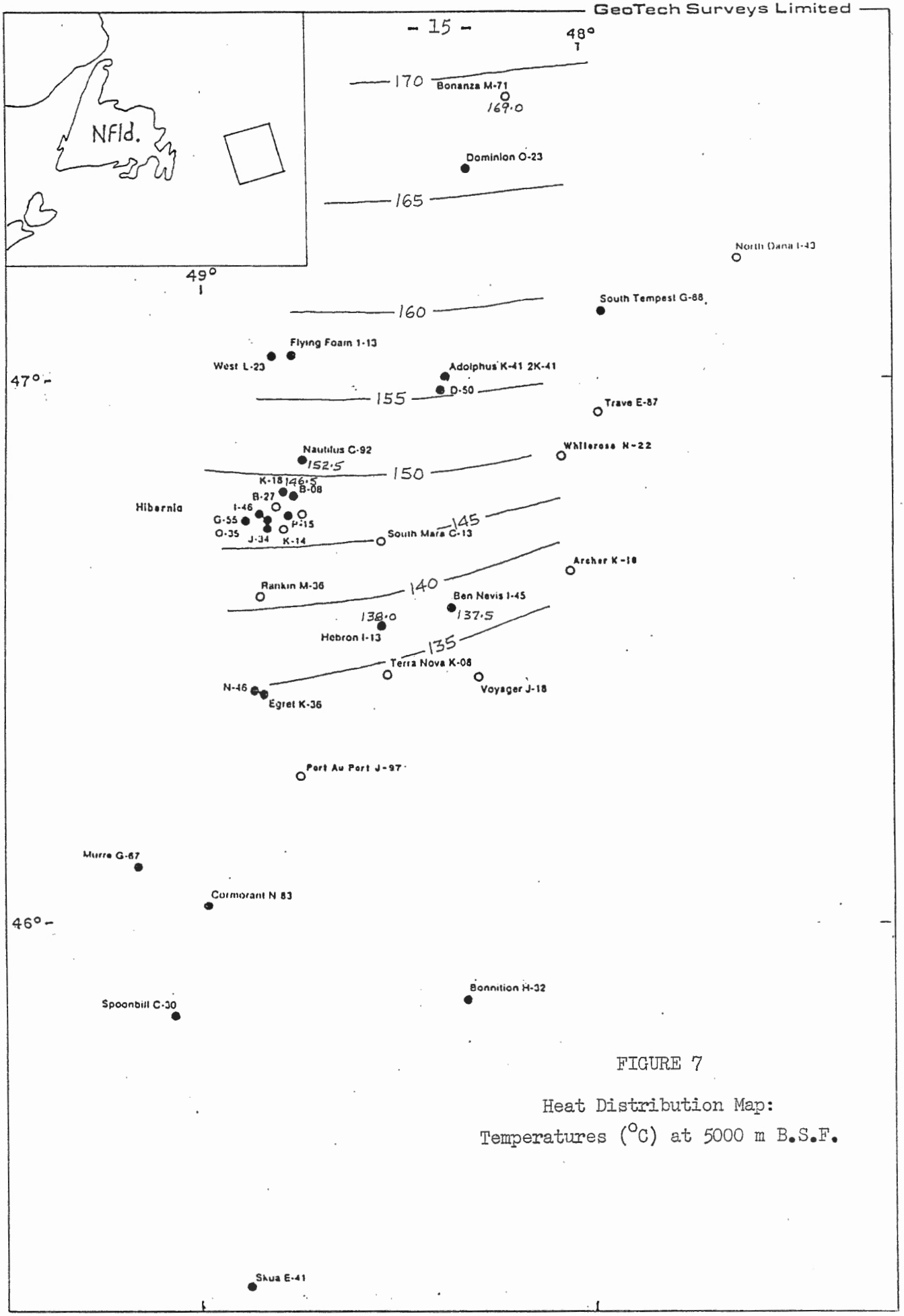

FIGURE 7

Heat Distribution Map:
Temperatures (°C) at 5000 m B.S.F.

with depth. This may be caused by thick salt beds lying not far above the Paleozoic basement. The high conductivity of the salt (i.e. low gradient) would give rise to higher heat flow (and higher gradient) in the overlying rocks. This change in gradient shows as an upward curve in the depth-temperature plot (see Appendix) and as the diminishing temperature contrast mentioned above.

(c) A zone at Egret N-46 shows only slight changes with depth. This is probably due to its proximity to a salt ridge (Figure 8).

2. The eastern part of the Hibernia group shows below-average temperatures but this effect is more subtle at depth.

3. The values at 4000 and 5000 metres indicate a considerable northward increase in temperatures which at 5000 m amounts to 35°C in about 120 km.

C. Relationship to Tectonic Framework

The geology and tectonic framework of the East Newfoundland Basin has been described most recently by Benteau et al, 1982; and Arthur et al, 1982; and summarized by Procter et al, 1984. The area lies about 300 km east-southeast of St. John's, Newfoundland, on the northeastern flank of the Avalon Uplift. Several northeasterly trending, graben-generated subbasins trend northeastward across the Uplift. The largest of these, the Jeanne D'Arc Subbasin, is bounded on the west by the Bonavista Platform, the eastern margin of which forms the hinge line for the Basin as a whole, and the Outer Ridge Complex about which little is known (Figure 8). Triassic, Jurassic and thick Lower Cretaceous clastic sediments filling these subbasins lie unconformably beneath thin Upper Cretaceous clastics and limestone and eastward thickening Tertiary shales. Salt beds, some of which have formed diapirs, occur not far above the Paleozoic basement. Post-Paleozoic sedimentary thickness in the Jeanne D'Arc Subbasin ranges from a few 1000 m at its margins to more than 12,000 m near the middle (Figure 8).

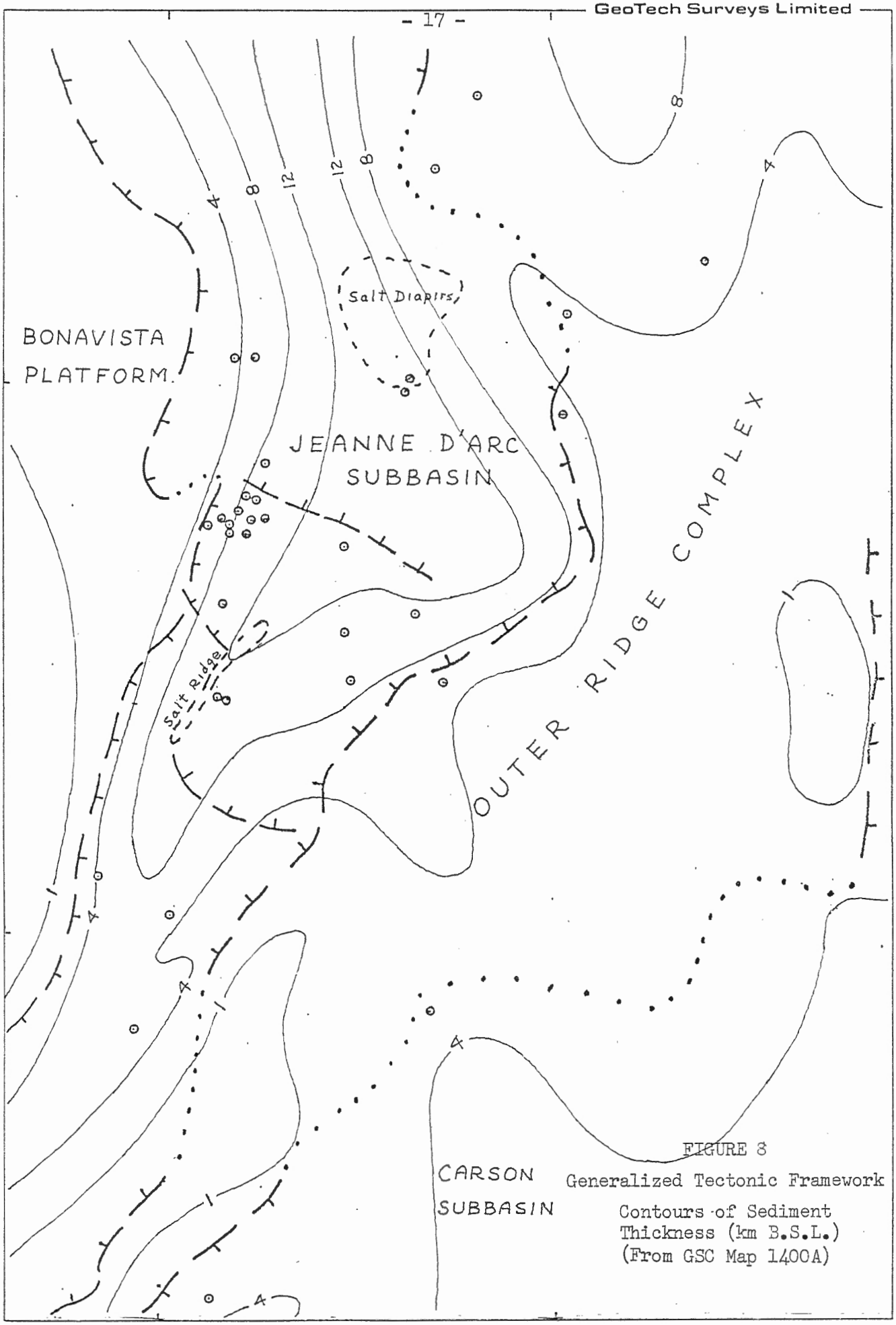

FIGURE 8

Generalized Tectonic Framework

Contours of Sediment Thickness (km B.S.L.)
(From GSC Map 1400A)

In order to reveal any relationship between the thermal regime and the tectonic framework, a simple approximation of the geothermal gradient at each well was determined by the slope of a straight line joining the deepest temperature with the sea-floor temperature. The single value for each well was plotted on the tectonic map and contours drawn at intervals of 0.25°C/100m (Figure 9).

There appears to be considerable correlation between the thermal pattern of contoured geothermal data and the tectonic framework. The pattern is similar in shape, size and position to the basement physiography of the Jeanne D'Arc Subbasin. The highest gradients occur in the middle and narrow southwestern "arm" of the Subbasin where the sediments are thickest, and decrease both easterly and westerly towards a shallower basement. Both patterns appear to continue northward but in a somewhat narrower configuration. The greatest lateral change in temperature gradients occurs along the western side corresponding to the relatively steep slopes along the basement hinge zone; a less rapid change in temperature reflects the more gentle slopes of the eastern side of the Subbasin.

A similar relationship has been found on the Scotian Shelf where low gradients occur over basement highs and near-shore areas, and high gradients occur seaward over thickening sedimentary sequences. Also, in the Vienna Basin (Boldizar, 1968) the highest gradients are found near the middle where the sediment is thickest, whereas the lowest gradients characterize the margins. Gradients in the North Sea (Evans et al, 1974) range from 4.0°C/100m in the middle of the basin to 2.6°C/100m or less near the British, Norwegian and Netherland coasts.

The reason for this basinward increase in gradients is not readily obvious. Theoretically, the generally higher thermal conductivities of basement rocks tend to give rise to relatively high gradients in the sedimentary cover

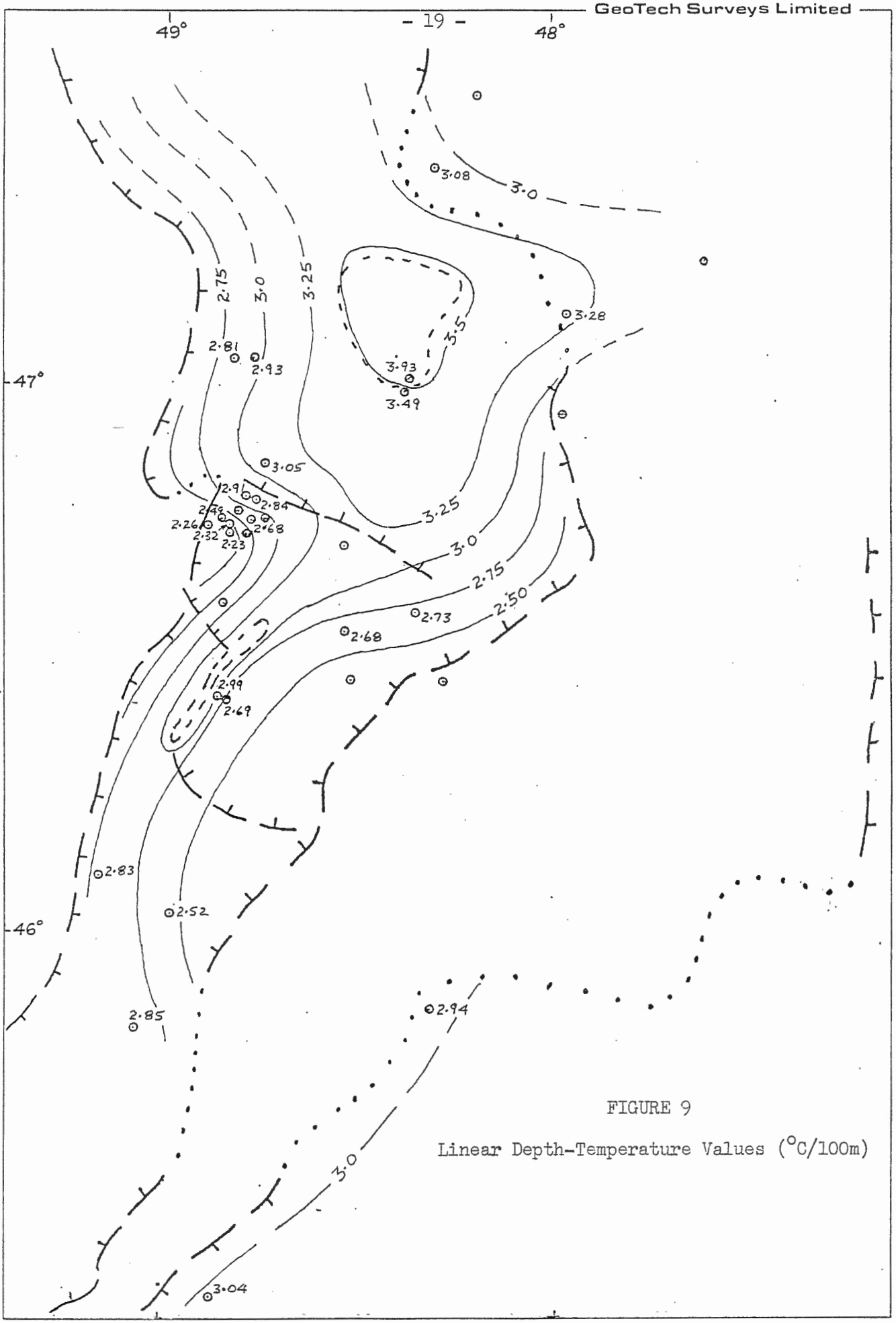

FIGURE 9

Linear Depth-Temperature Values (°C/100m)

overlying basement highs. Conversely, low gradients should be characteristic of thick sedimentary sequences, especially those of relatively low thermal conductivity. However, in the above examples just the reverse is the case.

Three possibilities can be suggested for the observed increase in geothermal gradients. The higher gradients could reflect the lower thermal conductivity of the Tertiary shales which thicken seaward. However, while it is popular to call upon low thermal conductivities to explain high geothermal gradients, other factors may be of greater influence.

The higher gradients might be caused by greater heat flow. Since it is now generally accepted that most of the heat leaving the earth is radiogenic in origin (i.e. the heat generated from the spontaneous decay of uranium, thorium and radiometric potassium in the earth's upper crust), it is possible that radioactive materials buried with the seaward thickening, post-Paleozoic sediments could enhance the heat production and cause greater heat flow. Such materials could include potassium-bearing minerals, including clays (e.g. illites), and organic matter which readily concentrates uranium and thorium.

Evidence that radiogenic heat may increase heat flow in the East Newfoundland Basin is indirect at best. High heat flows in Nova Scotia are associated with the Devonian granites and extensive (early Paleozoic) Meguma slates and quartzites because these rocks have high radioactive heat production (Hyndman et al, 1979). The Meguma sediments inherited their high heat production from the Northwestern African craton from which they were eroded (Schenk, 1971). Since these radioactive Paleozoic rocks are the source for the post-Paleozoic sediments comprising the Scotian Shelf, they may also have imparted their radioactivity as well.

Since the Devonian granites and Proterozoic metasedimentary rocks of mainland Newfoundland, especially eastern Newfoundland, are probably the source for the clastic material which fills the East Newfoundland Basin, it is possible

by analogy to think that these source rocks, if they could be shown to be equally radioactive, are also the origin for any radioactivity that the offshore sediments might contain.

Local increases in heat flow could be caused by piercement salt diapirs. Because salt has a relatively high thermal conductivity, diapirs can act as conduits, conducting heat from the hotter basement to the stratigraphically higher levels of the sedimentary section. Adolphus D-50 and 2K-41 are both drilled near a salt diapir so that the particularly high values in the middle of the Basin may simply be due to their proximity to salt diapirs.

In summary, the basinward increase in geothermal gradients in the East Newfoundland Basin is probably caused by a combination of three factors. Seaward-thickening Tertiary shales have low conductivity and may contain organic matter with a significant uranium and thorium content. Mesozoic clastic sediments form thick sequences and may contain significant amounts of potassium-bearing minerals. Together, these rocks could produce considerable radiogenic heat which could escape only very slowly through the uppermost strata. Salt diapirs, such as at Adolphus D-50 and 2K-41, may locally increase the thermal regime. Only a more detailed study can determine the relative importance of each factor.

III. TIME-TEMPERATURE INDEX

A. Theory of Lopatin's Model

It has been widely established in recent years that both time and temperature are important factors in the process of oil generation and in the subsequent cracking of oil to methane (Waples, 1980). Lopatin (1971) has developed a method which considers the effects of time and temperature for calculating the thermal maturity of organic material in buried sediments. His mathematical model uses a "time-temperature index" (TTI) as a theoretical measure of maturity of the buried organic material.

The model is based on the generally accepted principle that chemical reaction rates involving organic material will double for every 10°C increase in temperature or with a doubling of exposure time (Dow, 1977; Hood et al, 1975; Lopatin, 1971). In other words, reaction rates vary linearly with time, but exponentially with temperature. It also means that the two factors are interchangeable: a high temperature acting for a short time can have the same maturation effect as a low temperature acting over a long time. The model, then, consists of determining the total of the maturation effects due to the time and temperature factors.

A maturation value, or TTI, can be calculated if it can be determined how long a particular sediment has occupied a place in each thermal regime to which it has been subjected during its burial. To do this, Lopatin (1971) divided the temperature scale into even 10°C intervals and assigned to each a factor, r^n, which reflects the exponential dependence of maturity on temperature. The exponent of this factor was arbitrarily given the value of zero for the temperature interval 100 - 110°C (i.e. r^0) and the exponent was increased by one, or decreased by one for every 10° interval of higher temperature, or of lower

temperature, respectively, in which the sediment was involved (Table 3). Subsequent work by Waples (1980) showed that r, itself, probably has a value of 2, which seems realistic in light of the doubling effect of temperature.

Because there is a linear relationship between maturity and time, Lopatin simply measured the time factor in millions of years. This means that the maturity added in any temperature interval, i, is expressed by the relationship:

$$\Delta \text{ Maturity} = (\Delta T_i)(r^{ni})$$

where ΔT_i is the length of time spent by the sediment in the temperature interval, i; and r^{ni} is the temperature factor for the i^{th} interval. Because maturation effects on the organic material are additive, the total maturity (or TTI) of a given sediment is given by the sum of the maturities acquired in each interval. Thus:

$$TTI = \sum_{nmin}^{nmax} (\Delta T_n)(r^n)$$

where nmax and nmin are the n-values of the highest and lowest temperature intervals encountered (Waples, 1980). Therefore, the calculated values for TTI are derived from a mathematical model which simulates the natural processes acting on buried organic material as it matures.

B. Constructing the TTI Model

Using geothermal gradients to construct temperature grids and dated statigraphy to construct burial history curves, Lopatin (1969, 1971), Waples (1980), Issler (1982, 1984), and Cercone (1984) were able to demonstrate that a very good understanding of the maturity of organic material in sedimentary basins is indeed possible. A similar procedure was followed in this study except that small, though conceptually significant changes were made in graphically displaying the historical development of the present geothermal gradient. These changes are explained in more detail in the section dealing with temperature grids.

TABLE 3

Temperature Factors for Different Temperature Intervals

Temperature Interval (^{o}C)	Temperature Factor	Value (where r = 2)
0 - 10	r^{-10}	0.0009765625
10 - 20	r^{-9}	0.001953125
20 - 30	r^{-8}	0.00390625
30 - 40	r^{-7}	0.0078125
40 - 50	r^{-6}	0.015625
50 - 60	r^{-5}	0.03125
60 - 70	r^{-4}	0.0625
70 - 80	r^{-3}	0.125
80 - 90	r^{-2}	0.25
90 - 100	r^{-1}	0.5
100 - 110	r^{0}	1.0
110 - 120	r^{1}	2.0
120 - 130	r^{2}	4.0
130 - 140	r^{3}	8.0
140 - 150	r^{4}	16
150 - 160	r^{5}	32
160 - 170	r^{6}	64
170 - 180	r^{7}	128

The steps taken to construct the model are shown in a flow chart (Figure 10). Data was gathered from well log headings, well history reports, published literature, and from Geological Survey of Canada internal reports on lithological, paleontological and geochemical analyses for most wells in the basin. This information provided the basis for generating a temperature grid and a set of burial history curves for each of the wells. The grids and curves were combined on the same graph so that TTI values could be calculated.

1. Burial History Curves

A burial history curve represents a graphical record of a single selected grain from the time it is deposited until it is intersected by drilling in the present. The curve indicates the rate at which the grain becomes buried (or uplifted) with the passage of time. All that is required is the depth to specifically dated horizons, usually the top of a biostratigraphic stage. Identification of the stage is made by paleontology, palynology, lithology or a combination of these and other techniques. The specific age of the stage is then established by referring to a recent geologic time scale (e.g. Palmer, 1983).

This age/depth information is the basis for deriving the thickness of each biostratigraphic stage in the well. The depths to specific horizons for which TTI values are desired are then calculated by summing the thicknesses beginning at the horizon chosen and progressing one horizon at a time to the present surface. An example is shown in Table 4. When these values are plotted on an age-depth graph, the depth chronology (i.e. burial history) for each horizon selected becomes obvious (Figure 11). The end result is a series of sub-parallel curves separated by different, yet consistent, spacings of depth.

It should be noted that gradual compaction of the sediments should affect the shape of the burial history curve. However, this effect has been neglected because it needlessly complicates the construction of the subsidence curves without adding appreciably to the accuracy of the TTI values.

Figure 10

Flow Chart: Procedure for Constructing TTI Model

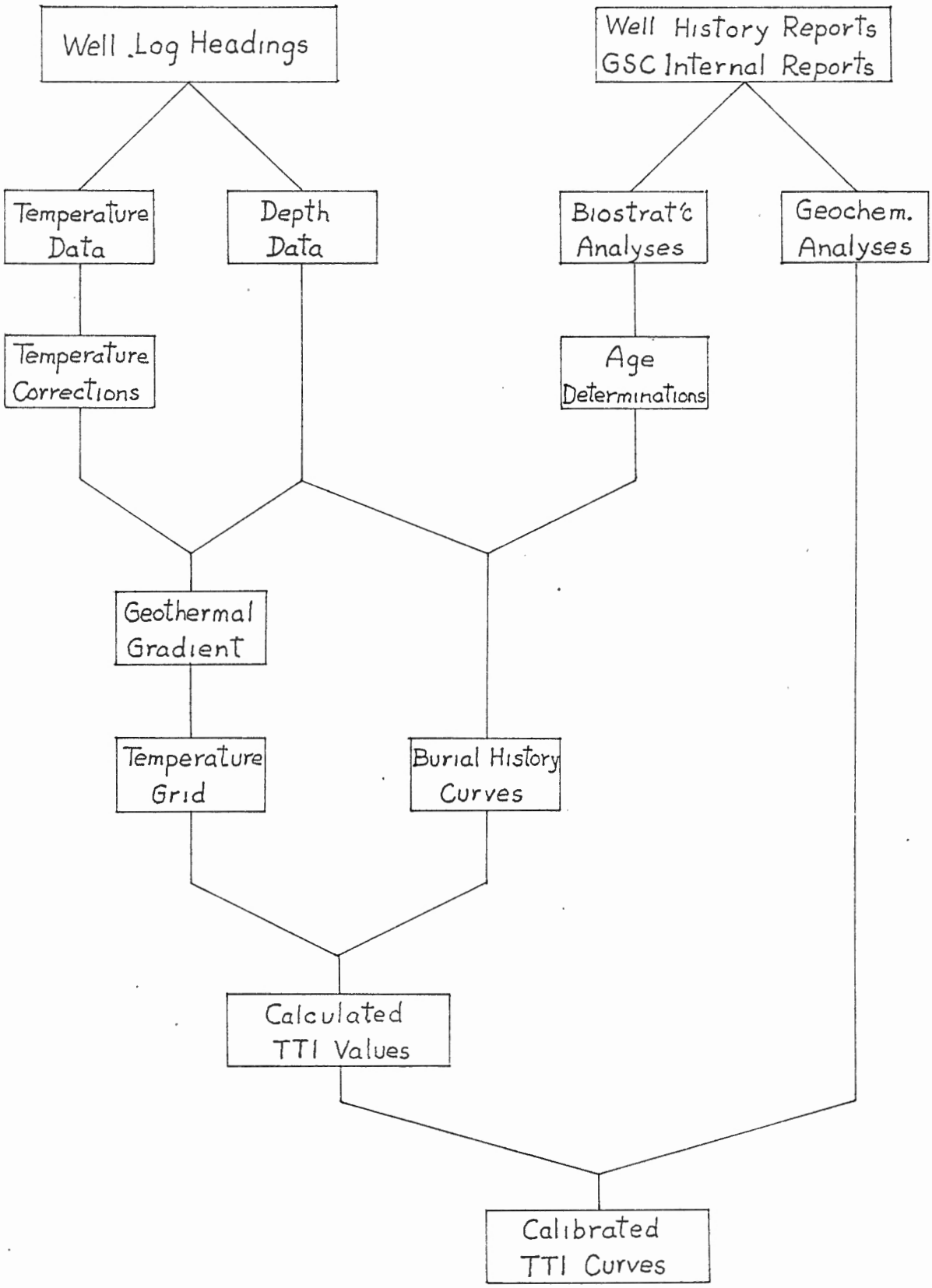

GeoTech Surveys Limited

			Age	RT	B.S.E	Th.	Depth Bottom	J/C	Berr/Val	Haut/Barr	Tur/Con	Eo/Olig
		Now	0.00				3641	3383	2296	2026	1966	996
		Pleist	0.01									
TERTIARY	Neogene	Plio	1.6									
		Mio-L	5.3			431						
		-M	11.2									
		-E	16.6									
	Paleogene	Olig-L	23.7									
		-E	30.0	540	431		3210	2952	1865	1595	1535	565
		Eoc-L	36.6	1105	996	565	2645	2387	1300	1030	970	0
		-M	40.0	1435	1326	330	2315	2057	970	700	640	
		-E	52.0									
		Paleo-L	57.8			160						
		-E	63.6	1595	1486		2155	1897	810	540	480	
CRETACEOUS	U	Maast	66.4									
		Camp	74.5			240						
		Sant	84.0	1835	1726		1915	1657	570	300	240	
		Coni	87.5			240						
		Turon	88.5	2075	1966		1675	1417	330	60	0	
		Ceno	91.0									
	L	Albion	97.5			60						
		Aptian	113									
		Barr	119									
		Haut	124	2135	2026		1615	1357	270	0		
		Val	131			270						
		Berr	138	2405	2296		1345	1087	0			
JURASSIC	U	Tith	144	3492	3383	1087	258	0				
		Kimm	152	3750	3641	258	0					
		Oxf	156									
	M	Call	163									
		Bath	169									
		Baj	176									
		Aal	183									
	L	Toar	187									
		Plien	193									
		Sin	198									
		Hett	204									
TRIASSIC	U	Nor	208									
		Carn	225									
	M	Lad	230									
		Anis	235									
	L	Scyth	240									

← paly (Davies)

paly (Bujak) →

TABLE 4

Cumulative Thicknesses for Specified Horizons:
Hibernia B-08

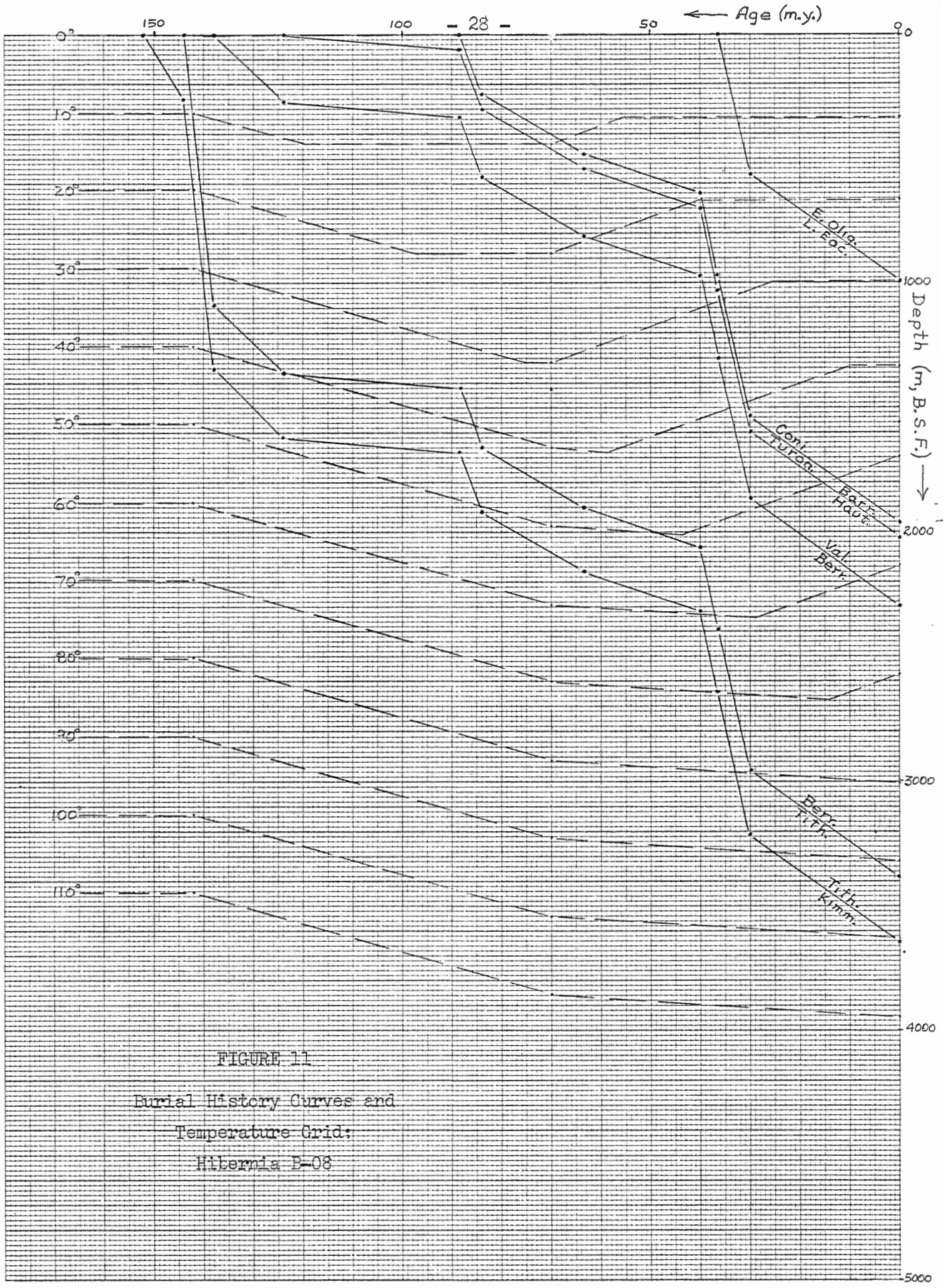

FIGURE 11

Burial History Curves and
Temperature Grid;
Hibernia B-08

METRIC

Corrections for compaction have been discussed by Perrier et al, 1974; Van Hinte, 1978; and Sclater et al, 1980.

2. Temperature Grids

The temperature grid is a graphical record of the changes in the geothermal gradient through geological history. The geothermal gradients developed in the early part of this report are used as a basis for calculating the depths to specific 10° intervals of increasing temperature.

Four assumptions have been made.

1. Heat flow from the basement is assumed to have been relatively constant throughout the geologic past.
2. The slope of each segment of the geothermal gradient is assumed to be some net function of the physical characteristics of the sedimentary strata occurring between the upper and lower depth limits of that segment. This relationship with lithology is assumed to have remained constant throughout the geologic past despite the compaction undergone by the sediments over this time.
3. It is assumed that the temperature of the sea floor has always been the same, in this case $0^{\circ}C$.
4. The effect of heat from radiogenic material and from mobile fluids is assumed not to be significant.

These assumptions are probably realistic for this level of sophistication in the model. They will probably have to be reconsidered along with other factors not mentioned above (e.g. tectonic age, etc.) if the model is to be developed for greater accuracy.

With these assumptions in mind, two tables are constructed. The first (Table 5) shows depth and temperature data picked from each segment of the geothermal gradient (Figure 12) so that numeric values (in $^{\circ}C/100$ m) can be calculated for each of the gradient segments. The time interval through which

TABLE 5

Segment Data of Geothermal Gradient:

Hibernia B-08

Time (m.y.)	Depth (m)	Thickness (m)	Temp. Range (°C)	Temp. Diff. (°C)	Gradient (°C/100m)
0 - 70	0 - 1560	1560	0 - 47	47	3.01
70 - 142	1560 - 2983	1423	47 - 79.5	32.5	2.28
142 - 152	2983 - 3641	658	79.5 - 100.5	21	3.19

FIGURE 12

Geothermal Gradient: Hibernia B-08

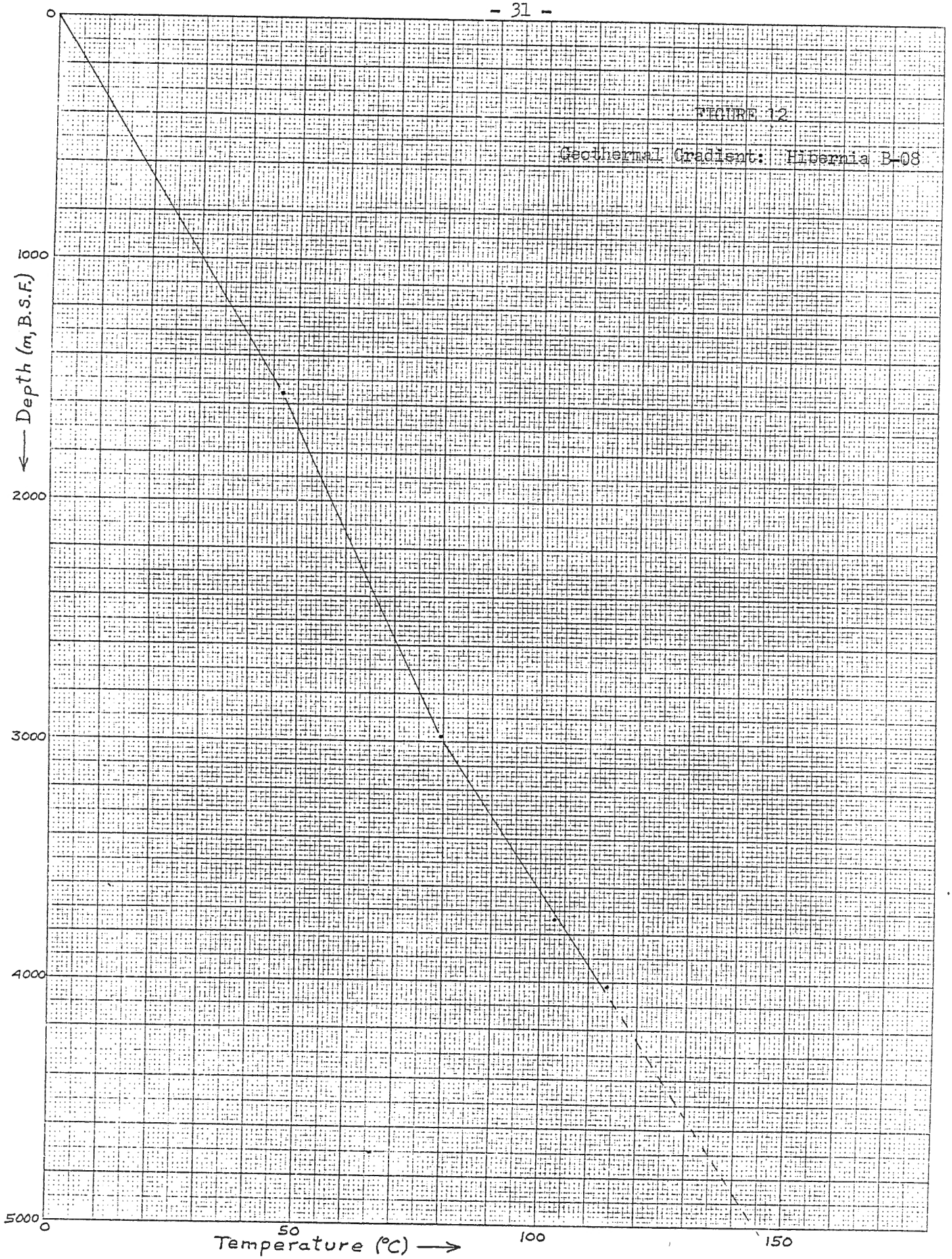

each segment is relevant is determined from the lithological ages at the upper and lower depth limits of the segment. The burial history curves are helpful in this regard, i.e. imagine that there are horizons at the upper and lower depth values so that the ages (B.P.) at which they were laid down can be read from the graph. These time intervals and their appropriate gradient values are then used to calculate the depth to each successively greater 10° geotherm, beginning at the sea floor with 0°C (Table 6).

Because each segment of a geothermal gradient (e.g. there are 3 indicated in Figure 12) is assumed to be a function of the lithology (assumption #2), the geothermal gradients in the historical past must change or shift according to the rate and conductivity of the accumulating sediments. This means that, as we regress into the past, the sea-floor environment (i.e. 0°C and 0 m depth) would seem to move progressively down the present-day geothermal gradient according to the corresponding age (i.e. depth). The gradient at any time in the past would simply be comprised of those segments appropriate to the underlying lithology for that time.

This shift in the geothermal gradient during sediment accumulation is an important conceptual aspect of the TTI model but was not considered in the graphical presentations of previous workers.

When the depth values for the different gradients (Table 6) are calculated and plotted at their respective ages on Figure 11, isotherms at 10° intervals can then be constructed to show how the geothermal gradients have changed through time. The isotherms must be drawn in such a way as to reflect the gradual change in gradient with time. It can be seen from Figure 11 that these isotherms are horizontal while each section (segment) is "built up", but becomes distorted (i.e. slopes up or down) when sediments of a different conductivity are deposited on top. However, the vertical spacings between each isotherm remain constant, reflecting the "burial" of each segment of the gradient.

Table 6

Depth Values of Temperature Grid: Hibernia B-08

Temp. (°C)	142 m.y. – 152 m.y.		70 m.y. – 142 m.y.		0 m.y. – 70 m.y.	
	Temp. Diff. / Grad. x100	Depth	Temp. Diff. / Grad. x100	Depth	Temp. Diff. / Grad. x100	Depth
0	0	0	0	0	0	0
10	313	313	439	439	332	332
20	313	626	439	878	332	664
30	313	939	439	1317	332	996
32.5			110	1427		
40	313	1252	235	1662	332	1328
47					233	1561
50	313	1565	313	1975	132	1693
60	313	1878	313	2288	439	2132
70	313	2191	313	2601	439	2571
79.5					417	2988
80	313	2504	313	2914	16	3004
90	313	2817	313	3227	313	3317
100	313	3130	313	3540	313	3630
110	313	3443	313	3853	313	3943

C. Calculation of TTI Values

TTI values are easily calculated by combining the appropriate burial history curve and temperature grid for each of the wells (Figure 11). For each horizon drawn on the burial history curve, the "time spent" in each temperature interval is determined and the result multiplied by the appropriate temperature factor to give an interval maturity (ΔTTI). All interval values are then summed to give the TTI value for that horizon.

The TTI values for most of the important horizons have been calculated and stated in tabular form (see Appendix).

IV. COMPARISON OF TTI VALUES WITH GEOCHEMICAL MEASUREMENTS

Because TTI values have been derived from a mathematical model, they must be correlated with data obtained using other, more direct methods for evaluating the thermal maturity of organic material.

A. Correlation with Vitrinite Reflectance (R_o) Data

A wide variety of geochemical measurements have been used to indicate levels of maturity, but vitrinite reflectance data are probably the most reliable. The effects of temperature and cumulative time on particles of kerogen are essentially irreversible so that the measured reflectance is an indication of the maximum rank attained. No other material provides such a direct measure of maturity without being affected by composition (Dow, 1977).

Vitrinite reflectance data for 13 of the 23 wells in the East Newfoundland Basin (e.g. Adolphus D-50, Ben Nevis, Bonnition, Dominion, Egret K-36, Flying Foam, Hebron, Hibernia G-55, K-18, O-35, P-15, Murre, and Nautilus) have been correlated with their corresponding TTI values for the same depth. These data, together with a best-fit correlation line, are displayed graphically in Figure 13. Mathematically, this correlation is expressed by the relationship:

$$\log TTI = 5.570 \log R_o + 1.946$$

or:

$$TTI = 88.308\ R_o^{5.570}$$

This compares with:

$$\log TTI = 6.7367 \log R_o + 2.7317$$

or:

$$TTI = 539\ R_o^{6.7367}$$

obtained by Issler (1982) for the Scotian Shelf. This curve is "lower" and "steeper" than the one for the East Newfoundland Basin. That is, for any value of R_o, the TTI values for the Scotian Shelf are higher and increase more rapidly

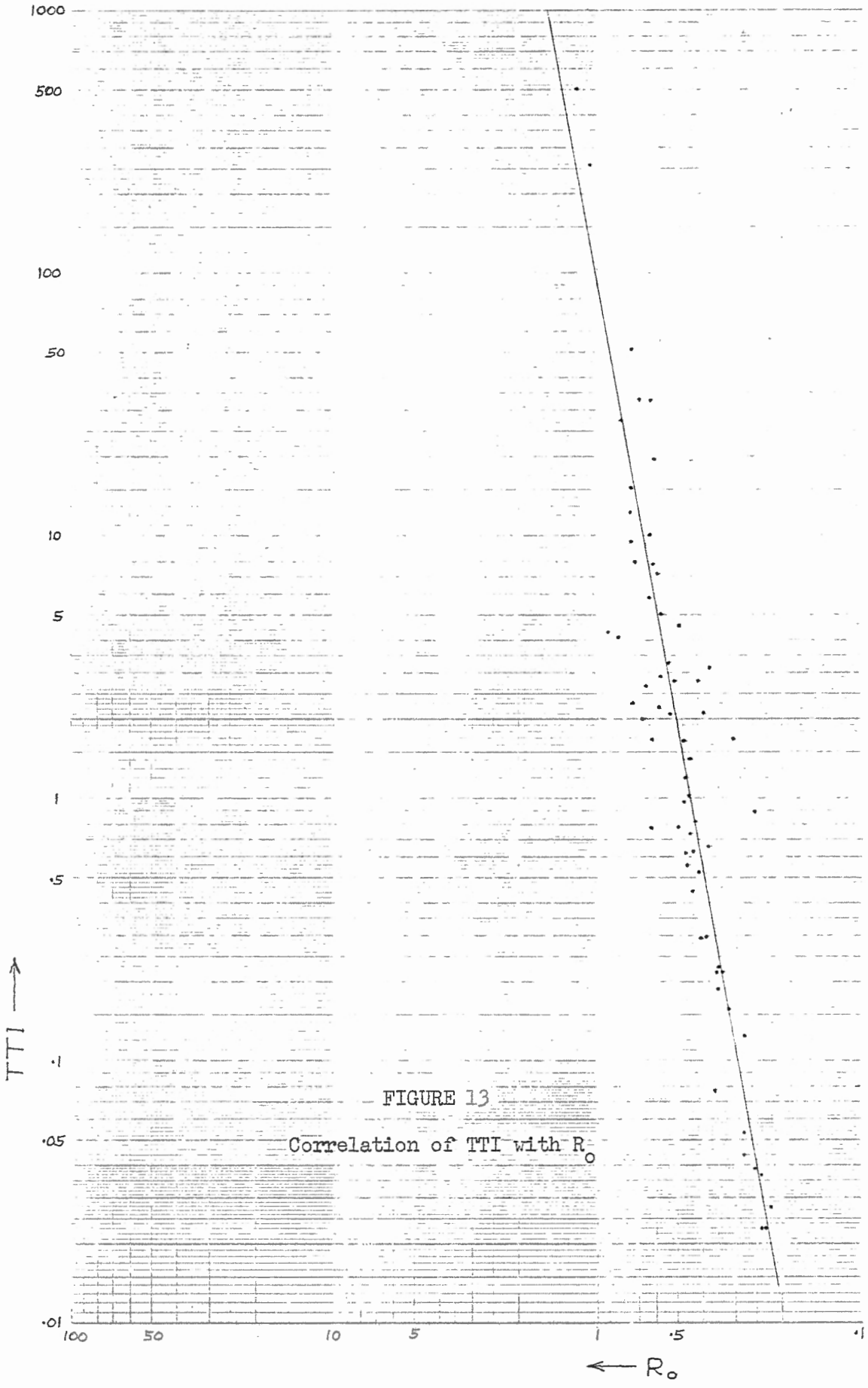

FIGURE 13

Correlation of TTI with R_o

Full Logarithmic, 3 × 5

than those for the East Newfoundland Basin.

Although there are a few data points at a considerable distance from the correlation line, the line is consistently straight and passes through the greatest density of data points over a range of 5 magnitudes TTI.

B. Correlation with Other Geochemical Information

An attempt was made to correlate the TTI values against all other available geochemical information, such as the thermal alteration index, fluorescence (both colour and intensity), and carbon preference index. The results of these correlations are discussed below.

Thermal Alteration Index (TAI): The thermal alteration index is a measurement of the level of maturation based on the colour and intensity of colour for dispersed organic material (Bujak et al, 1977). Because it is rather subjective, the method is not quite as reliable an indicator of maturation as R_o data (Issler, 1982).

A correlation of TTI values and TAI values at matching depths is shown in Figure 14. (The unusual scale marking the TAI coordinate is the same as that used in the TAI reports from which the data were taken.) Although there is considerable scatter, there is a marked trend of increasing TAI values with TTI values. The relationship can be expressed:

$$\log TTI = 4.126\ TAI - 6.298$$

or:

$$TTI = 5.04 \times 10^{-7} \times 13366^{TAI}$$

Fluorescence: The results of fluorescence tests with respect to both colour and intensity were correlated with their corresponding TTI values. A graphic display of colour values is shown in Figure 15 where the spectral colours from blue to red are designated by the numbers from 0 to 9. A correlation with fluorescence intensity is shown in Figure 16 where intensities increase from 0 to 5.

FIGURE 14

Correlation of TTI with TAI

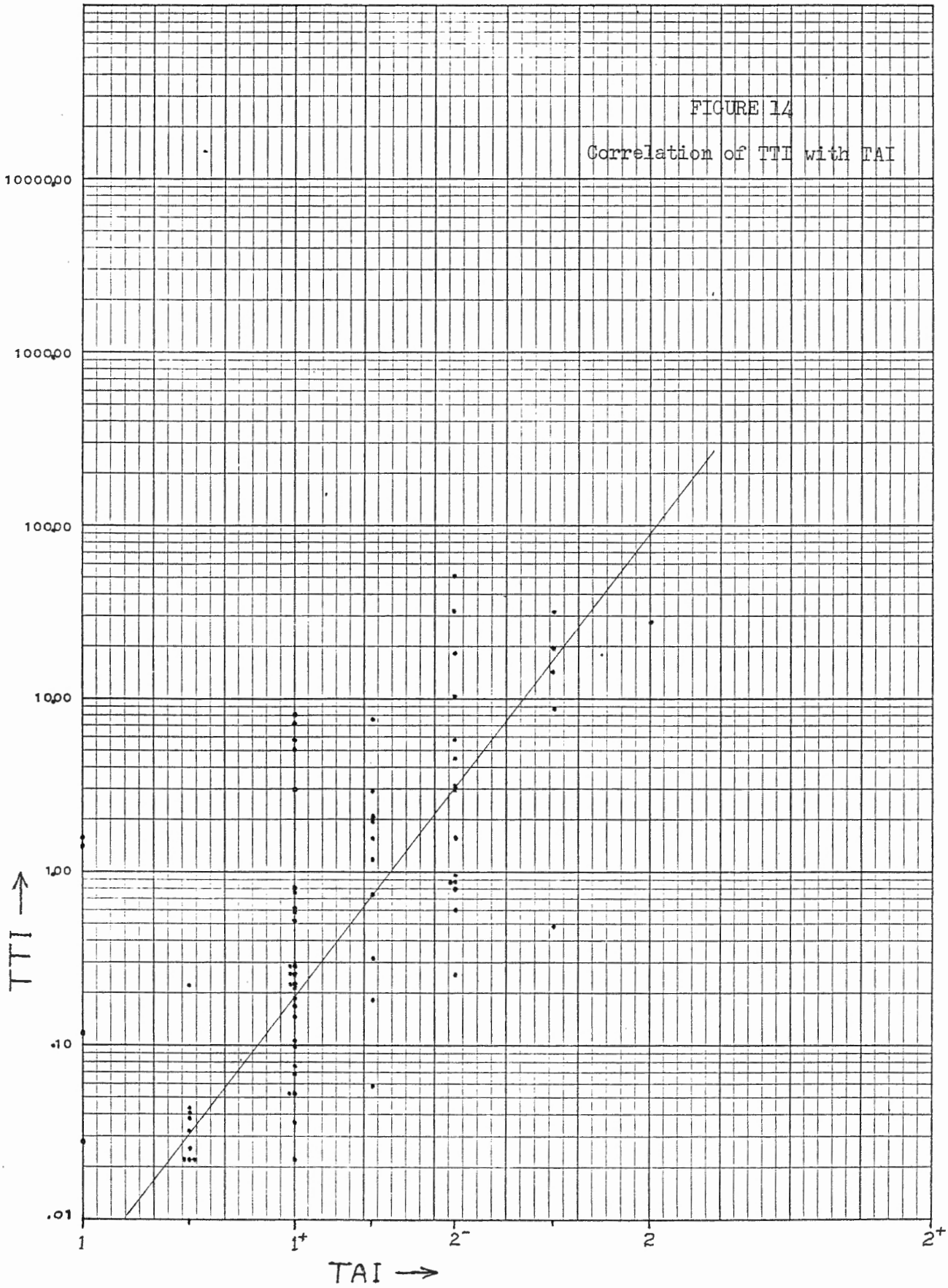

FIGURE 15

Correlation of TTI with Fluorescence Colour

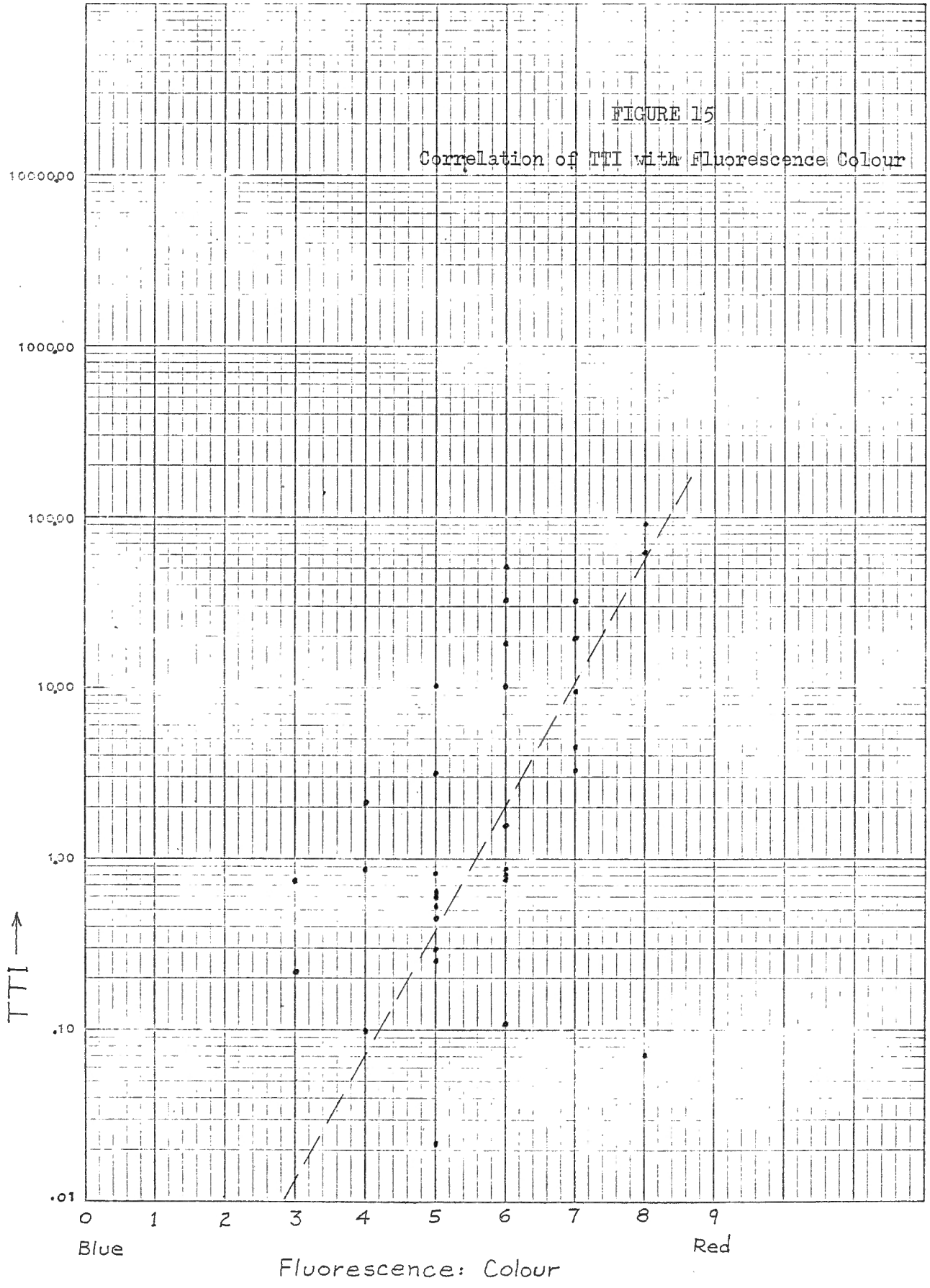

FIGURE 16

Correlation of TTI with Fluorescence Intensity

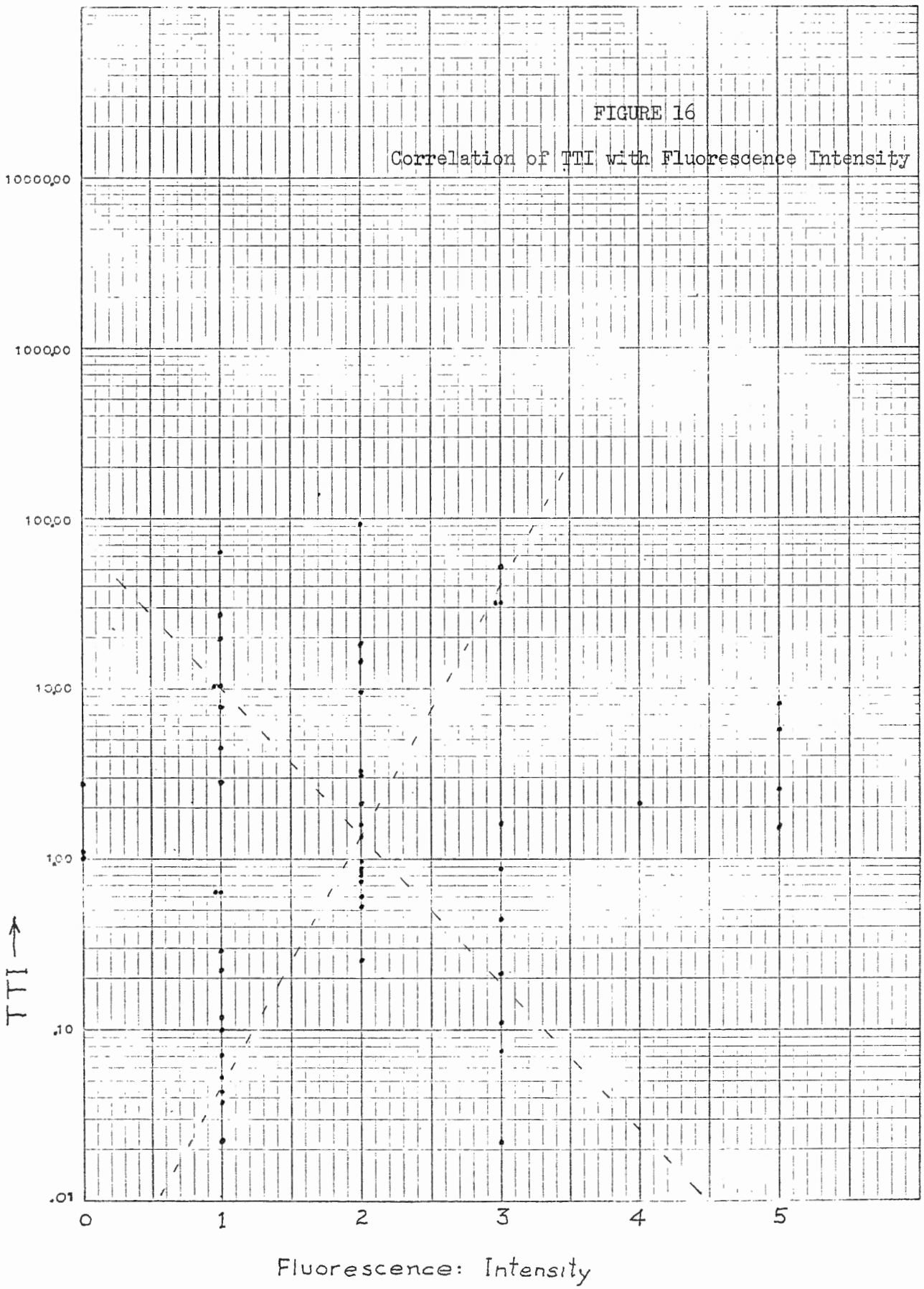

The correlation with respect to colour shows a broad trend of increasing TTI values as fluorescence colour changes from blue to red. No particular trends are shown with fluorescence intensity.

Carbon Preference Index (CPI): It is generally accepted that CPI values decrease with increasing thermal maturity. That is, CPI values for immature samples tend to range from low to very high, but among the more mature samples, very high values do not occur (Waples, 1980). Although only a few CPI values were available for wells in the East Newfoundland Basin (e.g. Cormorant, Egret K-36, Murre), their correlation with corresponding TTI values seems to bear this out (Figure 17).

C. Correlation with Depth, and with Temperature

Although both depth and temperature are integral factors in the calculation of TTI values, it may be useful to correlate each with its appropriate TTI value. Figure 18 shows a correlation of depth with the logarithm of corresponding TTI values. The resulting best-fit curve is linear which can be expressed by the relationship:

$$\log TTI = 0.0006945 \text{ Depth} - 1.36601$$

A nominal TTI value can then be calculated or deduced graphically for any given depth, or vice versa.

From this, it appears that the top of the oil window (i.e. where $R_o = 0.5$ or TTI = 2.0) would occur nominally at 2400 metres. Similarly, the peak of oil generation (i.e. where $R_o = 0.8$ or TTI = 25) would occur nominally at 4000 metres. Note that here we are using generally accepted values of R_o (Dow, 1977).

A similar correlation with temperature is shown in Figure 19. Again, the resulting curve is linear, and can be expressed by the relationship:

$$\log TTI = 0.0289248 \text{ Temperature} - 1.6585391$$

FIGURE 17

Correlation of TTI with CPI

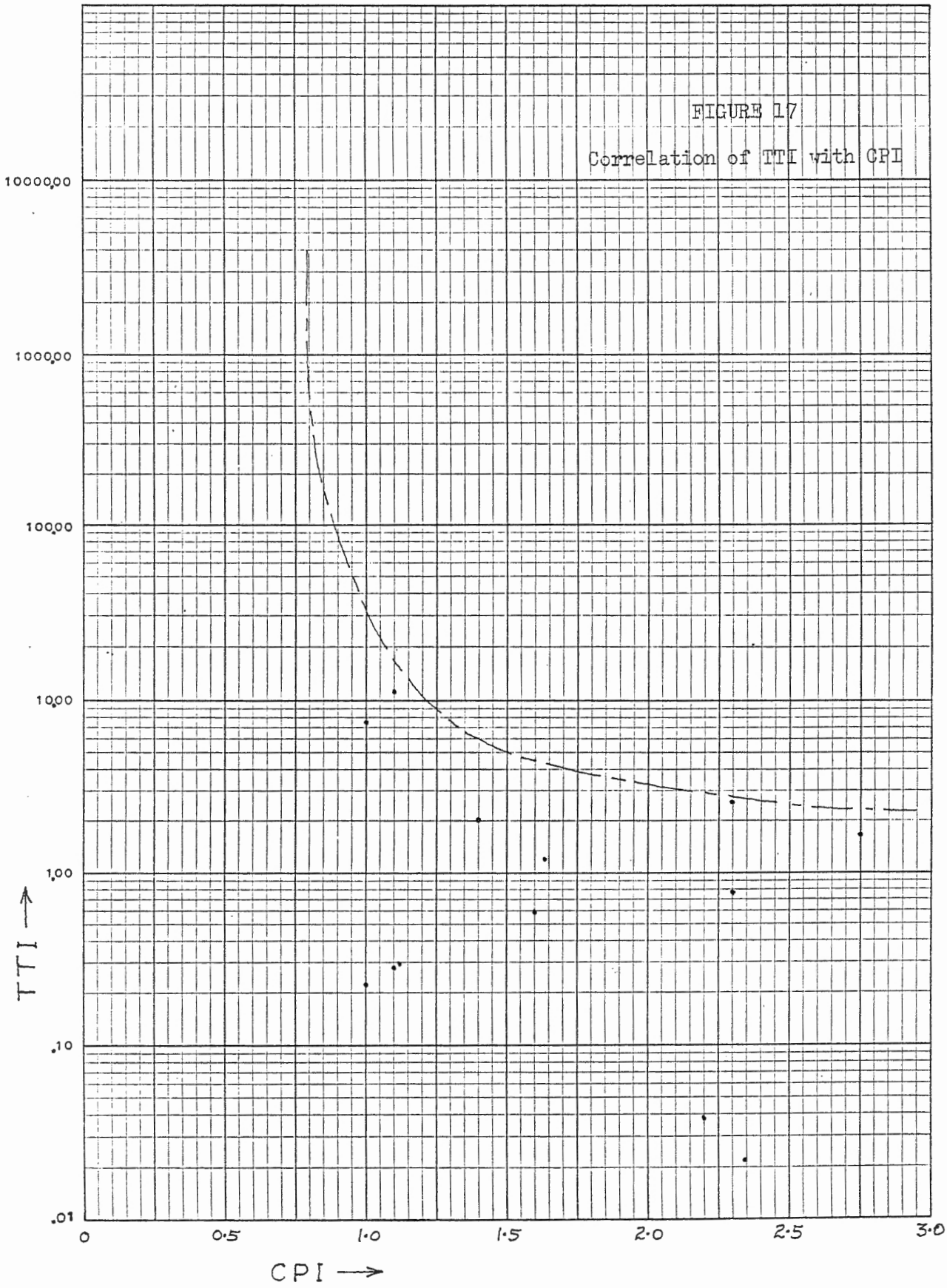

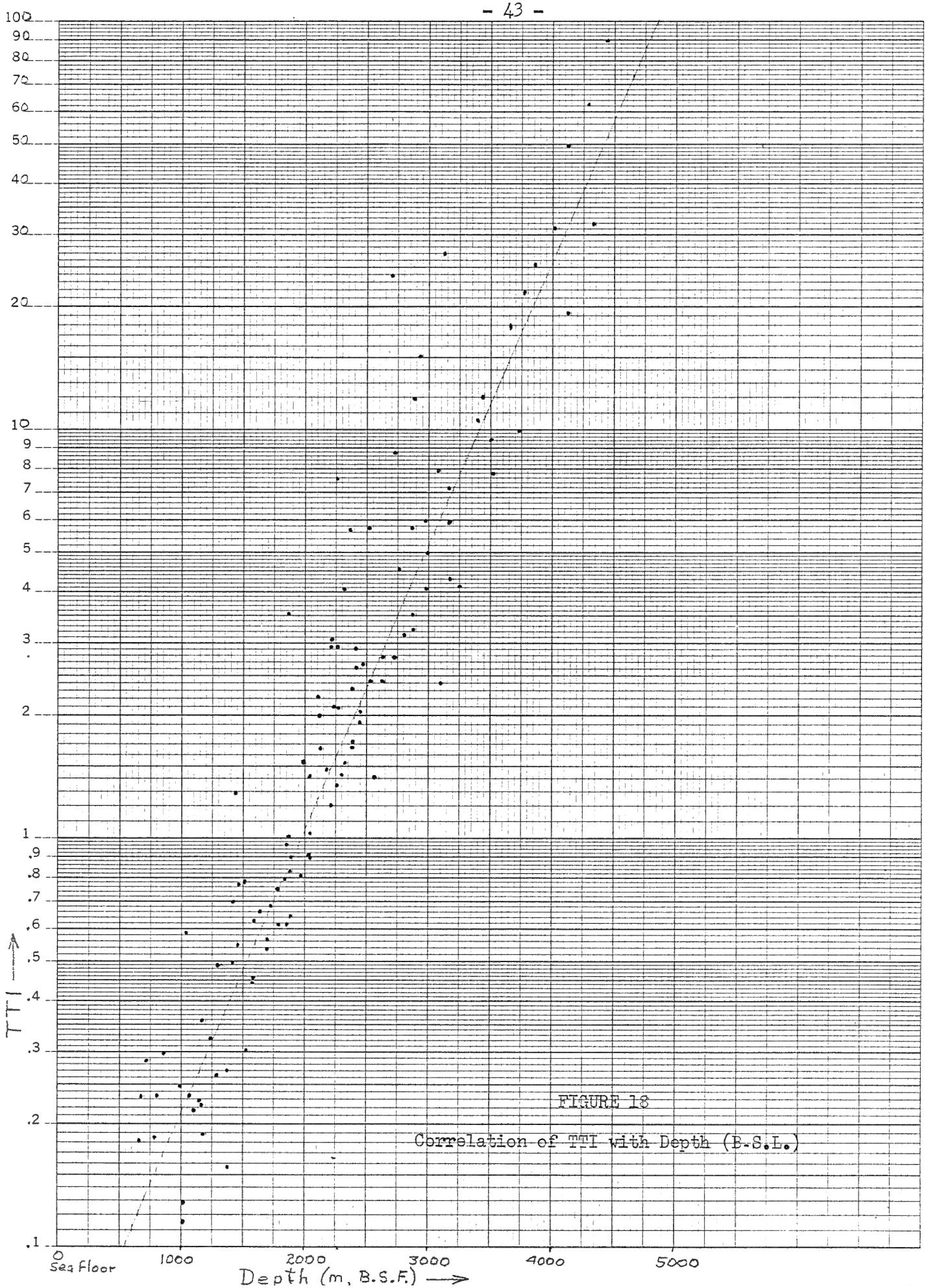

FIGURE 18

Correlation of TTI with Depth (B.S.L.)

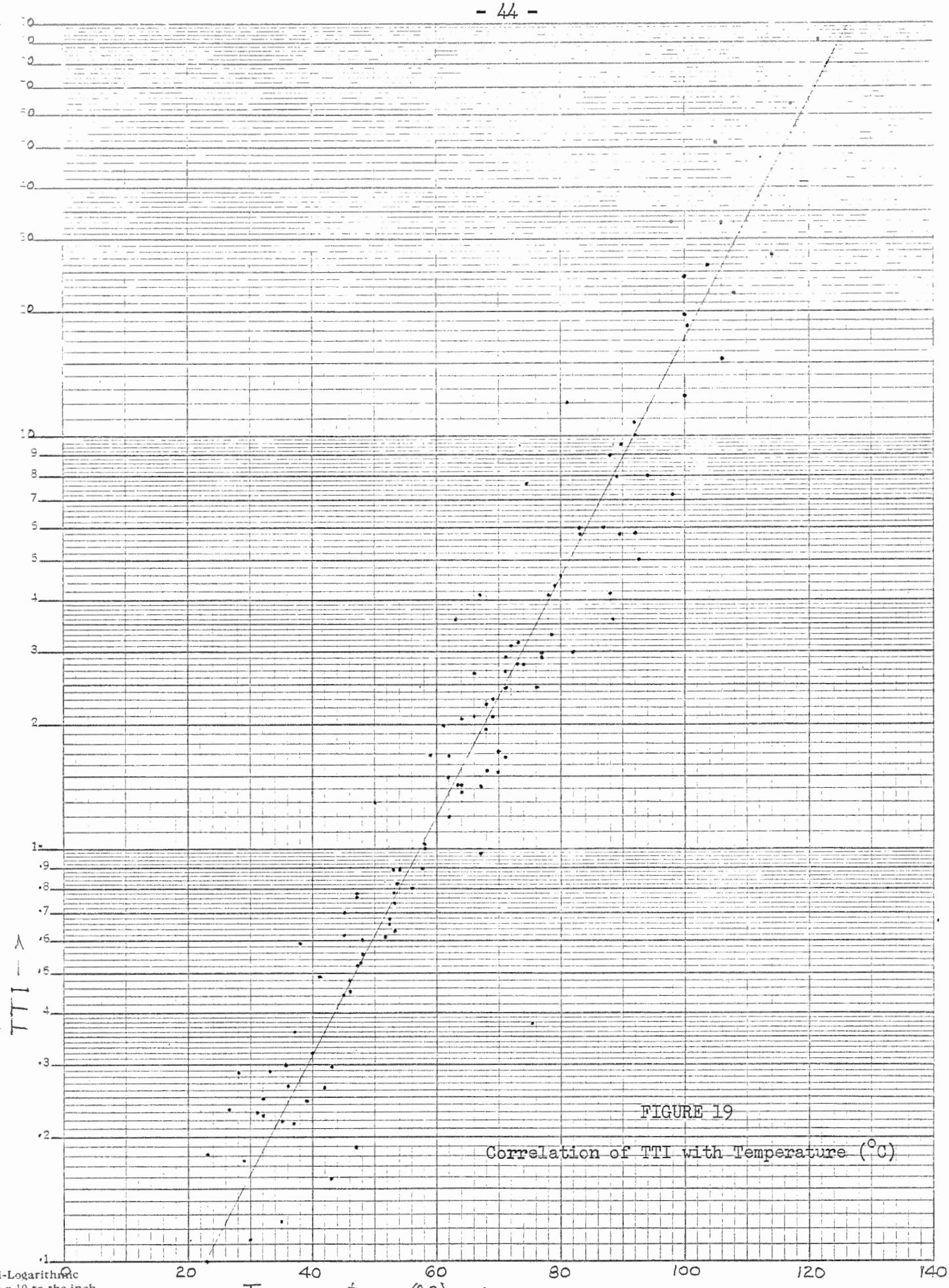

FIGURE 19

Correlation of TTI with Temperature (°C)

From this equation, a nominal TTI value can be calculated (or deduced graphically from the curve) for any given temperature, and vice versa.

V. ORGANIC MATURATION

Calibrated TTI values obtained by application of Lopatin's model can be useful for indicating where organic maturation has occurred. Dow (1977) suggests that the onset of oil generation should begin at about R_o = 0.5, reach a peak at about R_o = 0.8, and end at about R_o = 1.2. The TTI equivalent values for each of these as derived in this study (see Figure 13) are 2, 25 and 240 respectively (Table 7). The TTI values of similar stages in other areas such as the Scotian Shelf (Issler, 1982, 1984) and worldwide (Waples, 1980) are included in Table 7.

A. Establishing the "Oil Window"

The relative timing of the development of the "oil window" in any given well can be established by calculating the age at which the TTI values for each horizon reach 2, 25 and 240 respectively. When equivalent values for beginning, peak and end of oil generation are plotted on a diagram showing burial history curves and a temperature grid, the area covered indicates the zone (time and source rock) which could have the potential for generating oil, i.e. have adequate physical conditions. The Nautilus C-92 well is used as an illustration in Figure 20.

B. Establishing the "Oil Kitchen"

Using data calculated in a similar manner from all 23 wells, the depth to the "oil kitchen" can be established. These depths have been plotted on a map of the area and contoured to show the changes in depth to the top of the "oil kitchen" (Figure 21). There were insufficient data to construct maps at other levels (i.e. at peak and end depths).

TABLE 7

TTI Equivalents for the "Oil Window"

R_o Values		TTI Values		
		East Nfld. Basin (This study)	World Wide (Waples, 1980)	Scotian Shelf (Issler, 1982)
Begin:	0.5	2	3	5
Peak:	0.8	25	34	120
End:	1.2	240	123	1300

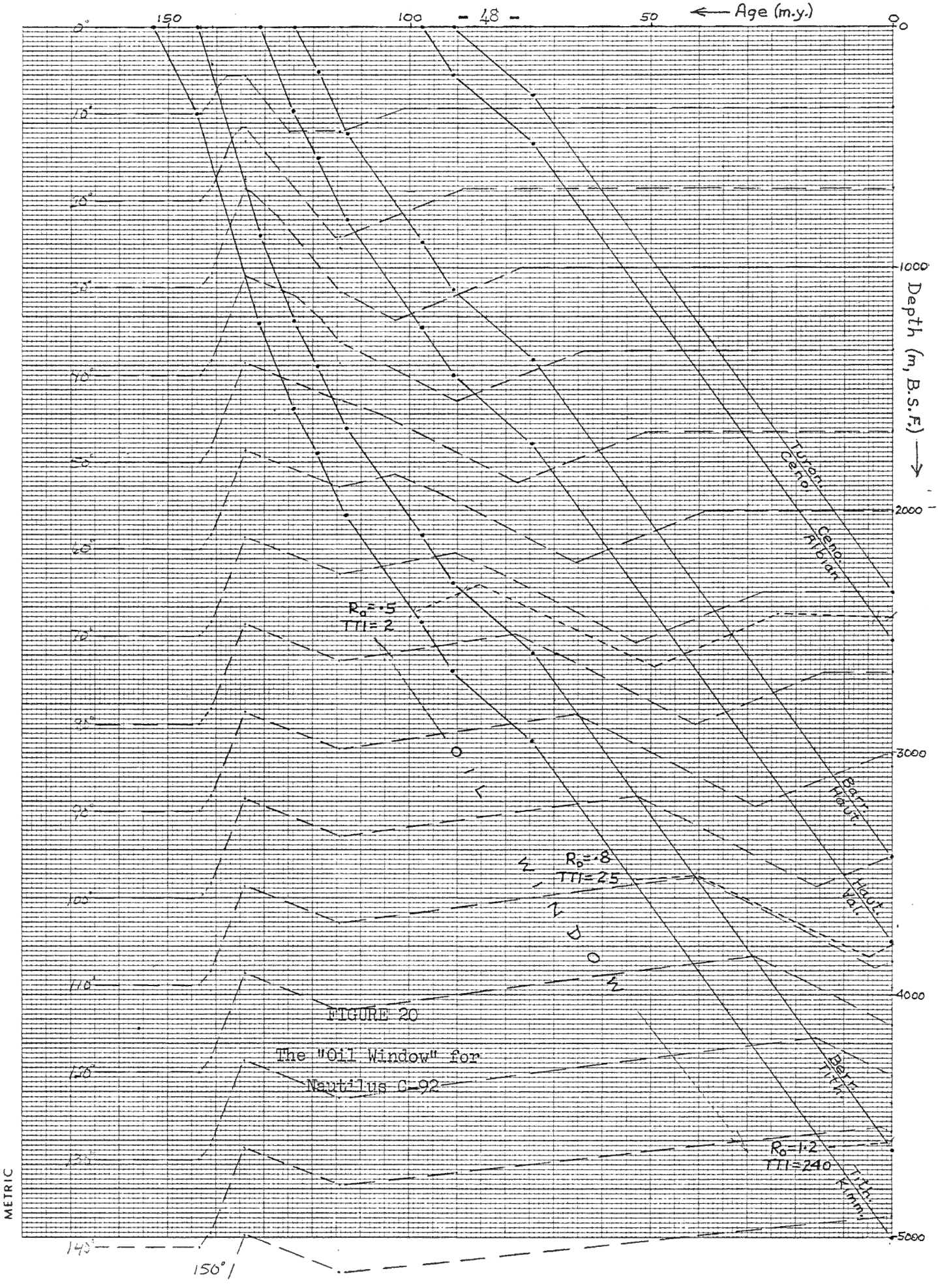

FIGURE 20

The "Oil Window" for Nautilus C-92

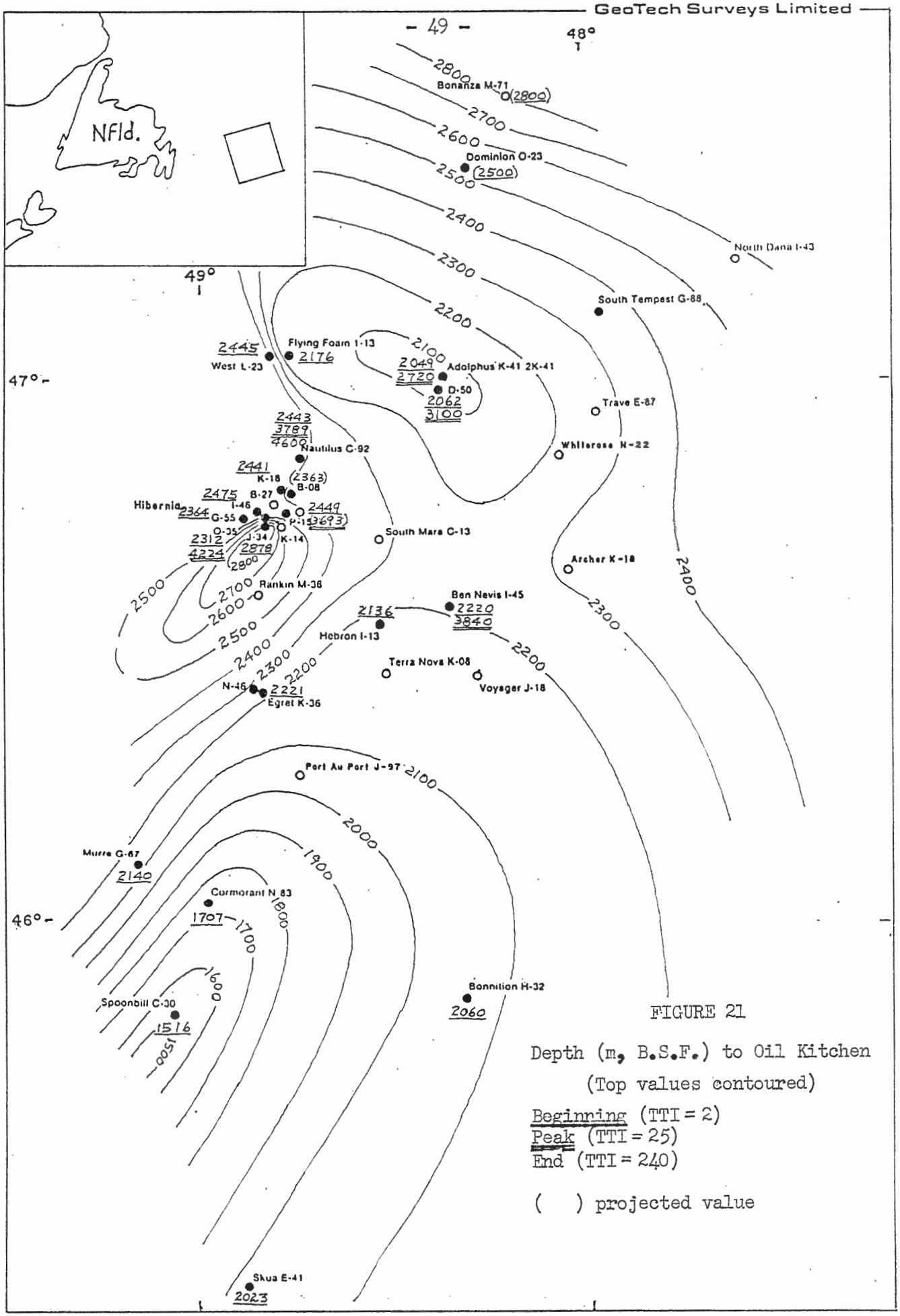

FIGURE 21

Depth (m, B.S.F.) to Oil Kitchen
(Top values contoured)

Beginning (TTI = 2)
Peak (TTI = 25)
End (TTI = 240)

( ) projected value

VI. HYDROCARBON GENERATION MODEL

A. Outline of the Model

A hydrocarbon generation model has been devised for the East Newfoundland Basin based on five major parameters.

1. Observed hydrocarbon occurrences
2. Quantity of organic material
3. Quality (type) of organic material
4. Maturation
5. Geology

All available information pertinent to each of these parameters and related to the generation of hydrocarbons has been collected and summarized in tabular form (Table 8). This table forms the basis of the following comments.

1. Observed Hydrocarbon Occurrences

Observed hydrocarbon occurrences serve as the major criterion for selecting those horizons for which related information was sought. Most occurrences are listed in either the Offshore Schedule of Wells or in company well history reports.

Except for one occurrence in the Upper Cretaceous (i.e. Adolphus 2K-41), all hydrocarbon discoveries are located in the Lower Cretaceous or Upper Jurassic. There are as well, minor stains and shows in the Tertiary (i.e. Adolphus 2K-41) and Lower Jurassic (Spoonbill, Cormorant).

Measurable hydrocarbons have been discovered in the Lower Cretaceous in at least seven wells (Table 8). Drill stem tests indicate that oil flows range between 41.5 and 592 m^3/d, and gas flows range between 3500 and

TABLE 8

Age / Well Name	Depth Interval m (RT)	Hydrocarbon Occurrances: Oil (m^3/d)	Gas (m^3/d)	GOR	Organic Matter: Quantity TOC (%)	Quality: A	H	W	C	Type	Maturation: R_o (%)	TAI	TTI	Geology	
TERTIARY															
Adolphus D-50	1250 - 2700				2.0 - 3.0	60	30	10	0	II	.31 - .63	1^+ - 2^-	.10 - 2.0	Sh(ls)	E.?
	1150 - 2140				4.0 - 4.3	65	35	0	0	II	.42 - .50	(1^+) - 2^-	.52 - 1.4	Sh(ls)	Eoc.
Adolphus 2K-41	1135 - 1234	oil stains			4.0 - 5.0	55	45	0	0	II	--	$1^+(2^-)$	—	SlsT(sh)	Olig
	1465 - 1960	oil stains			4.0 - 5.0	75	25	0	0	II	—	$1^+(2^-)$	.28 - 1.0	Sh, slsT	Eoc.
Bonnition	1139 - 1261				3.5 - 5.0	65	35	0	0	II	.30 - .34	1^+	? - .20	Sh	Eoc.
Dominion	1875 - 3139				2.5 - 3.0	50	45	5	0	II	.36 - .57	1^+	.29 - 4.0	Sh(slsT)	Eoc.
	2615				3.4	50	40	10	0	II	.53	1^+	1.4	Sh, slsT	Eoc.
Flying Foam	1480 - 1946				3.0 - 5.0	70	15	5	0	II	.33 - .4	1	.29 - .84	ClysT, sh	Eoc.
Murre	341				2.2	50	40	0	10	II	—	—	—	ClysT	Olig
Skua	864				2.4	10	40	25	25	III	—	$<1^+$	—		Eoc.

TABLE 8

Age / Well Name	Depth Interval m (RT)	Hydrocarbon Occurrances: Oil (m^3/d)	Gas (m^3/d)	GOR	Organic Matter: Quantity TOC (%)	Quality: A	H	W	C	Type	Maturation: R_o (%)	TAI	TTI	Geology
U. CRETACEOUS														
Adolphus 2K-41	2609-2647	42.6	5.7	133		60	30	0	10	II	—	1+(2-)	3.5-4.5	Ss, ls
	2714				4.0	15	25	35	25	III	—	2--2	12.0	Sh
Hibernia B-08	609-1829					55	40	5	0	II	—	1+	?-.49	Clyst.
L. CRETACEOUS														
Adolphus 2K-41	2817				3.8	10	30	40	20	III	—	3-	24.0	Slst, red b, salt
Ben Nevis	2378-4340	stain-41.5	trace-293	1024							.4-.6	—	9.6-50	Ss, sh (slst, coal)
Bonnition	1614				2.5	35	40	15	10	III	.38	1+	.40	Slst
Egret K-36	1750-1850				6.4-20.0	0	35	60	5	III	.35	1+	.68-.70	Ss (clyst, coal)
Egret N-46	1460				4.5						—	—	.57	Slst (ss, sh)
Flying Foam	2393-2960				3.0-5.0	10	45	45	0	III	.45-.63	1+	2.2-5.0	Slst, ss (ls)
Hebron	1794-1916	110-121	3.5-4.3	32-36							.46-.48	—	.55-.73	Ss (sh, mlst)
	2722-2986	show-357	0-30.3	0-86							.40-.62	—	3.0-3.7	Ss (sh, ls)
Hibernia B-08	2648-3261	80-489	59.5-306	122-3823		0	40	45	15	III	—	2-	2.3-5.0	Ss (slst, ls, coal)
Hibernia G-55	2461, 3319	2 stains									.42-.44	—	1.75-?	Ss (slst)
Hibernia K-18	2282-3217	205-574	25.2-93.2	106-162							.47-.57	—	1.15-4.8	Ss (sh, slst)
Hibernia O-35	2055-2476	64-494	17.5-62.3	88-179							.44-.46	2-	.92-2.3	Ss (slst)
Hibernia P-15	2422-2443	185	12.4	67	1.0	0	30	40	30	III	0.3	2-	1.5	Ss
	3192-3856	343-592	52.3-125	126-211	0.3-0.7	0	40	40	20	III	0.6	2-	16-18.5	Ss (slst)
	3695-3905		gassy water		0.7	0	40	40	20	III	0.62	2-	21.3	Slst, ss
Nautilus	3205-4001	show-418	0-152	0-164							.69-.69	—	7.0-30	Ss (sh, slst, ls)
West Flying Foam	2476-2550	stain									—	—	1.7-1.9	Ss, sh

TABLE 8

Age / Well Name	Depth Interval m (RT)	Hydrocarbon Occurrances: Oil (m^3/d)	Gas (m^3/d)	GOR	Organic Matter: Quantity TOC (%)	Quality: A	H	W	C	Type	Maturation: R_o (%)	TAI	TTI	Geology
U. JURASSIC														
Ben Nevis	4426 - 4436	4.4									~1.1	—	61 - 63	Sh, ss
	4535 - 4550	254	340	1337							~1.1	—	78 - 81	Ss, (sh, coal)
Egret K-36	2550 - 2700		dry gas		6.0 - 8.0	40	40	0	10	II	.50	(1+)2-	2.7 - ?	Ls (sh, ss, coal)
Egret N-46	1650 - 2320	0 - trace			1.5 - 5.0						—	—	~9 - ?	Sh (ss, s/st, coal)
Flying Foam	3258 - 3318				4.0 - 5.0	45	25	15	15	II	.75 - .76	1+ - 2-	6.8 - 8.2	Ls, ss (sh, coal)
	3449 - 3618				3.0 - 4.0	10	40	30	20	III	.82 - .88	1+ - 2-	9.6 - 13.5	Ss, s/st, sh
Hebron	3842 - 4381	0 - 487	0 - 90.6	99 - 245	1.0 - 4.3						1.25 - 1.5	—	—	Ss (s/st, sh, coal)
Hibernia B-68	3485 - 3715	386 - 577	64 - 515	167 - 1133		0	50	40	10	III	—	2-	10.5 - 17	Ss (s/st, coal)
Hibernia K-18	3735 - 3854	130 - 731	43 - 193	246 - 332							.63 - .65	—	8.9 - 10	Ss (s/st, sh)
Hibernia P-15	4113 - 4142	show - 127	0 - 12.8	84 - 101	1.0 - 2.2	0	40	50	10	III	.7 - .72	2-	32 - 37	Ss (ls)
Murre	1185				1.6	0	30	40	30	III	—	—	~40	Sh
M. JURASSIC														
Skua	2705				2.0	0	35	45	20	III	—	2-	6.4	Sh
L. JURASSIC														
Cormorant	2335 - 2524	stains			0.2 - 0.8	10	40	40	10	III	—	1+ - 2-	7.2 - 8.0	Delta (ank, salt)
Spoonbill	1007				5.0	15	52	20	15	III	—	1+ (2-)	—	Ls (delta)
	1204 - 1433	shows				0	33	33	33	III	—	1+ - 2-	3.5 - 5.7	Salt (delta)
TRIASSIC														
Spoonbill	1530, 2580				3.3 - 3.7	25	25	25	25	III	—	1+ - 2-	4.4 - 5.0	Red sh (salt)

293,000 m^3/d. Gas to oil ratios (GOR) calculated from these values, range between 32 and 7024.

Similarly, measurable hydrocarbons have been discovered in the Upper Jurassic in five wells (Table 8). Drill stem tests indicate that oil flows range up to 731 m^3/d and gas flows range up to 515,000 m^3/d. Gas to oil ratios for these measurements range between 89 and 1337. It should be noted that the highest GOR in the Lower Cretaceous (i.e. 7024) and the highest GOR in the Upper Jurassic (i.e. 1337) occur in the same well, Ben Nevis.

Notwithstanding the high gas values in both the Lower Cretaceous and the Upper Jurassic, the East Newfoundland Basin is undoubtedly oil prone.

2. Quantity of Organic Material

The amount of organic carbon is commonly used as a simple and direct measure of the capability of the source rock for generating hydrocarbons. Although a commonly accepted minimum organic carbon content for a potential source rock is 0.5%, values of one per cent or more are usually necessary for viable source rocks.

Total organic carbon (TOC) as a percentage of rock weight is indicated in Table 8 together with its respective depth interval. This information is available from corporate well history reports and a detailed study of ditch cuttings gas ($C_1 - C_4$ analysis) (Hardy and Jackson, 1980). TOC values range up to 5.0 wt. % in many places, even over considerable sections; some are as high as 8 wt. % (Upper Jurassic) and 20 wt. % (Lower Cretaceous).

3. Quality of Organic Material

The type of organic material trapped in buried sediments depends on the depositional environment (i.e. marine, terrestrial, lacustrine) and, in turn, greatly influences the hydrocarbon source potential (or yield) and the nature

(i.e. oil, gas, condensate) and timing of the hydrocarbon products (Powell and Snowdon, 1983). When organic material becomes buried, it matures by undergoing diagenesis (or catagenesis) and produces kerogen which is the raw material for generating oil and gas. Geochemical analyses of kerogen can provide accurate C, H, O, and N contents from which H/C and O/C ratios can establish the type of organic matter (Figure 22). Because kerogen Types I, II, III, and IV have different initial hydrogen contents and therefore different chemical structures, their maturation thresholds are different as is the nature of the hydrocarbon products. This is summarized graphically in Figure 23. The hydrocarbon potential or yield from each type will also be different (Figure 24).

The organic matter from many of the wells used in this study has been examined by optical microscope, and identified according to a botanical classification as amorphous, herbaceous, woody, or coaly (Burgess, 1974). This scheme, while useful for palynological dating, does not consider the wide ranging chemical and structural differences inherent in the various kinds of kerogen. For example, kerogen commonly identified as being amorphous can have a wide range in hydrogen content (Powell et al, 1982). Nevertheless, there appears to be sufficient similarities between the kinds of organic materials grouped in the 4-fold botanical classification and those classified into the four Types (i.e. I, II, III, and IV) that, for this study, reasonable conclusions can be made about the depositional environment (Table 9).

The composition of the organic matter is stated in percentages of amorphous, herbaceous, woody or coaly fragments in the total organic mix (Table 8). From this and other information, it was then possible to classify the organic matter as to which Type was predominant in the sample.

In general, the organic matter from Tertiary sediments is dominantly amorphous with most of the remainder being herbaceous (Table 8). This is relatively analogous to Type II material which indicates a marine source for the

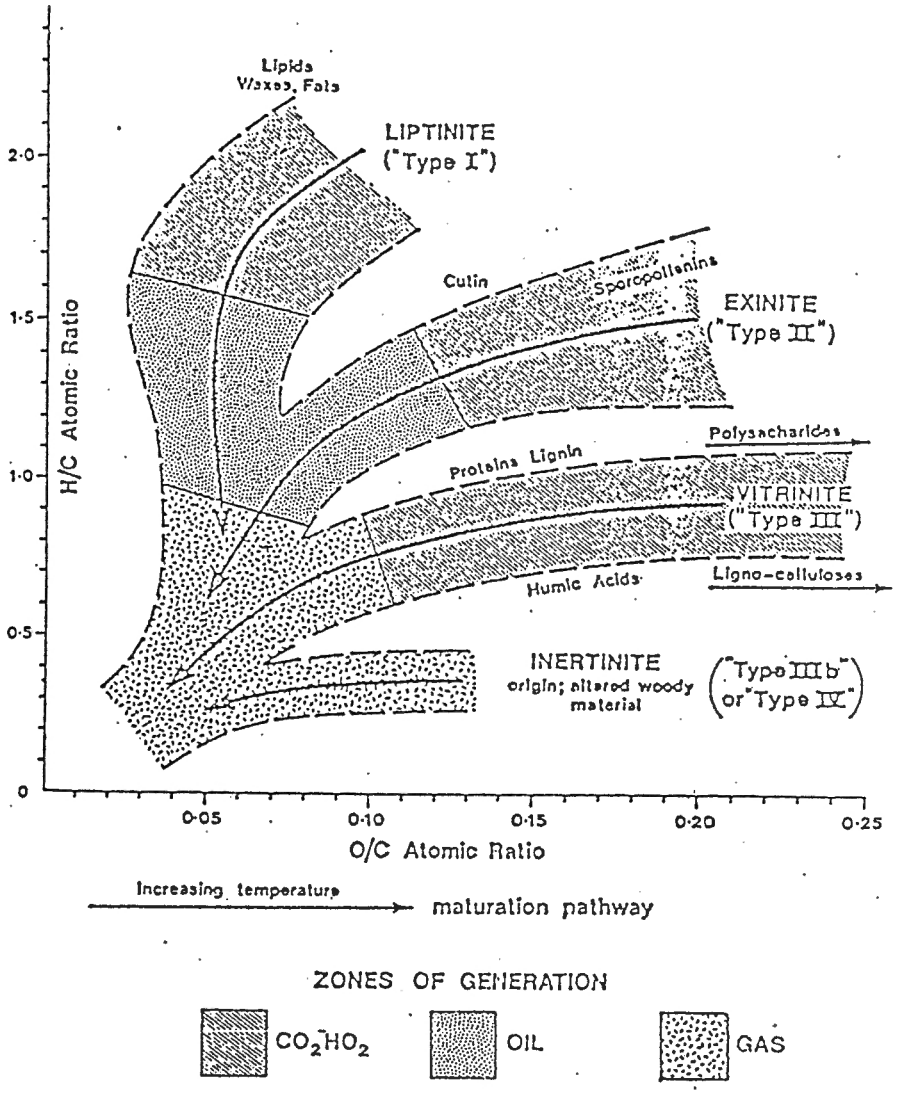

FIGURE 22

Hydrocarbon Model Based on Atomic H/C Ratio
(After Tissot, 1974; Brooks, 1981)

FIGURE 24

Effect of Increasing Temperature on Kerogen Type
(After Hunt, 1979)

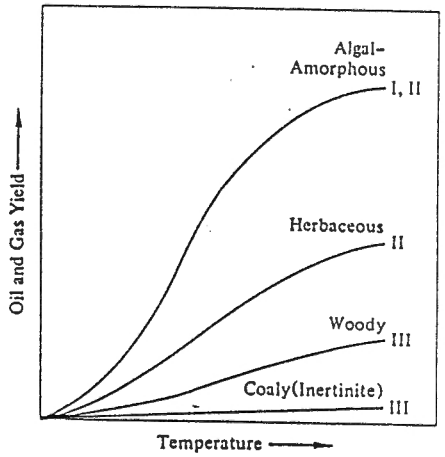

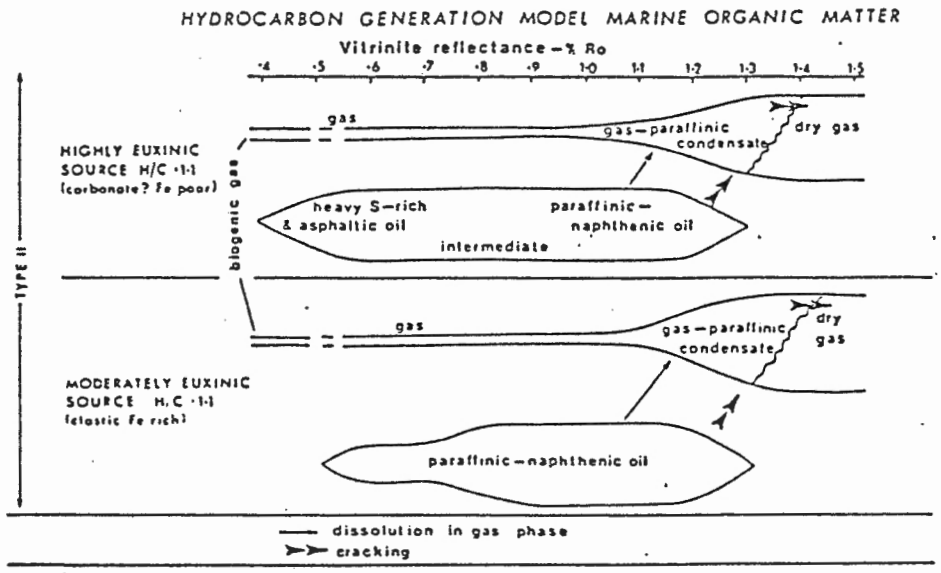

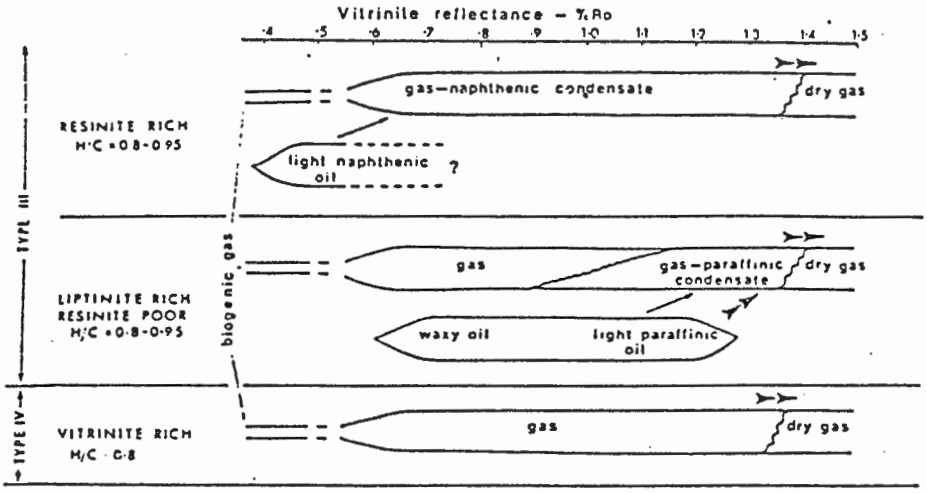

FIGURE 23

Revised Oil and Gas Generation Model
(After Powell and Snowdon, 1983)

	SAPROPELIC			HUMIC	
KEROGEN (by transmitted light)	Algal	Amorphous	Herbaceous	Woody	Coaly (Inertinite)
COAL MACERALS (by reflected light)	Liptinite (Exinite)			Vitrinite	Inertinite
	Alginite	Amorphous	Sporinite Cutinite Resinite	Telinite Collinite	Fusinite Micrinite Sclerotinite
KEROGEN (by evolutionary pathway)	Types I, II		Type II	Type III	Type III
H/C	1.7–0.3		1.4–0.3	1.0–0.3	0.45–0.3
O/C	0.1–0.02		0.2–0.02	0.4–0.02	0.3–0.02
ORGANIC SOURCE	Marine and lacustrine		Terrestrial	Terrestrial	Terrestrial and recycled
FOSSIL FUELS	Predominately oil Oil shales, boghead and cannel coals		Oil and gas	Predominately gas Humic coals	No oil, trace of gas

TABLE 9

Classification of Organic Matter in Sedimentary Rocks
(After Hunt, 1979)

material (Powell and Snowdon, 1983). Similar inferrences and results were drawn from the quality of organic matter found in the Upper Cretaceous.

The organic matter from Lower Cretaceous sediments is approximately evenly divided between herbaceous and woody particles with only minor amounts of amorphous and coaly material (Table 8). These are the characteristics of Type III which would suggest a dominantly terrestrial source (Powell and Snowdon, 1983). A few analyses of organic matter from the Middle Jurassic, Lower Jurassic and Triassic indicate similar environments.

Both Type II and Type III organic material is indicated by analyses of different strata in the Upper Jurassic. This suggests that marine and non-marine influences alternately dominated the paleoenvironment during the period. It may be that during the Jurassic this area alternated between being wholly marine and wholly non-marine (i.e. terrestrial). However, it seems more likely that the depositional environment was more or less marine, but that it was close enough to the continental margin to receive periodic influxes of dominantly terrestrial material.

4. Maturation

Maturation of organic material in buried sediments can be measured by a variety of techniques, such as vitrinite reflectance in oil ($\%R_o$), thermal alteration index (TAI), and time-temperature index (TTI). Because maturation is essentially a measure of the duration and amount of heating, other factors such as age, depth, and temperature can individually give only a partial and perhaps misleading measure of maturation.

All available information on R_o, TAI, and TTI is shown appropriately in Table 8. Vitrinite reflectance values range between 0.30 and 0.63 in the Tertiary, 0.30 and 0.69 in the Lower Cretaceous, and between 0.50 and 1.5 in the Upper Jurassic. Thermal alteration indices range between 1 and 2$^-$ in the

Tertiary, 1^+ and 2 in the Upper Cretaceous, 1^+ and 3^- in the Lower Cretaceous and between 1^+ and 2^- in the Upper Jurassic. Time-temperature indices range between 0.16 and 6.0 in the Tertiary, 0.49 and 12 in the Upper Cretaceous, 0.4 and 50 in the Lower Cretaceous and between 0.4 and 81 in the Upper Jurassic.

Each of these series of values shows a progressive increase in their range with increasing age. This is particularly evident in the sequence of values stated for the upper end of each range. In general, R_o and TTI values appear to be more sensitive and more useful as a gauge of maturation.

5. Geology

Some indication of the lithology has been shown where possible (Table 8). This information has been taken mainly from interpretations by Canadian Stratigraphic Services Ltd.

In general, the zones with favourable geochemical information in the Tertiary are composed of shales, with minor siltstone and limestone. Similarly, the Lower Cretaceous is mainly sandstone, with minor siltstone and shale. There are also a few coal seams and, in the lower parts, the section has been penetrated by at least one salt diapir (at Adolphus 2K-41). Sandstones with a few limestone beds dominate the Upper Jurassic; coal seams are almost always present with some siltstones and shale. Salt overlain by anhydrite and dolomite occur in the lowermost Jurassic (e.g. at Spoonbill and Cormorant).

B. Source of Hydrocarbons

There is considerable evidence that Upper Jurassic rocks have been the major source of all the hydrocarbons discovered to date in both Upper Jurassic and Lower Cretaceous reservoirs.

1. The Lower Cretaceous lies immediately above the Upper Jurassic.
2. The flow rates for oil and gas in the Lower Cretaceous are very similar to those in the Upper Jurassic.

3. Some of the highest flow rates in the Lower Cretaceous occur in horizons which have R_o values indicating immature sediments.

4. Most of the R_o values for the Lower Cretaceous are less than 0.5, which is generally considered to be the minimum necessary to form oil.

5. TOC values in Upper Jurassic strata have a higher range than that for Upper Cretaceous strata.

6. The Lower Cretaceous contains dominantly Type III organic matter indicating terrigenous material and therefore a gas prone hydrocarbon potential which is in contrast to the relatively low GOR values for the Lower Cretaceous. The Upper Jurassic, on the other hand, contains significant amounts of Type II organic matter, that which has the highest potential for generating oil.

7. In at least six wells the top of the overpressure zone coincides with the Verrill Canyon shales at the top of the Upper Jurassic. These shales probably act as an impermeable barrier to any upward migrating hydrocarbons. Nevertheless, significant hydrocarbons have found conduits and leaked upwards into the Lower Cretaceous.

8. Powell (1984) determined the composition of gasoline-range compounds in Lower Cretaceous hydrocarbons of Hebron, Ben Nevis, South Tempest, Adolphus D-50, 2K-41, and Hibernia K-18, O-35, and P-15 wells to ascertain their maturity. Because the maturity of these hydrocarbons was considerably higher than the maturity of the reservoir rocks, he concluded that the hydrocarbon fluids had migrated from more mature source rocks.

9. From RockEval analyses of organic-rich intervals in Hibernia P-15, O-35, and K-18, Powell (1984) showed that the kerogen from Upper Jurassic rocks gave higher yields than that from Lower Cretaceous rocks.

C. Timing of Hydrocarbon Generation

Because of the great thickness of Lower Cretaceous rocks in the depocentre of the Basin, oil generation in the Upper Jurassic could have started here as early as late Cretaceous. The potential for loss of hydrocarbons from the Basin during the period of the Avalon unconformity is therefore considerable (Powell, 1984). However, if an R_o of 0.5%, or the equivalent TTI of 2.0, is accepted as a minimum value for the generation of oil, maturation calculations of this study indicate that no part of the Upper Jurassic drilled to date was mature enough to have generated oil before the beginning of the Tertiary. Further, the oil currently in reservoirs beneath the Avalon unconformity shows no evidence of extensive biodegradation (Powell, 1984). It is therefore concluded that loss of hydrocarbons during the period of the Avalon unconformity was negligible.

D. Summary

The generation of hydrocarbon products in the East Newfoundland Basin can be summarized by the following statements.

1. The occurrence of oil and gas is confined almost entirely to the rocks of the Lower Cretaceous and Upper Jurassic, both having good reservoir characteristics. The Lower Cretaceous is generally a light-brown sandstone with minor siltstone and shale. Organic material trapped in these rocks is Type III indicative of terrigenous sources and is at best only marginally mature. The oil and gas occurs most commonly in the uppermost sandstone beds lying beneath a section of shale or, in a few places, limestone. The Upper Jurassic is mainly a light-gray sandstone and oolitic limestone with some siltstone, shale and coal. Type II and Type III organic matter, indicative of both marine and non-marine sources, has a maturity within the generally accepted oil window of R_o = 0.5 to 1.3%.

2. The Upper Jurassic is the source rock for the hydrocarbons which now occur in both the Upper Jurassic and Lower Cretaceous reservoirs. These hydrocarbons have migrated to the Upper Cretaceous since the beginning of the Tertiary.

3. Although considerable organic matter occurs in the Tertiary, especially in the Eocene, only minor stains have been discovered. Measured vitrinite reflectances on organic matter trapped in these sediments (mainly shales) indicate that it is too immature for hydrocarbon generation.

4. In two wells (Spoonbill and Cormorant) oil and gas shows occur associated with salt beds in Lower Jurassic rocks where the oil may be indigenous. Significant recovery of oil occurred from a drill stem test in the Upper Cretaceous of the Adolphus 2K-41 well. This occurrence may be a result of leakage from nearby source rocks (i.e. Upper Jurassic) during the fissuring and fracturing commonly developed around piercement salt diapirs.

VII. IMPLICATIONS FOR FUTURE EXPLORATION

1. Because no part of the Upper Jurassic drilled to date was mature enough to have generated hydrocarbons before the beginning of the Tertiary, any post-Mesozoic structures, therefore, become entirely available for trapping hydrocarbons subsequently generated in the Basin.
2. Although the Tertiary rocks contain considerable marine (i.e. Type II) organic material, they are not mature enough in the study area to generate significant oil or gas. However, these rocks thicken to the north and northeast so it may have been possible for some of the deeper parts to have reached sufficient maturity to generate some hydrocarbons. Unfortunately, the Tertiary here is dominantly shale which does not make a good reservoir rock.
3. Similarly, some hydrocarbons may have been generated in some of the deeper Lower Cretaceous rocks. These indigenous hydrocarbons would probably be gas because of the predominantly Type III organic material in these rocks.

VIII. CONCLUSIONS AND RECOMMENDATIONS

A hydrocarbon generation model has been devised for the East Newfoundland Basin in offshore eastern Canada. The model is based on correlations of observed hydrocarbon occurrences, quantity and type of organic material, degree of organic maturity and geology. A synthesis of the data indicates that copious quantities of hydrocarbons have been generated in Upper Jurassic sediments since the beginning of the Tertiary, and that significant amounts of these fluids have since migrated into the overlying Lower Cretaceous. The Tertiary rocks, while they contain significant amounts of Type II (i.e. marine) organic material, are shales and claystones with little potential as a petroleum reservoir. The low maturity of the kerogen in these rocks may, however, give way to more profound catagenesis towards the northeast where the Tertiary sediments thicken and become deeper. A few salt diapirs in the Basin have local hydrocarbon accumulations.

The following suggestions or recommendations are made concerning aspects of this study.

1. The Lopatin method yields a good estimate of the present organic maturity and, along with vitrinite reflectance measurements, forms an important part of the hydrocarbon generation model. However, results from the method would be much more realistic if the influence of compaction, periodic uplift and varying heat flow could be more accurately determined.
2. Greater diligence in recording times and temperatures during logging runs would provide a more accurate and complete basis for calculating geothermal gradients and temperature grids.
3. Because it is becoming increasingly evident that the type of organic material greatly influences the yield, timing and nature of the hydro-

carbons generated, a more thorough and detailed analysis of the kerogen is required. Some of this might be done in conjunction with vitrinite reflectance measurements. (TAI values were not particularly useful for this study.)

4. Much more confidence is needed in the biostratigraphic age determinations carried out on each well. For example, determinations of depth to a given horizon made by different workers on material from the same well often vary as much as 1500 to 2000 m, and differences of 1000 m are common. These discrepencies presented the greatest difficulty in using the TTI method for assessing maturity.

5. Because the East Newfoundland Basin covers a relatively large area with rather sparse information (few wells), it may be worthwhile to construct a similar hydrocarbon generation model for the Hibernia field alone. Well density is considerably greater than for the Basin as a whole and the proven economic potential has heightened interest in this particular area. Such a study would have closer controls on each factor involved and might provide results having both academic and economic benefit.

IX. REFERENCES

Arthur, K. R., Cole, D. R., Henderson, G. G. L., and Kushnir, D. W., 1982, Geology of the Hibernia discovery, in The Deliberate Search For the Subtle trap, Halbou, M. T. (ed.): A.A.P.G. Mem. 32, pp. 181-196.

Benteau, R. I., and Sheppard, M. G., 1982, Hibernia — a petrophysical and geological review: J. Can. Pet. Tech., v. 22, no. 3, pp. 59-72.

Boldizsar, T., 1968, Geothermal data from the Vienna Basin: J. Geophy. Res., v. 73, no. 2, pp. 613-618.

Brooks, J., 1981, Organic maturation of sedimentary organic matter and petroleum exploration — a review, in Organic Maturation Studies and Fossil Fuel Exploration, J. Brooks, ed., Academic press, pp. 1-37.

Bujak, J. P., Barss, M. S., and Williams, G. L., 1977a, Offshore East Canada's organic type and color and hydrocarbon potential, Part I: Oil and Gas J., v. 75, pp. 198-202.

Bujak, J. P., Barss, M. S., and Williams, G. L., 1977b, Organic type and color and hydrocarbon potential, Part II: Oil and Gas J., v. 75, no. 15, pp. 96

Burgess, J. D., 1974, Microscopic examination of kerogen in petroleum exploration: Geol. Soc. Am., Spec. Paper 153, pp. 19-30.

Cercone, K. R., 1984, Thermal history of Michigan Basin: A.A.P.G. Bull., v. 68, no. 2, pp. 130-136.

Dow, W. G., 1977, Kerogen studies and geological interpretations: J. Geochem. Expl., v. 7, pp. 79-99.

Dowdle, W. L., and Cobb, W. M., 1975, Static formation temperature from well logs — an empirical method: J. Pet. Tech., Nov., pp. 1326-1330.

Evans, T. R., and Coleman, N. C., 1974, North Sea geothermal gradients: Nature, v. 247, pp. 28-30.

Fertl, W. H., 1978, How subsurface temperature affects formation evaluation: Oil and Gas J., July, pp. 54-62.

Fertl, W. H., and Wichmann, P. A., 1977, How to determine static BHT from well log data: World Oil, Jan, pp. 105-106.

Hardy, I. A., and Jackson, A. E., 1980, A compilation of geochemical data: east coast exploratory wells: G.S.C., O.F.R. 694.

Hood, A., Gutjahr, C. C. M., and Heacock, R. L., 1975, Organic metamorphism and the generation of petroleum: A.A.P.G. Bull, v. 59, pp. 986-996.

Hunt, J. M., 1979, Petroleum Geochemistry and Geology, W. H. Freeman and Co., Publ., 617 p.

Hyndman, R. D., Jessop, A. M., Judge, A. S., and Rankin, D. S., 1979, Heat flow in the Maritime Provinces of Canada: Can. J. Earth Sci., v. 16, pp. 1154-1165.

Issler, D. R., 1982, Calculation of organic maturation levels from downhole temperatures/burial history curves, Scotian Shelf: B.Sc. thesis, Univ. of Waterloo, 129 p.

Issler, D. R., 1984, Calculation of organic maturation levels for offshore eastern Canada — implications for general application of Lopatin's method: Can. J. Earth Sci., v. 21, pp. 477-488.

Jones, F. W., and Lam, H. L., 1979, An investigation of geothermal energy resources of Alberta: Alberta/Canada Energy Resources Research Fund Contract U-8 (Jones), 12-month report, 69 p.

Lopatin, N. V., 1969, Principle phase of crude oil formation (in Russian): Akad. Nauk SSSR Izv., Ser. Geol. 34, no. 5, pp. 69-77.

Lopatin, N. V., 1971, Temperature and geologic time as factors in coalification (in Russian): Akad. Nauk SSSR Izv., Ser. Geol., no. 3, pp. 95-106.

Palmer, A. R., 1983, The decade of North American geology: 1983 geologic time scale: Geology, v. 11, pp. 503-504.

Perrier, R., and Quiblier, J., 1974, Thickness changes in sedimentary layers during compaction history: Methods for quantitative evaluation: A.A.P.G., v. 58, no. 3, pp. 507-520.

Powell, T. G., 1982, Petroleum geochemistry of the Verrill Canyon Formation: A source for Scotian Shelf hydrocarbons: Bull. Can. Pet. Geol., v. 30, no. 2, pp. 167-179.

Powell, T. G., 1984, Hydrocarbon-source relationships Jeanne D'Arc and Avalon Basins, offshore Newfoundland: (pre-print), 14 p.

Powell, T. G., 1984, Paleogeographic implications for the distribution of Upper Jurassic source beds: offshore eastern Canada: (pre-print), 7 p.

Powell, T. G., Creany, S., and Snowdon, L. R., 1982, Limitations of use of petrographic techniques for identification of petroleum source rocks: A.A.P.G., Bull. v. 66, no. 4, pp. 430-435.

Powell, T. G., and Snowdon, L. R., 1983, A composite hydrocarbon generation model: Erdol und Kohle - Erdgas - Petrochemie, v. 36, no. 4, pp. 163-170.

Procter, R. M., Taylor, G. C., and Wade, J. A., 1984, Oil and Gas Resources of Canada, 1983: G.S.C. Paper 83-31, 59 p.

Schenk, P. E., 1971, Southeastern Atlantic Canada, northwestern Africa and continental drift: Can. J. Earth Sci., v. 8, pp. 1218 -1251.

Sclater, J. G., and Christie, P. A. F., 1980, Continental stretching: An explanation of the Post-Mid-Cretaceous subsidence of the central North Sea Basin: J. Geophy. Res., v. 85, pp. 3711-3739.

Tissot, B. P., and Welte, D. H., 1978, Petroleum Formation and Occurrence, Springer-Verlag Publ., 538 p.

Van Hinte, J. E., 1978, Geohistory analysis: Application of micropaleontology in exploration geology: A.A.P.G. Bull., v. 62, no. 2, pp. 201-222.

Waples, D. W., 1980, Time and temperature in petroleum formation: application of Lopatin's method to petroleum exploration: A.A.P.G. Bull., V. 64, pp. 916-926.

X. APPENDIX

A. Procedure for Deriving Geothermal Gradients

The geothermal gradient can be defined as the change in temperature of the earth with increasing depth, and is usually expressed in degrees per unit depth. Geothermal gradients were derived for 23 wells in the East Newfoundland Basin. Corrected bottomhole temperatures (BHT) plotted against depth provided the information for the calculations.

1. Collection of Data

All information and data required for establishing the temperature-depth curve at each well was obtained from the various well log headings for each log run. There were as many an 37 different kinds of logs used in this study with up to 10 of these available for any one well. The following data was used:

Date of Log: The date may vary as much as several days due to the time required to log the hole.

Elevation of Rotary Table: The rotary table or kelly bushing is the datum used for recording depth measurements on the log headings. Because it sits about 30 m or so above mean sea level (MSL), this information is necessary for future calculations of depth.

Water Depth: The depth of water at the well site must be known to calculate the exact location of the sea floor relative to the rotary table.

Depth (to Temperature Measurement): "First Reading" or "Bottom Log Interval" is the depth at which the logging run began and therefore the approximate location of the deepest (and presumably the hottest) temperature measurement.

Temperature: The most reliable temperature is "Temp. Max." (Maximum

Recorded Temperature). Unfortunately, this value has been recorded in only about half the wells. The BHT (Bottomhole Temperature) recorded in the "Remarks" or the BHT recorded for the "Rm" (Resistivity of the mud) was used where no other temperature information was available. In many cases, however, these values were found to be very unreliable.

Time Drilling Stopped: Although reported on only about half of the log headings, this information is vitally important if the temperature corrections are to be calculated to derive static (i.e. equilibrium) temperatures.

Time Circulation Stopped: This information is reported on most log headings.

Time of Temperature Measurement: This information is reported as "Tool on Bottom" or "Tool Last on Bottom".

Time Since Circulation: The time interval between ceasation of circulation and the temperature measurement is reported in about a third of the wells. Unfortunately, many of these values, when they are reported, are not in agreement with those calculated from the previous two pieces of information.

2. Depth Corrections

The sea floor (SF) was used as the datum for all depth caluclations in this study. Since all log depths are measured from the platform at the rotary table, it was therefore necessary to correct the measured depth (MD) for the elevation of the rotary table (RT) or kelly bushing (KB) and the water depth (WD). Thus:

$$\text{Depth from sea floor (SF)} = MD - RT - WD$$

If the values were not already in the metric system, they were converted.

3. Temperature Corrections

Obtaining realistic temperatures was relatively more difficult than depth determinations. The main problem is caused by the fact that circulating drilling muds tend to disrupt (i.e. lower) the local thermal regime at the

bottom of the well. If circulation were to stop, however, the temperature should return to some value not too different from the original or static value given enough time. Unfortunately, this could be a long time —— unrealistically so for the drilling operator.

It is possible, however, to apply a correction to the measured value (usually the maximum temperature for that depth of drilling) to approximate the static temperature. Two related methods have been used to calculate the corrections.

a. By CT Projection: The most accurate correction depends on the availability of the circulation times (CT). The approach is theoretically sound and has been discussed and used by others (Dowdle and Cobb, 1975; Evans and Coleman, 1974; Fertl, 1978; Fertl and Wichmann, 1977; Jones and Lam, 1979; and Issler, 1982, 1984).

To use such a correction, we must know how long the muds were circulated and how long circulation was shut down before the temperature measurements were made. Specifically, it is necessary to know the exact times when drilling stopped (DS), when circulation stopped (CS) and when temperature measurement began (TOB or TLB). From these values, it is easy to calculate circulation time (CT):

$$CT = CS - DS \qquad \text{(in hours)}$$

and time since circulation (TSC):

$$TSC = TLB - CS \qquad \text{(in hours)}$$

If we let CT = t, and TSC = Δt, then the relationship $\Delta t/\Delta t-t$ should tend to unity when Δt (i.e. the time since circulation) is infinitely long.

It is then possible to plot $\Delta t/\Delta t-t$ against the corresponding measured temperature (preferrably Temp. Max., otherwise BHT) on semi-logarithmic paper. Usually the points for any given depth fall on a reasonably straight line. When projected to unity, the line will give a value which theoretically should be the

static temperature. At least two data points are required, but three or more create greater confidence in the projected line and value.

b. By TSC Projection: A second method of calculating the temperature correction has been devised for this report because the data needed to calculate the circulation times were reported for only 8 of the 23 wells. For the other wells to be used in this study, it was necessary to develop some relationship which would give at least approximate static temperatures in the absence of circulation times. After trying several approaches, it was found that, by substituting TSC values (calculated or reported) for the relation $\Delta t/\Delta t-t$ and again plotting the corresponding measured temperatures on semi-logarithmic paper, the data points produce reasonably straight lines. When these lines were projected to TSC = 50 hours, the temperatures were very close to those derived by the CT projection.

To test the validity of this empirical approach, the data from the 8 wells for which there were circulation times reported was plotted using both methods. A correlation of the static temperatures derived by the two methods showed that 85% of the values fell within ±6% of the temperature of a 1:1 correlation (Figure A1). It was therefore assumed that static temperatures derived by the TSC projection for the remaining 16 wells are reasonable approximations of those which would have been derived by the CT projection had the circulation times been known.

B. Geothermal Gradients (Graphs)

1. Gradients for Individual Wells
2. Gradients for Groups of Wells

C. TTI Values for Specified Horizons in Each Well

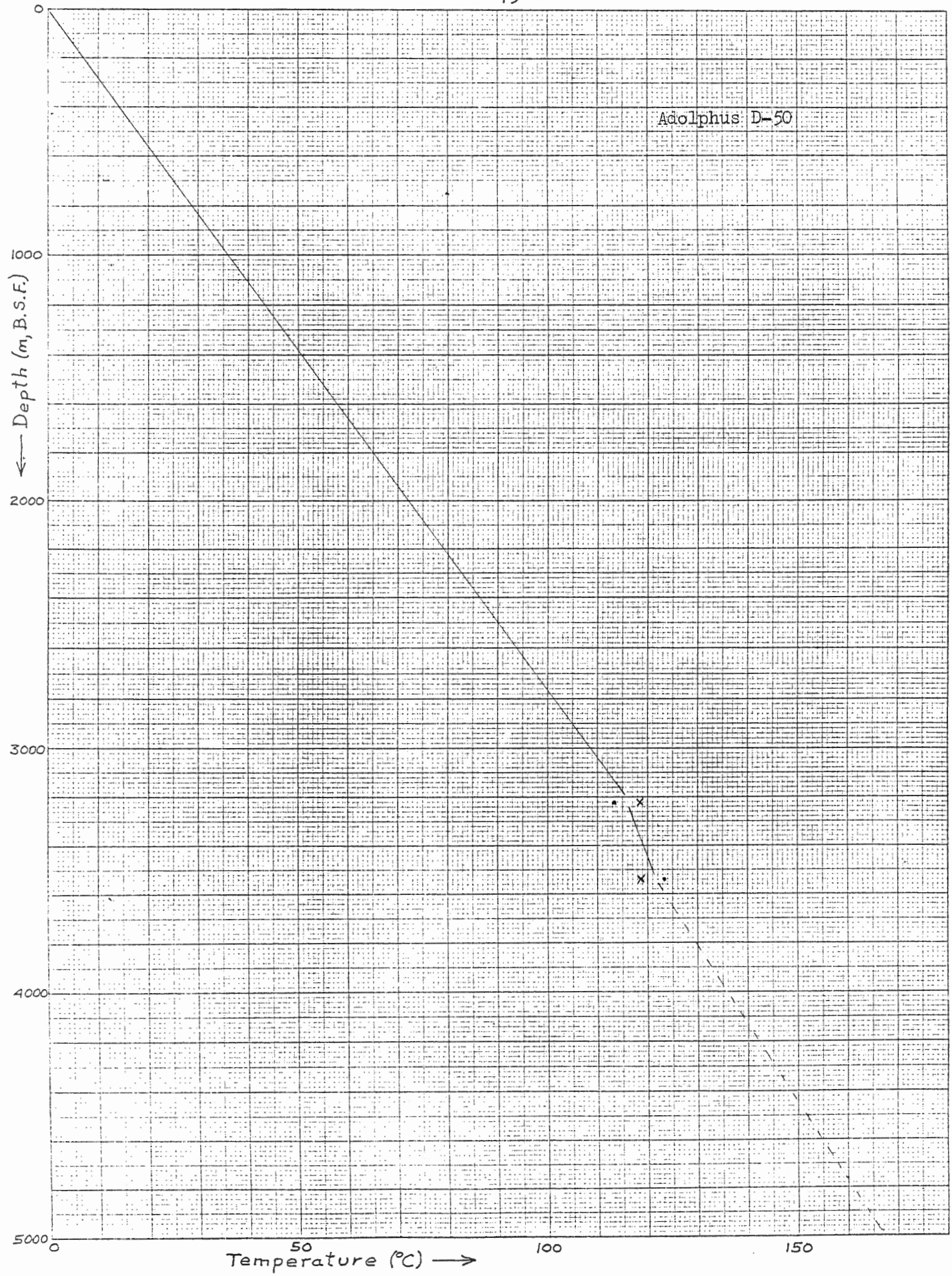
Adolphus D-50
0
1000
2000
3000
4000
5000
Depth (m, B.S.F.)
0
50
100
150
Temperature (°C) ⟶

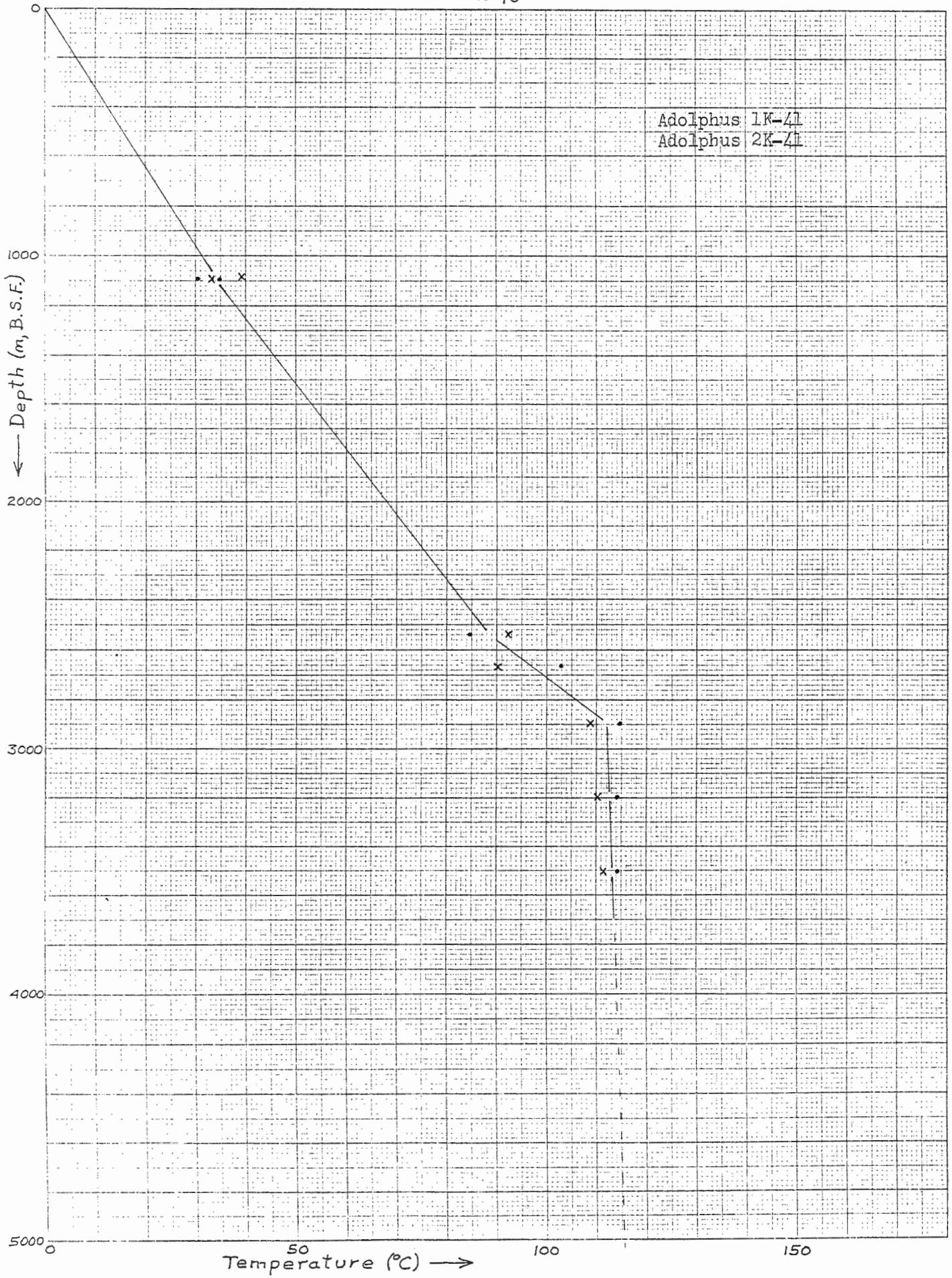
Adolphus 1K-41
Adolphus 2K-41
0
1000
2000
3000
4000
5000
← Depth (m, B.S.F.)
0
50
100
150
Temperature (°C) →

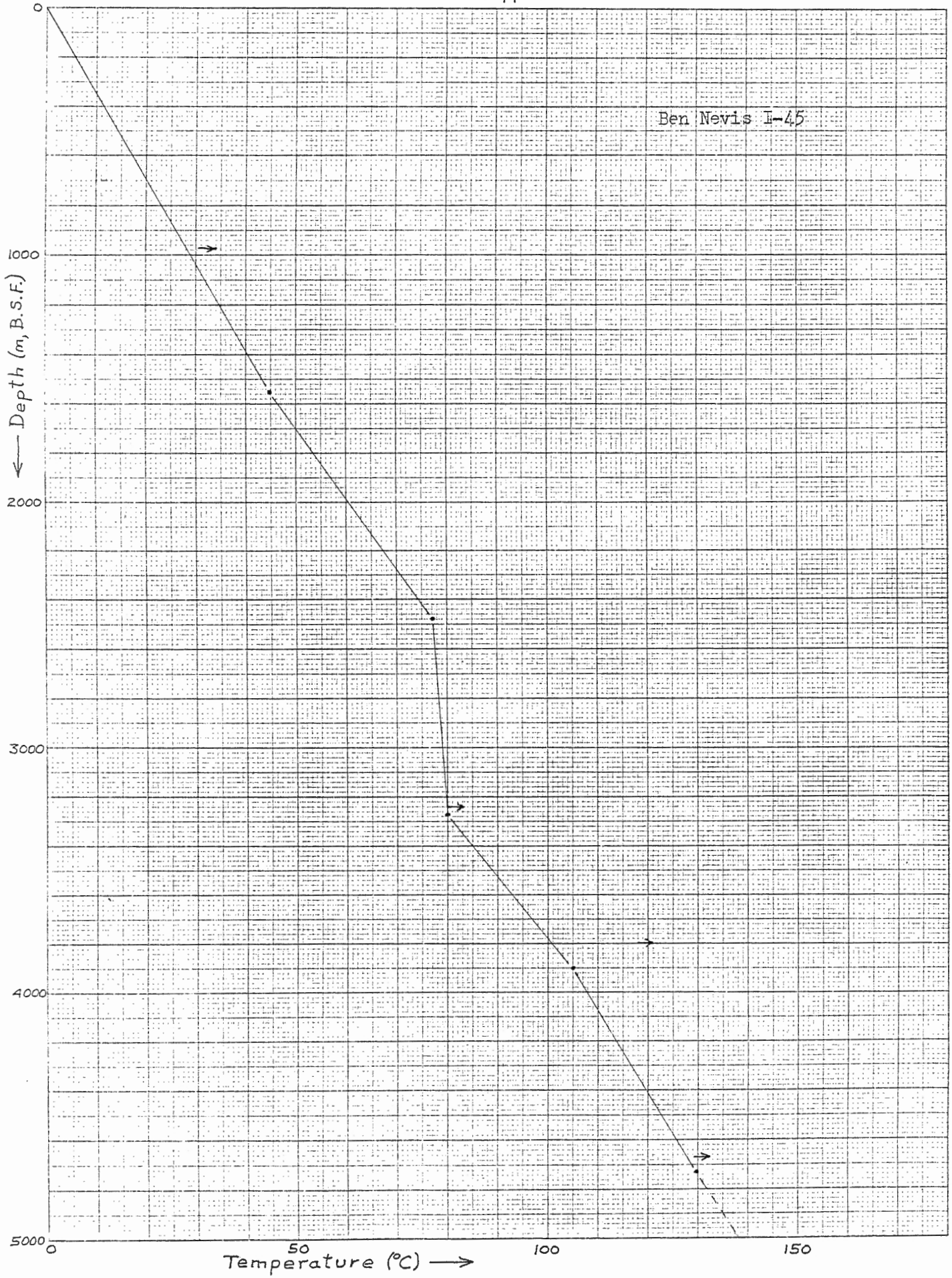
Ben Nevis I-45
0
1000
2000
3000
4000
5000
← Depth (m, B.S.F.)
0
50
100
150
Temperature (°C) →

PLEASE NOTE:

P. 78 is not missing.

It appears to be non-existent and may very well an error in the numbering of pages.

VEUILLEZ NOTER:

P. 78 ne manque pas. Il semblerait que ce soit une erreur dans le numérotage des pages.

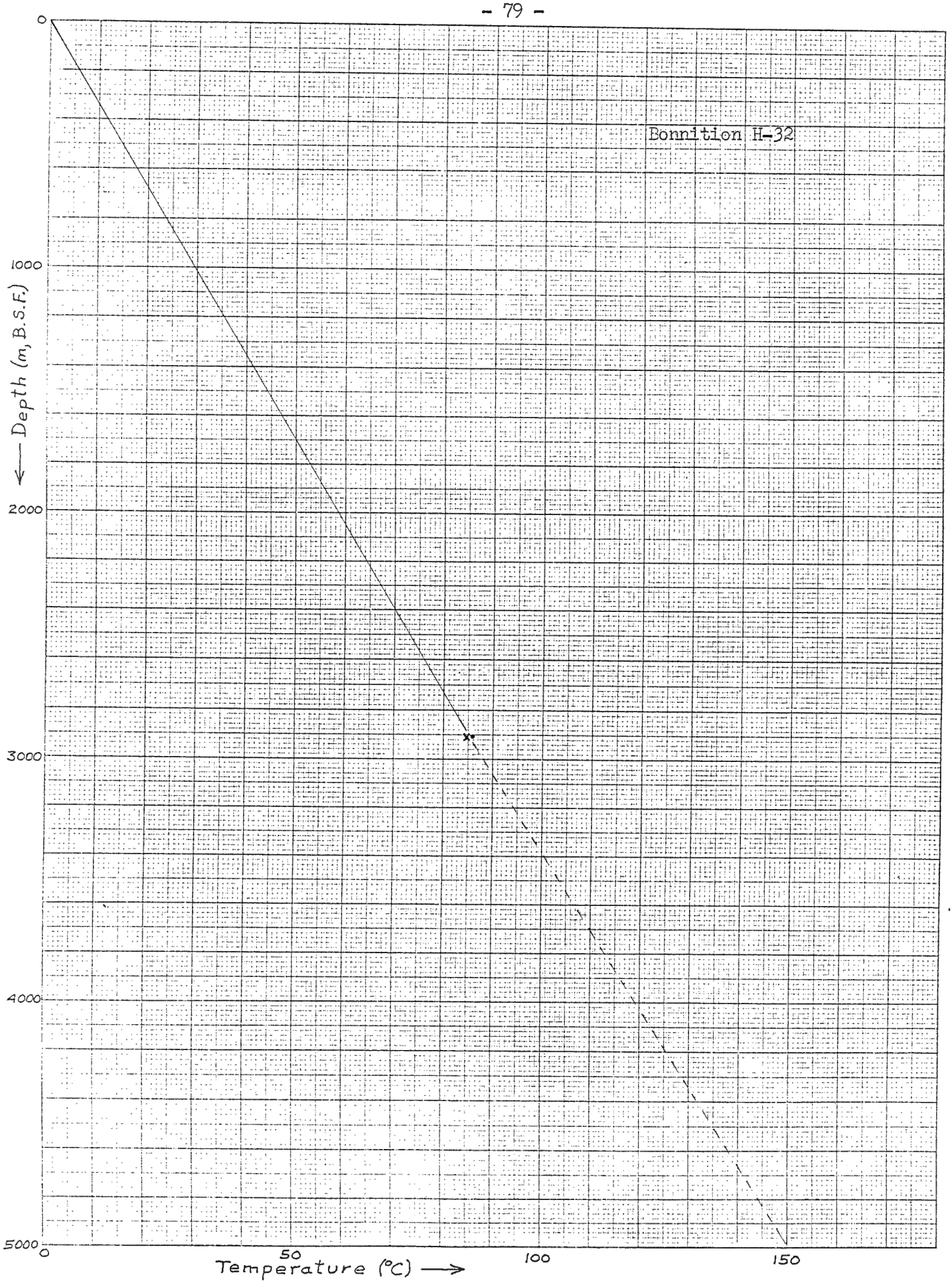
Bonnition H-32
0
1000
2000
3000
4000
5000
← Depth (m, B.S.F.)
0
50
100
150
Temperature (°C) →

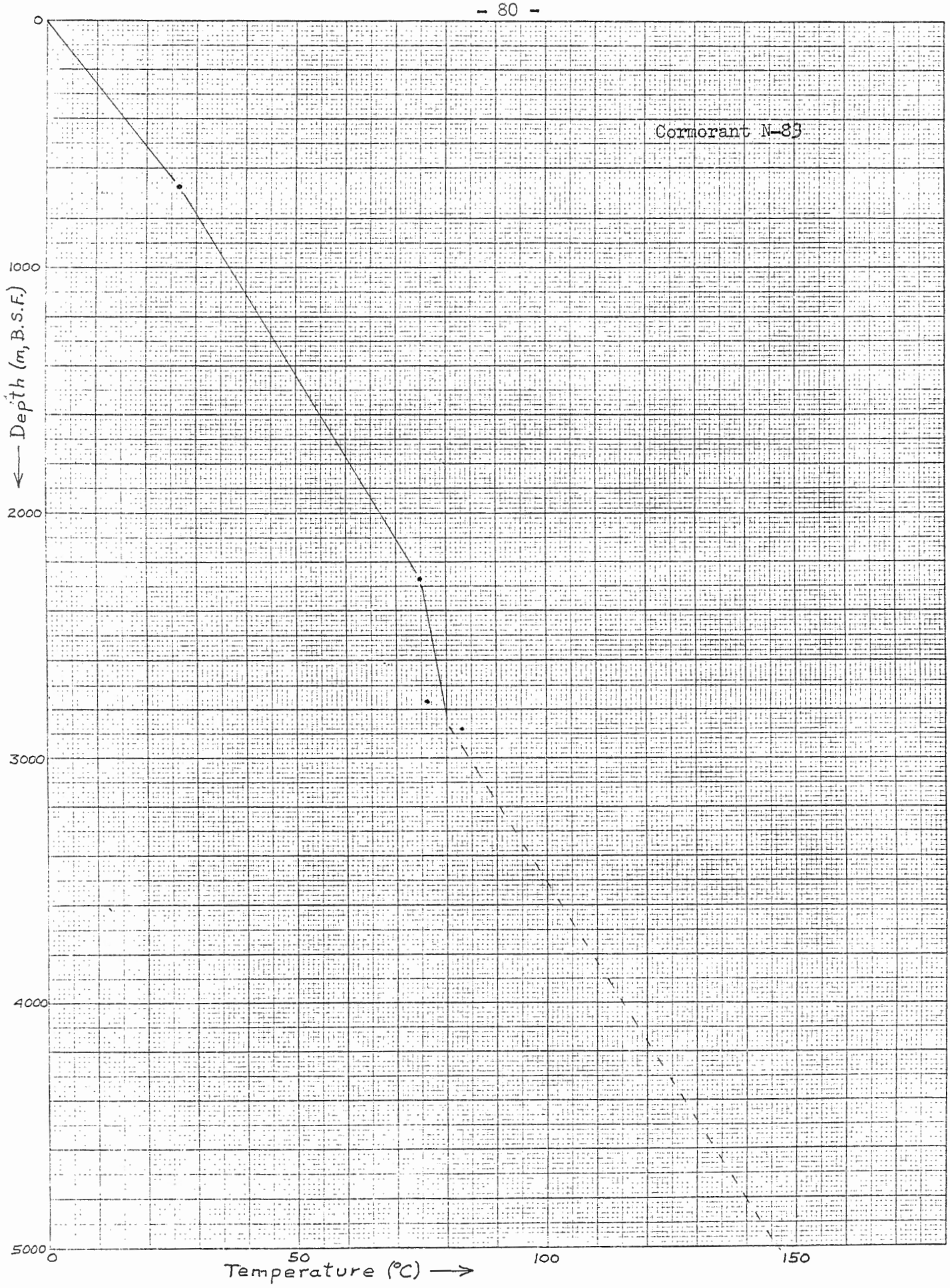
Cormorant N-83
0
1000
2000
3000
4000
5000
← Depth (m, B.S.F.)
0
50
100
150
Temperature (°C) →

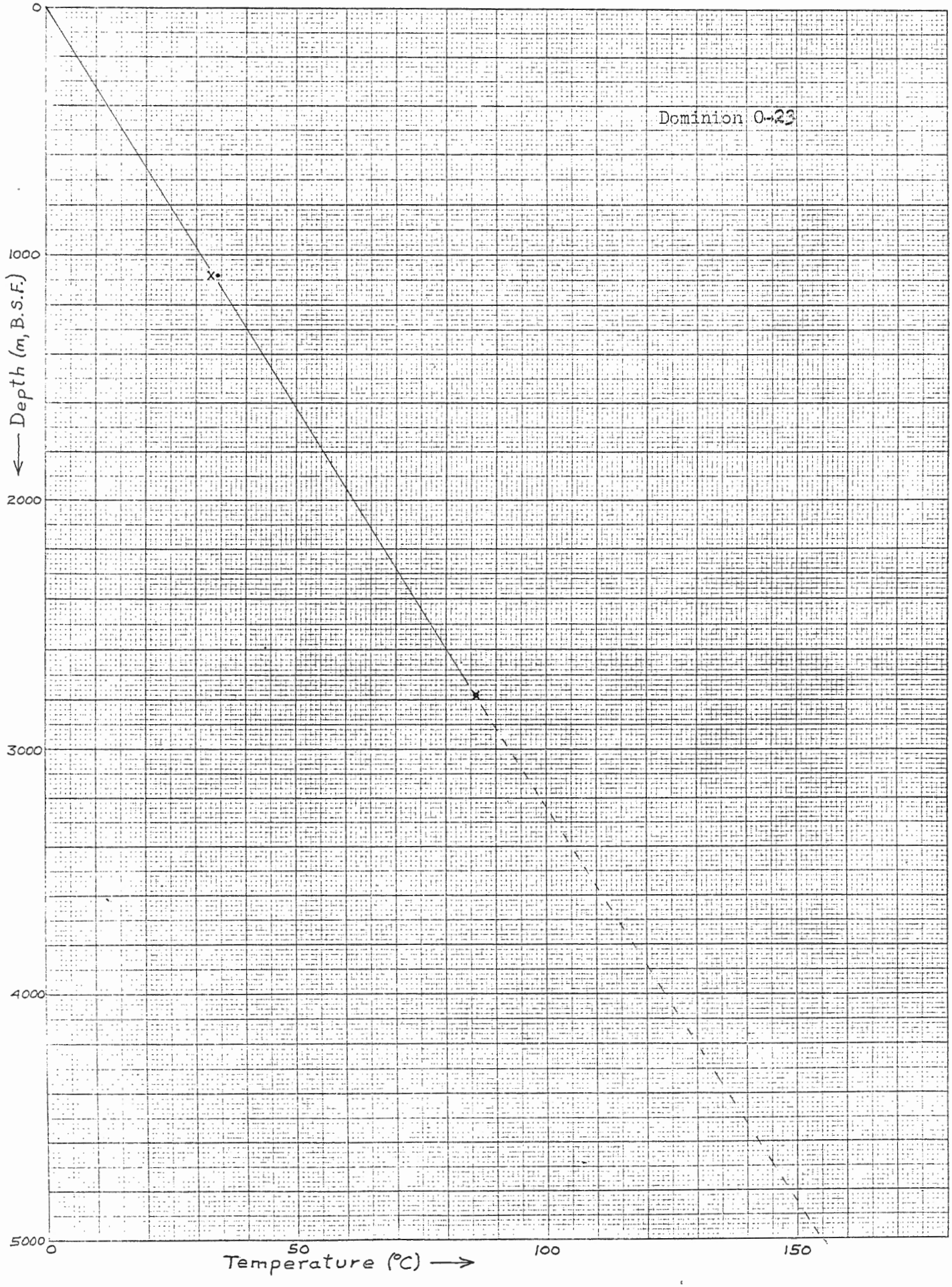
Dominion O-23
0
1000
2000
3000
4000
5000
Depth (m, B.S.F.)
0
50
100
150
Temperature (°C)

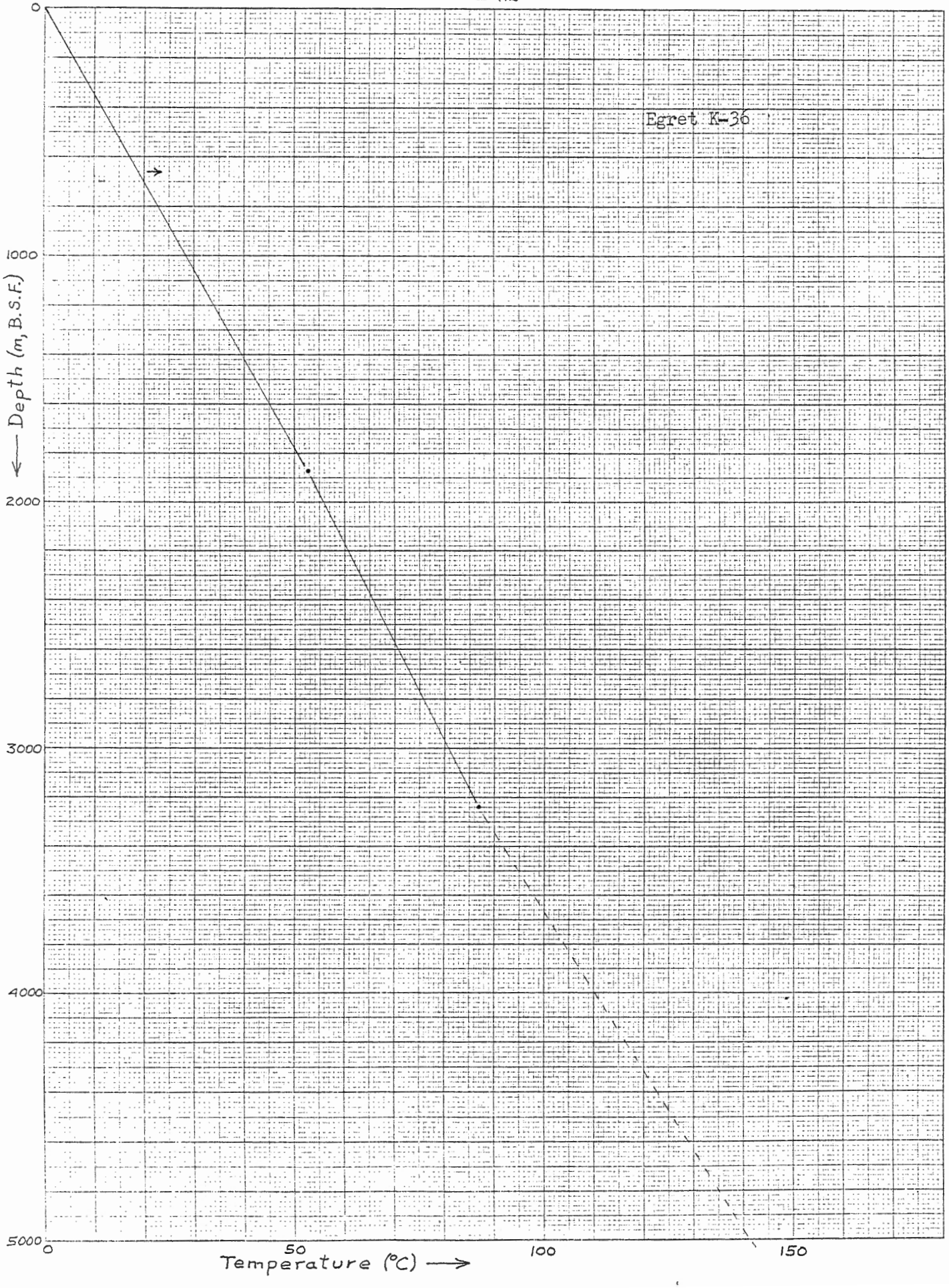
Egret K-36
0
1000
2000
3000
4000
5000
← Depth (m, B.S.F.)
0
50
100
150
Temperature (°C) →

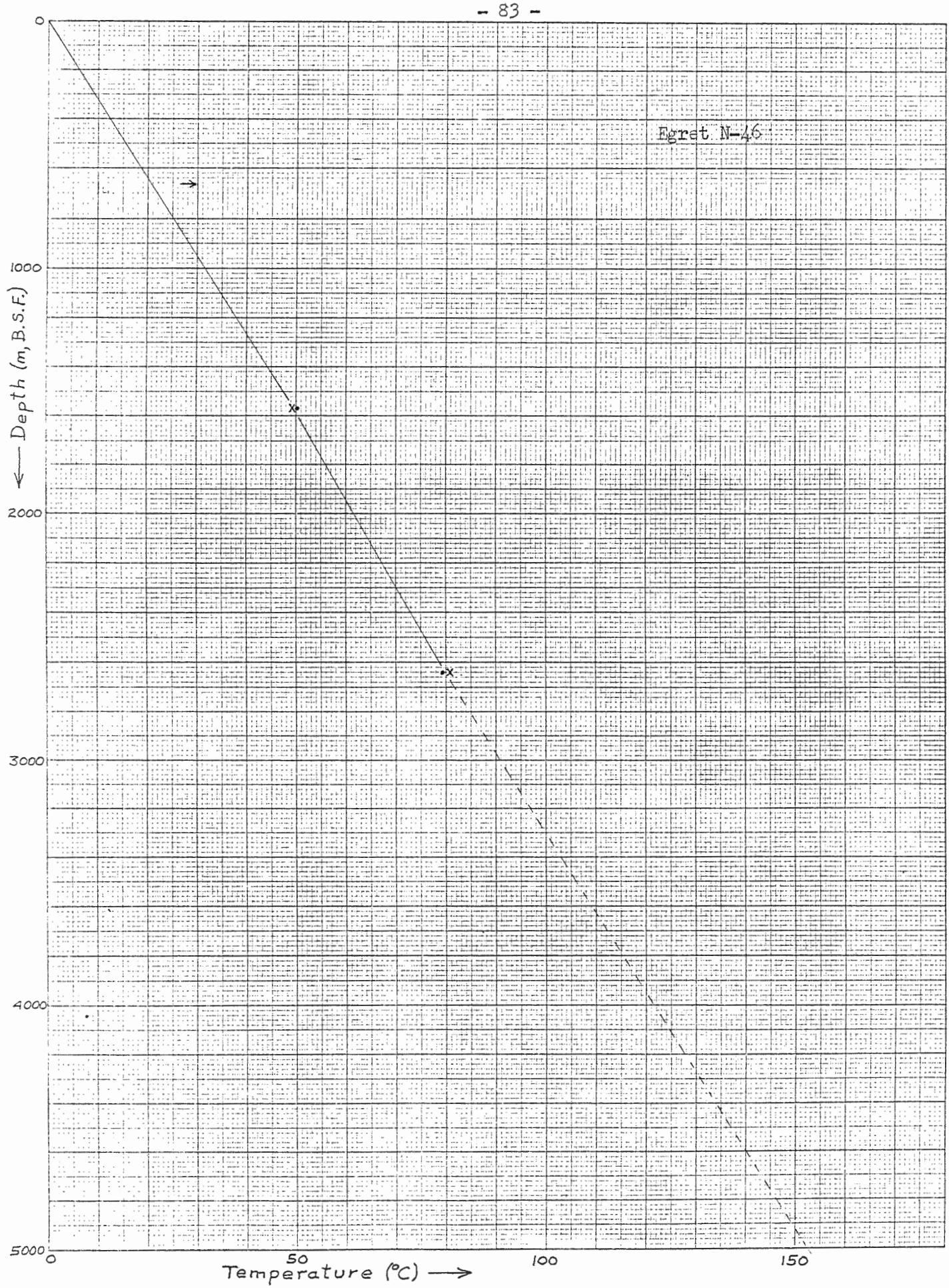
Egret N-46
0
1000
2000
3000
4000
5000
← Depth (m, B.S.F.)
0
50
100
150
Temperature (°C) →

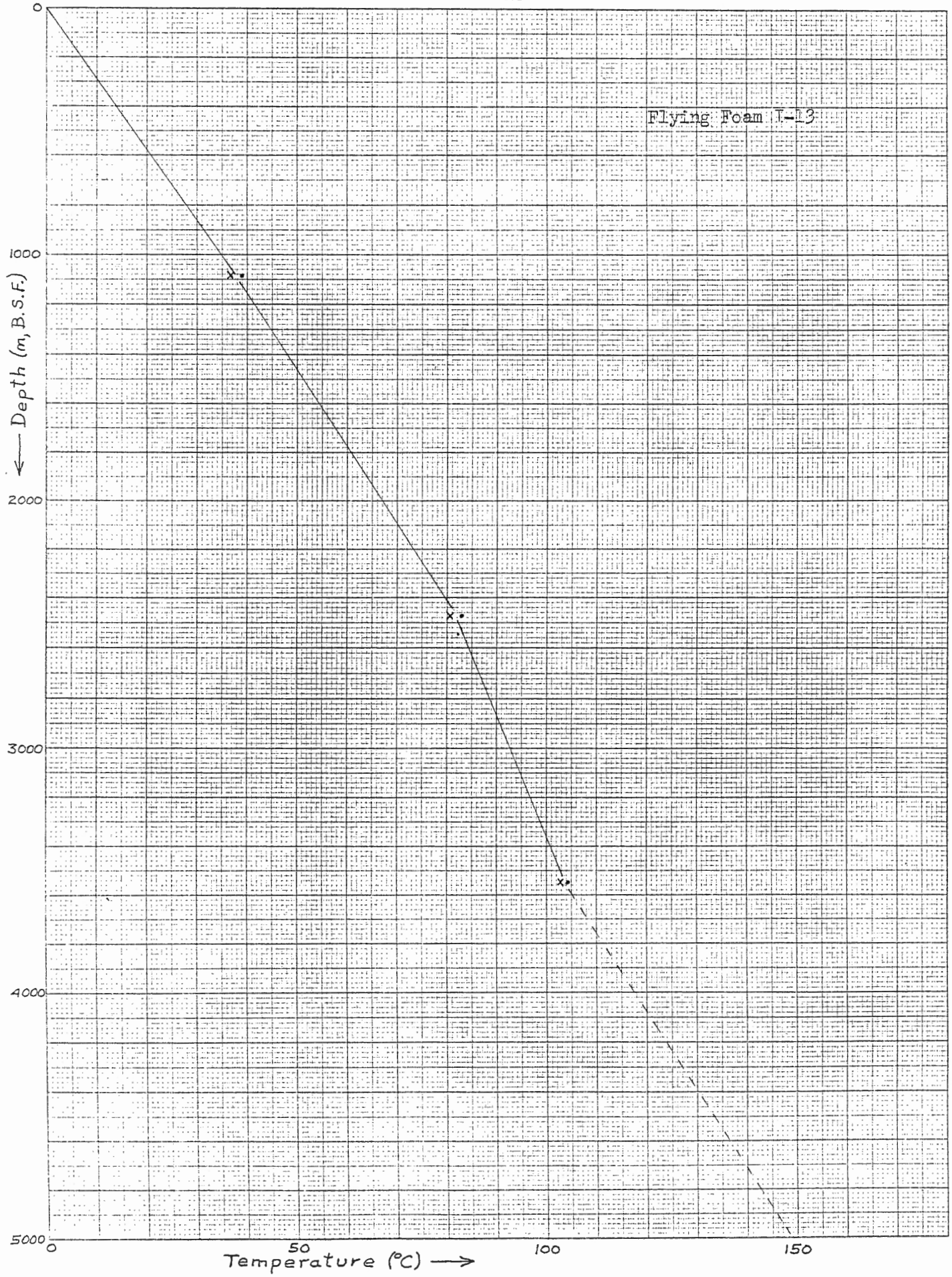
Flying Foam I-13
0
1000
2000
3000
4000
5000
Depth (m, B.S.F.)
0
50
100
150
Temperature (°C) ⟶

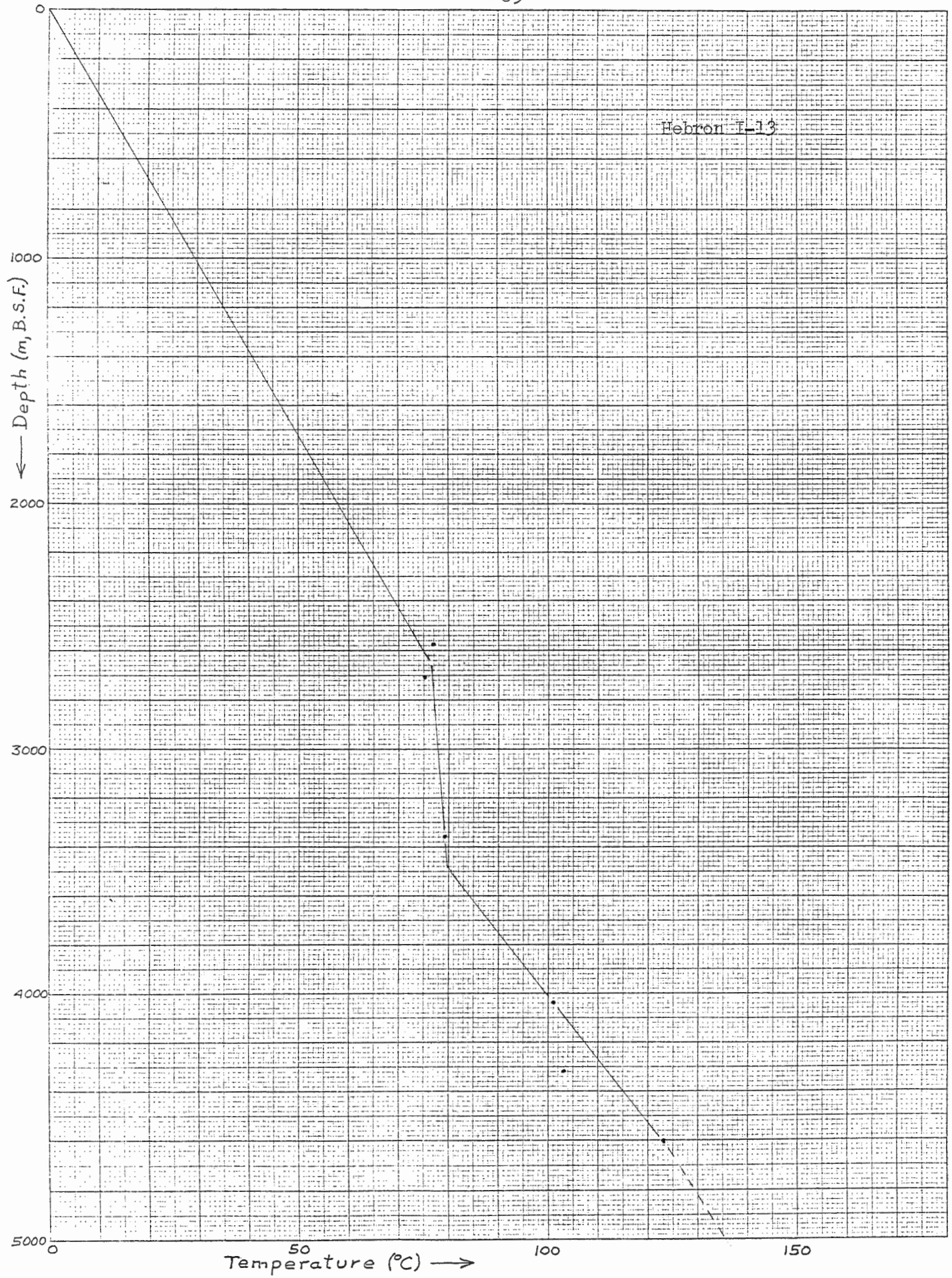
Hebron I-13
0
1000
2000
3000
4000
5000
Depth (m, B.S.F.)
0
50
100
150
Temperature (°C) ⟶

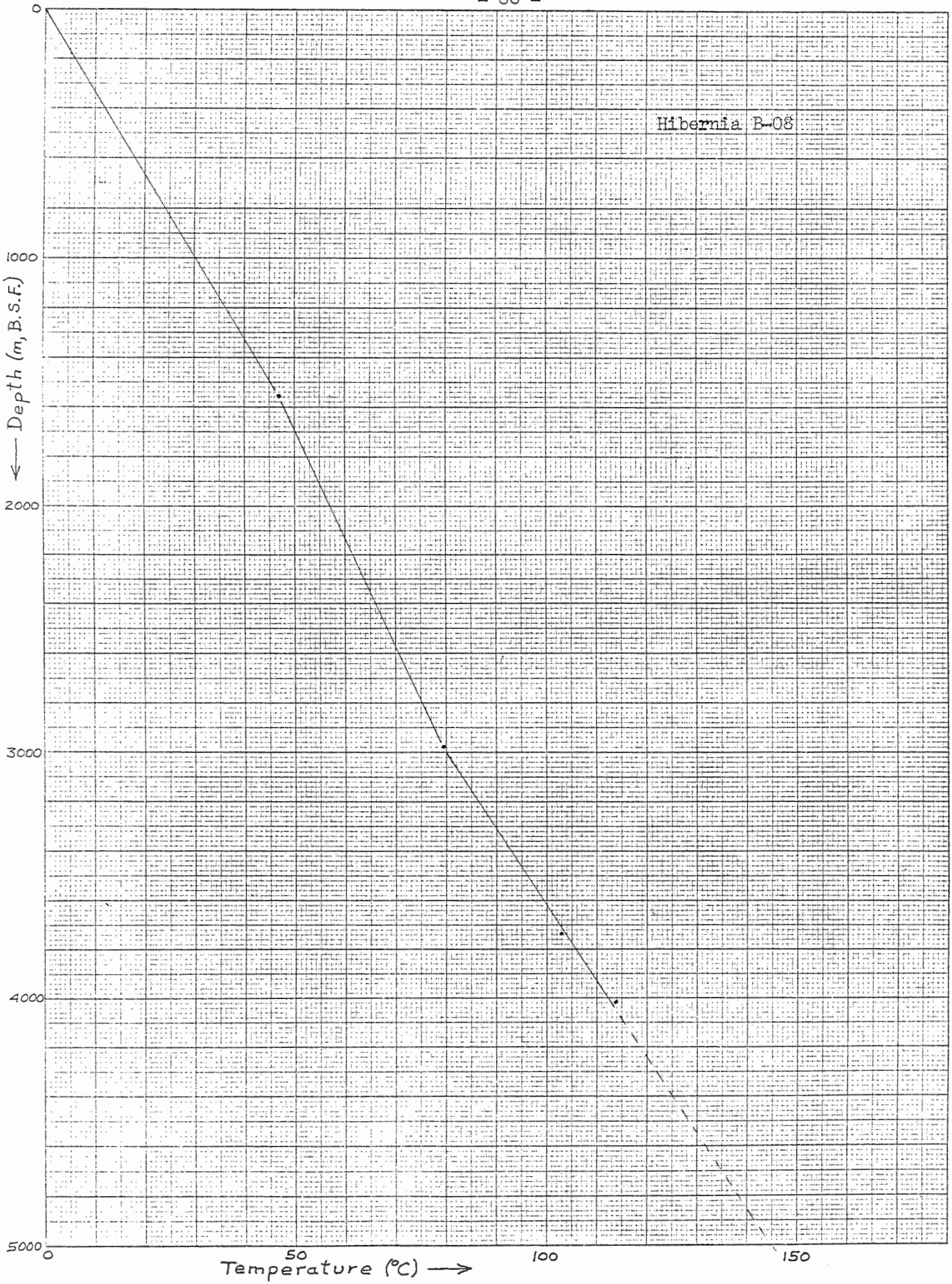
Hibernia B-08
Depth (m, B.S.F.)
0
1000
2000
3000
4000
5000
0
50
100
150
Temperature (°C) ⟶

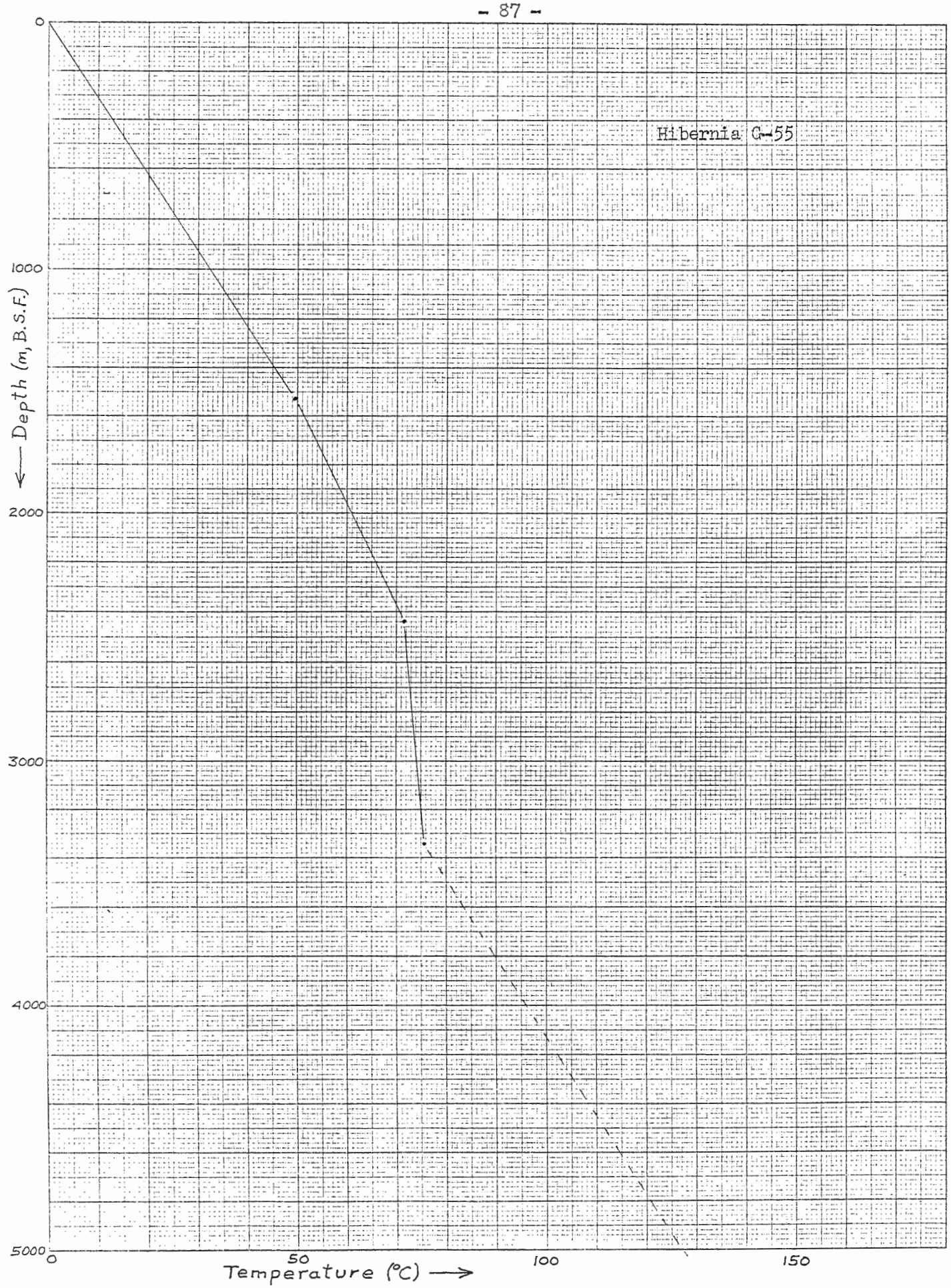
Hibernia G-55
0
1000
2000
3000
4000
5000
← Depth (m, B.S.F.)
0
50
100
150
Temperature (°C) →

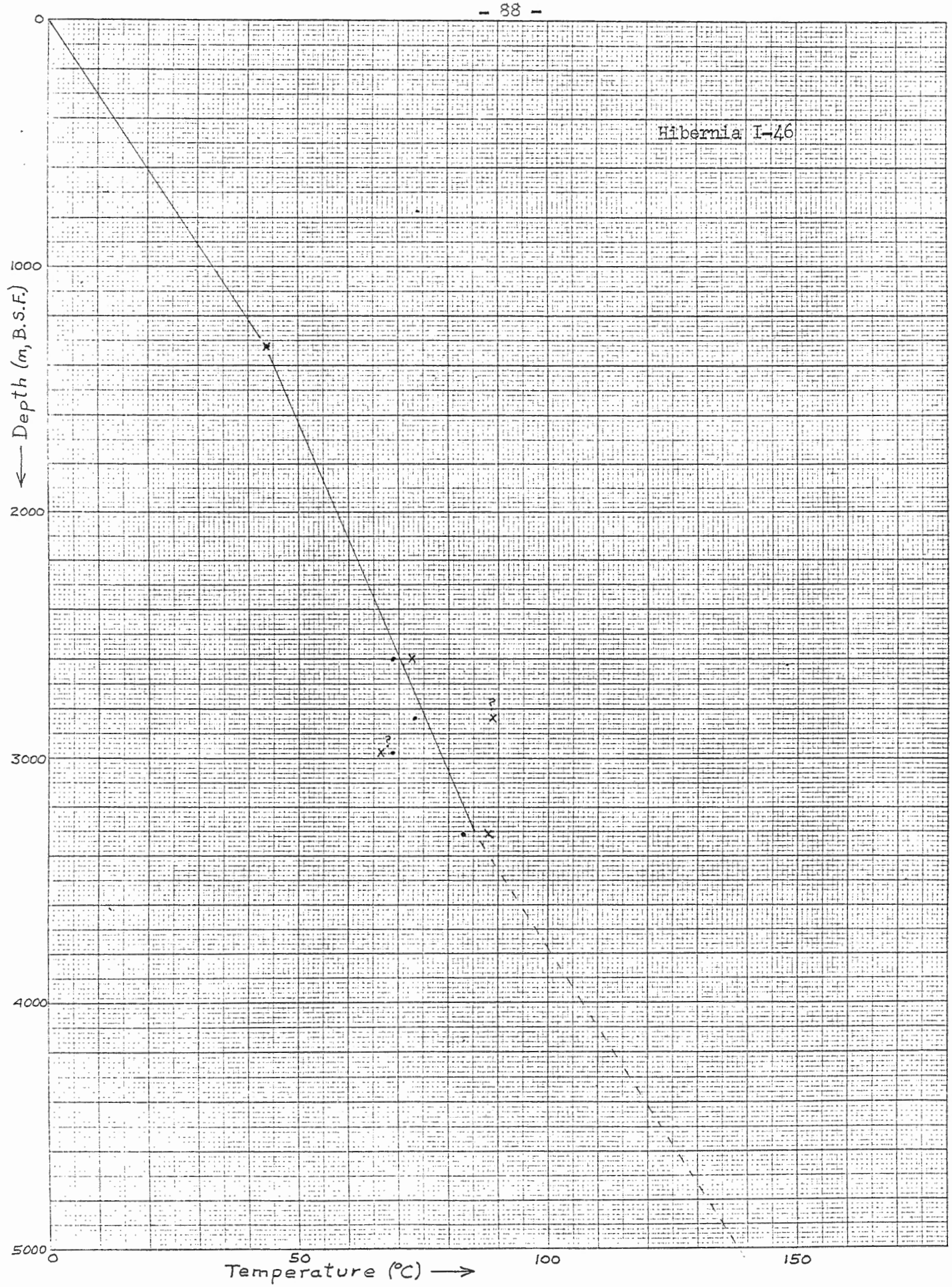
Hibernia I-46
0
1000
2000
3000
4000
5000
← Depth (m, B.S.F.)
0
50
100
150
Temperature (°C) →

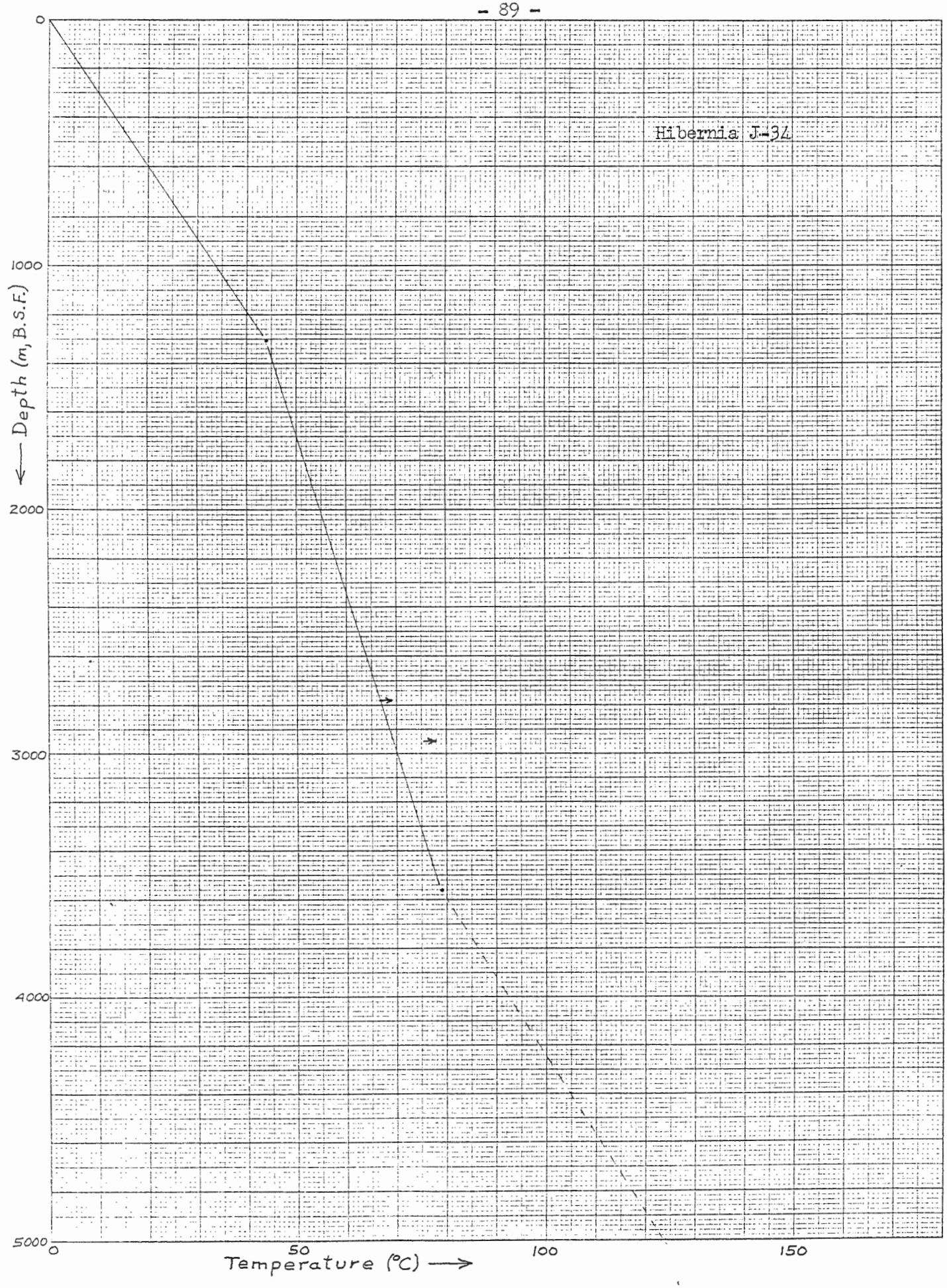
Hibernia J-34
Depth (m, B.S.F.)
0
1000
2000
3000
4000
5000
0
50
100
150
Temperature (°C) ⟶

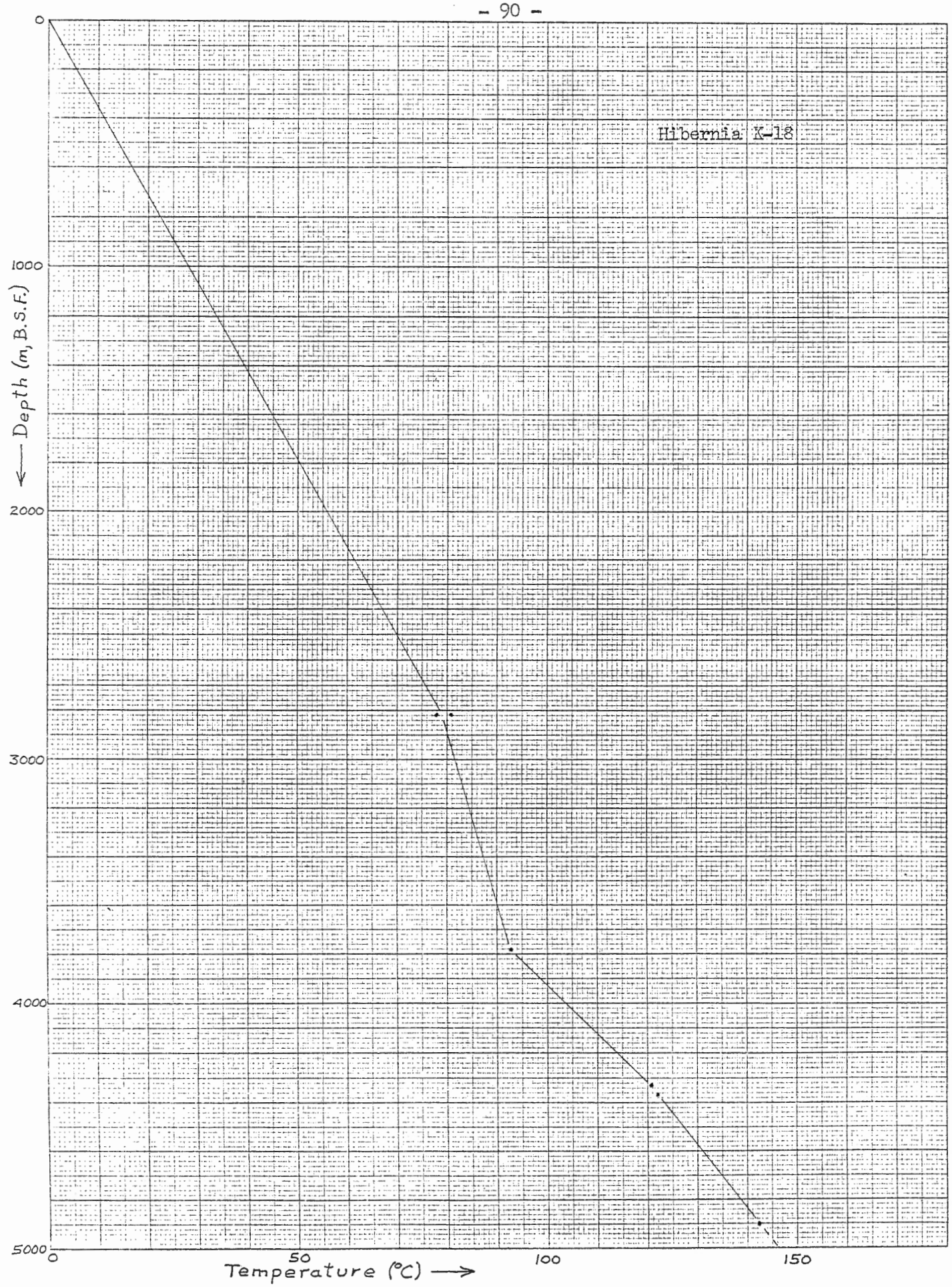
Hibernia K-18
0
1000
2000
3000
4000
5000
← Depth (m, B.S.F.)
0
50
100
150
Temperature (°C) →

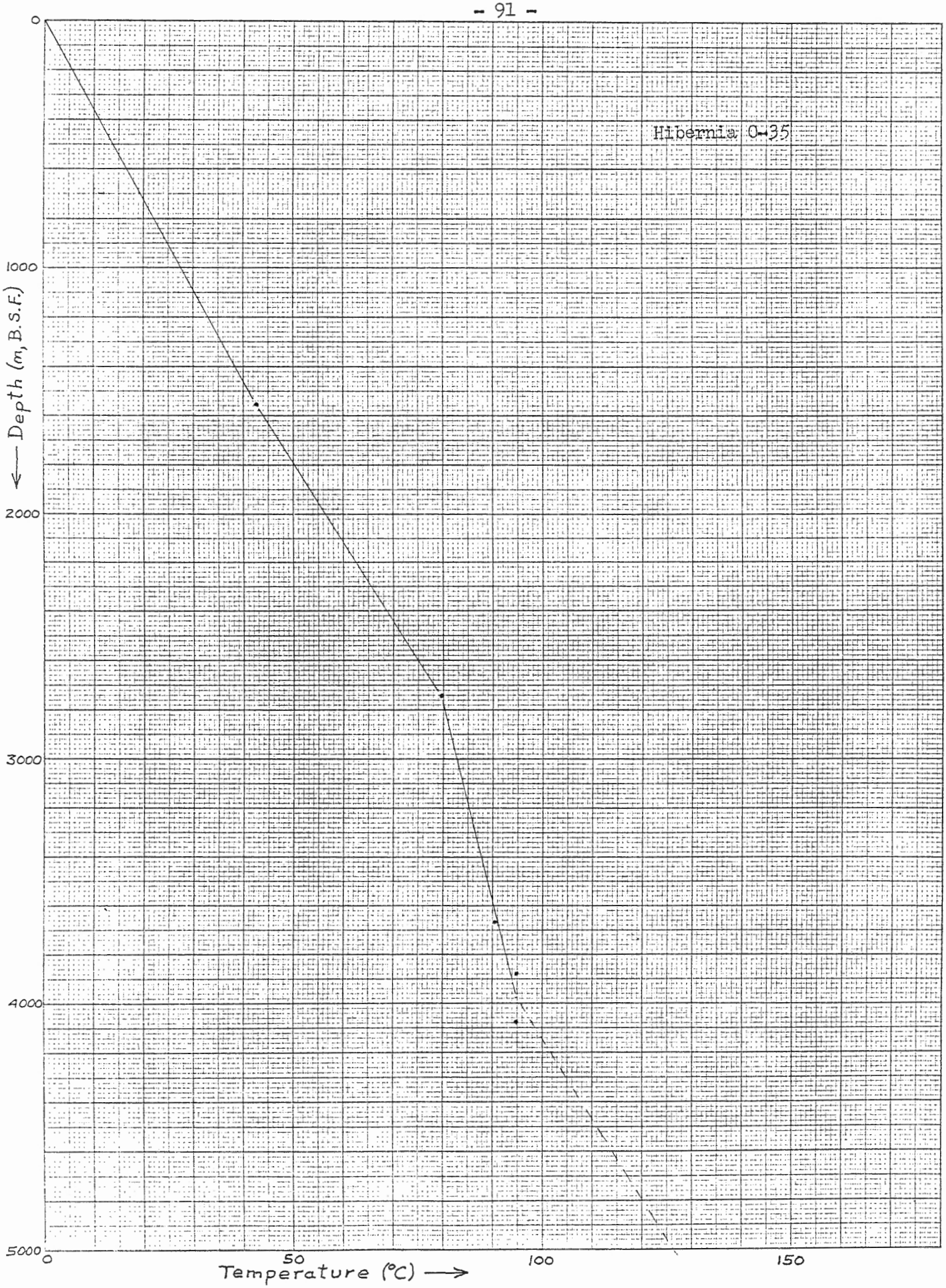
Hibernia O-35
0
1000
2000
3000
4000
5000
Depth (m, B.S.F.)
0
50
100
150
Temperature (°C) ⟶

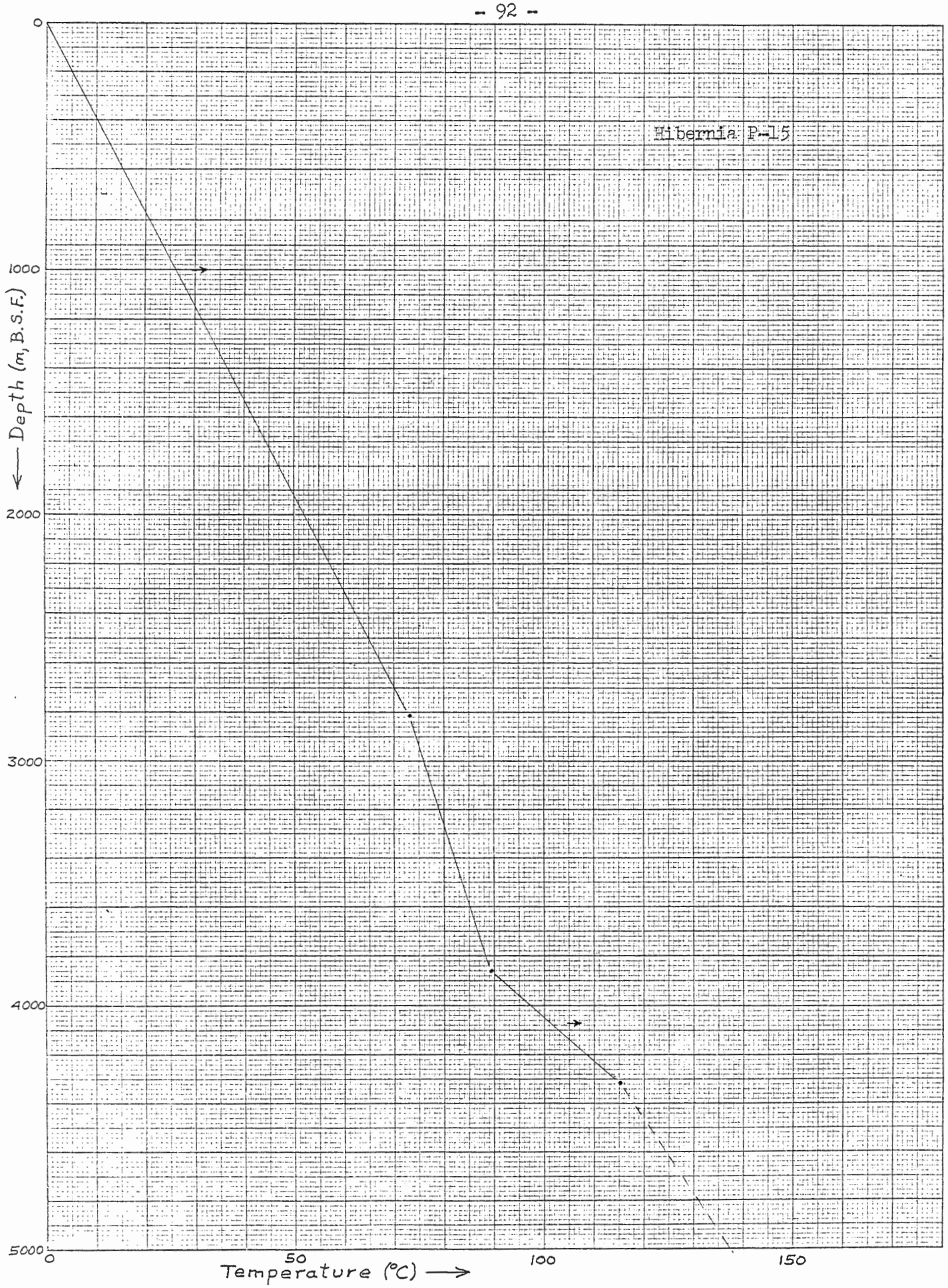
Hibernia P-15
0
1000
2000
3000
4000
5000
Depth (m, B.S.F.)
0
50
100
150
Temperature (°C) ⟶

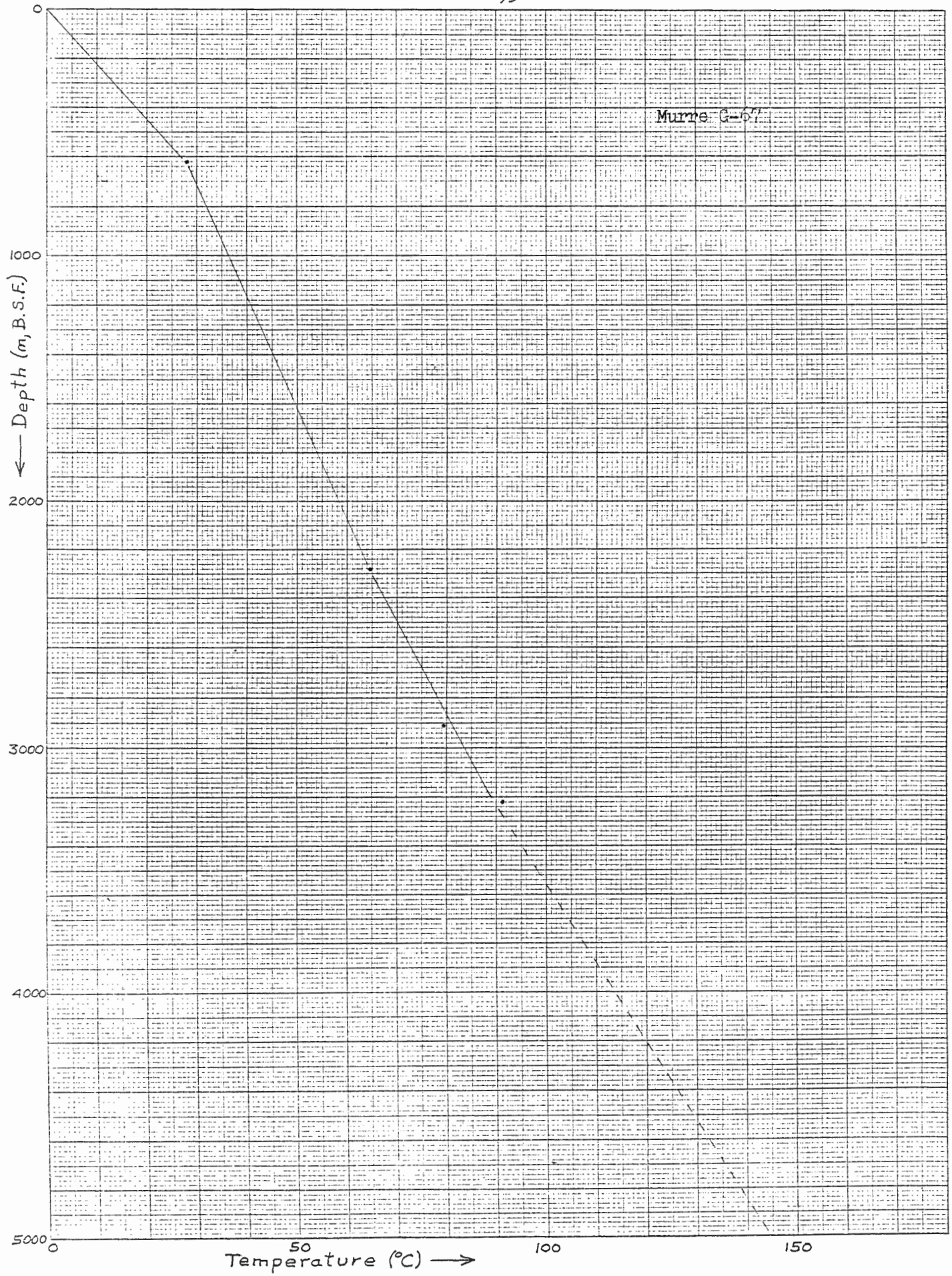
Murre G-67
0
1000
2000
3000
4000
5000
Depth (m, B.S.F.)
0
50
100
150
Temperature (°C)

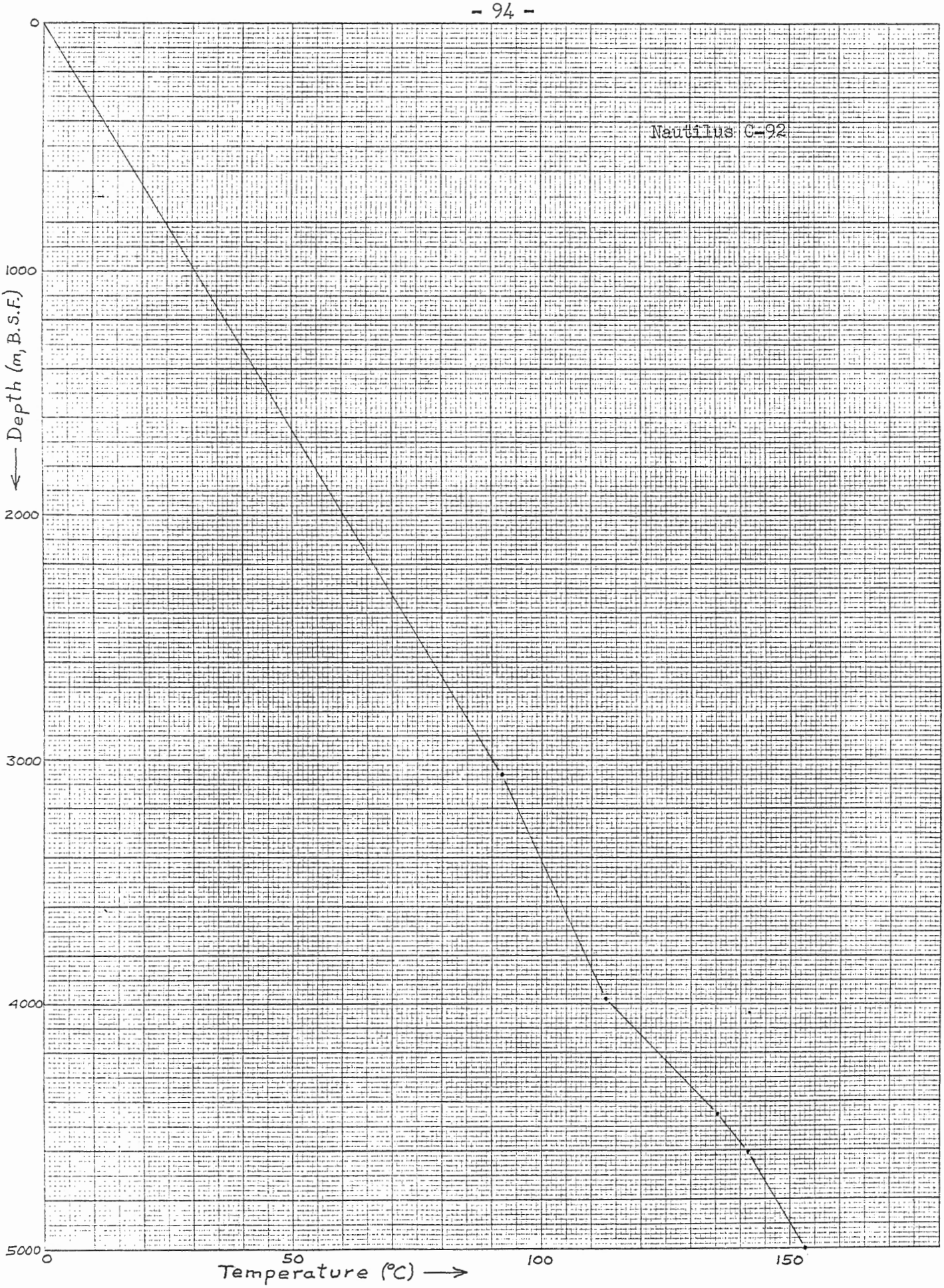
Nautilus C-92
0
1000
2000
3000
4000
5000
← Depth (m, B.S.F.)
0
50
100
150
Temperature (°C) →

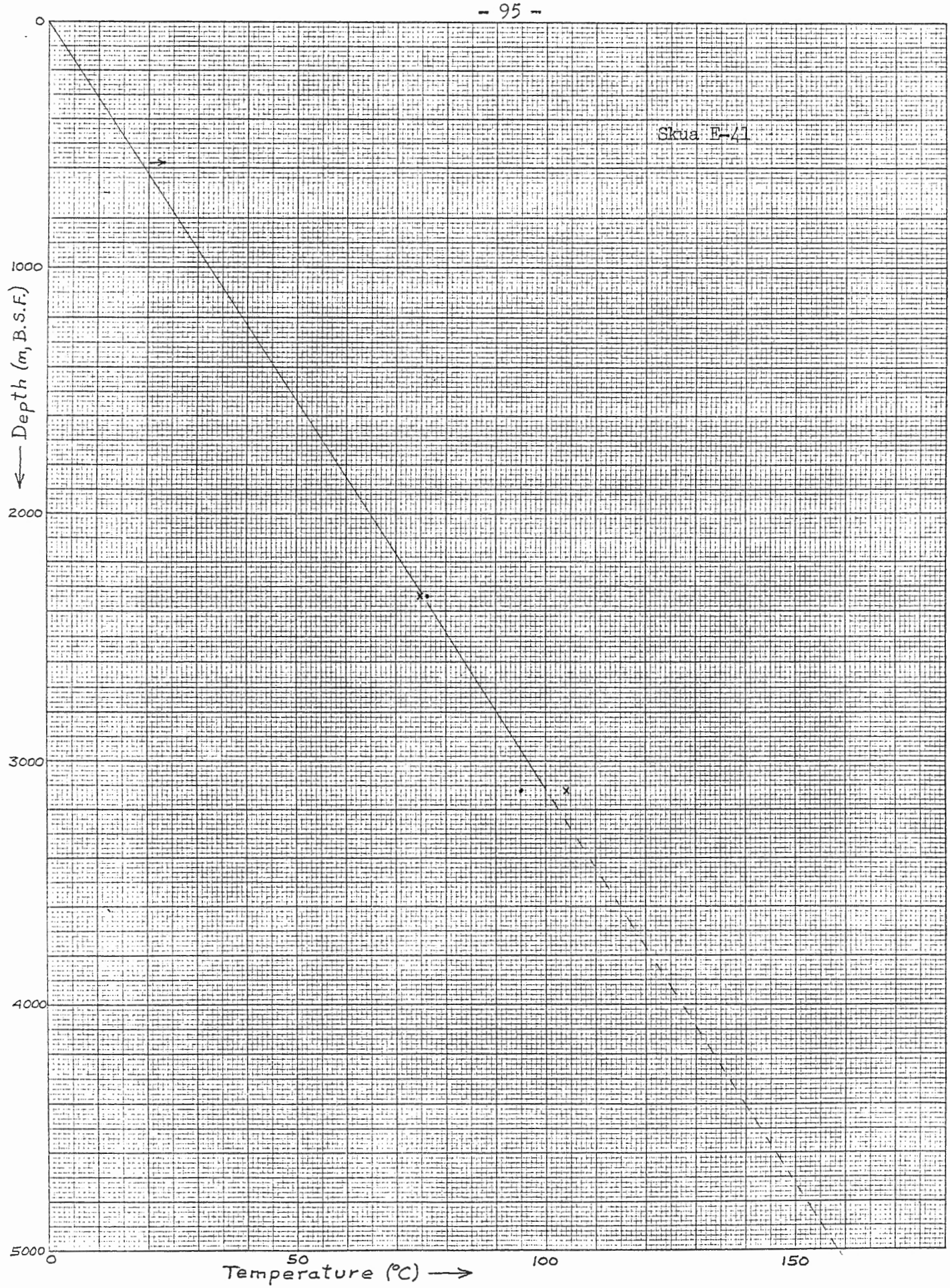
Skua E-41
0
1000
2000
3000
4000
5000
Depth (m, B.S.F.)
0
50
100
150
Temperature (°C)

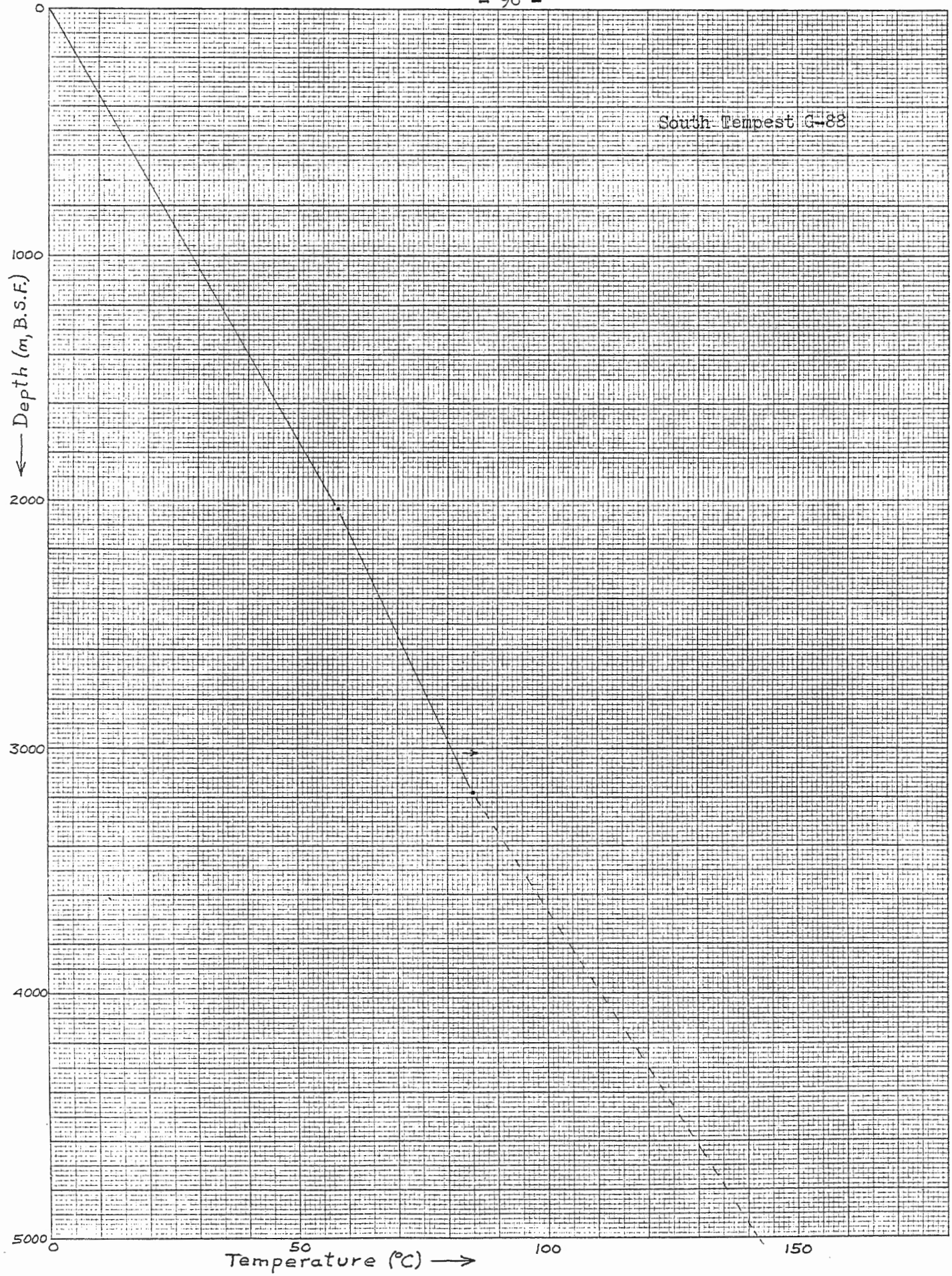
South Tempest G-88
0
1000
2000
3000
4000
5000
Depth (m, B.S.F.)
0
50
100
150
Temperature (°C) →

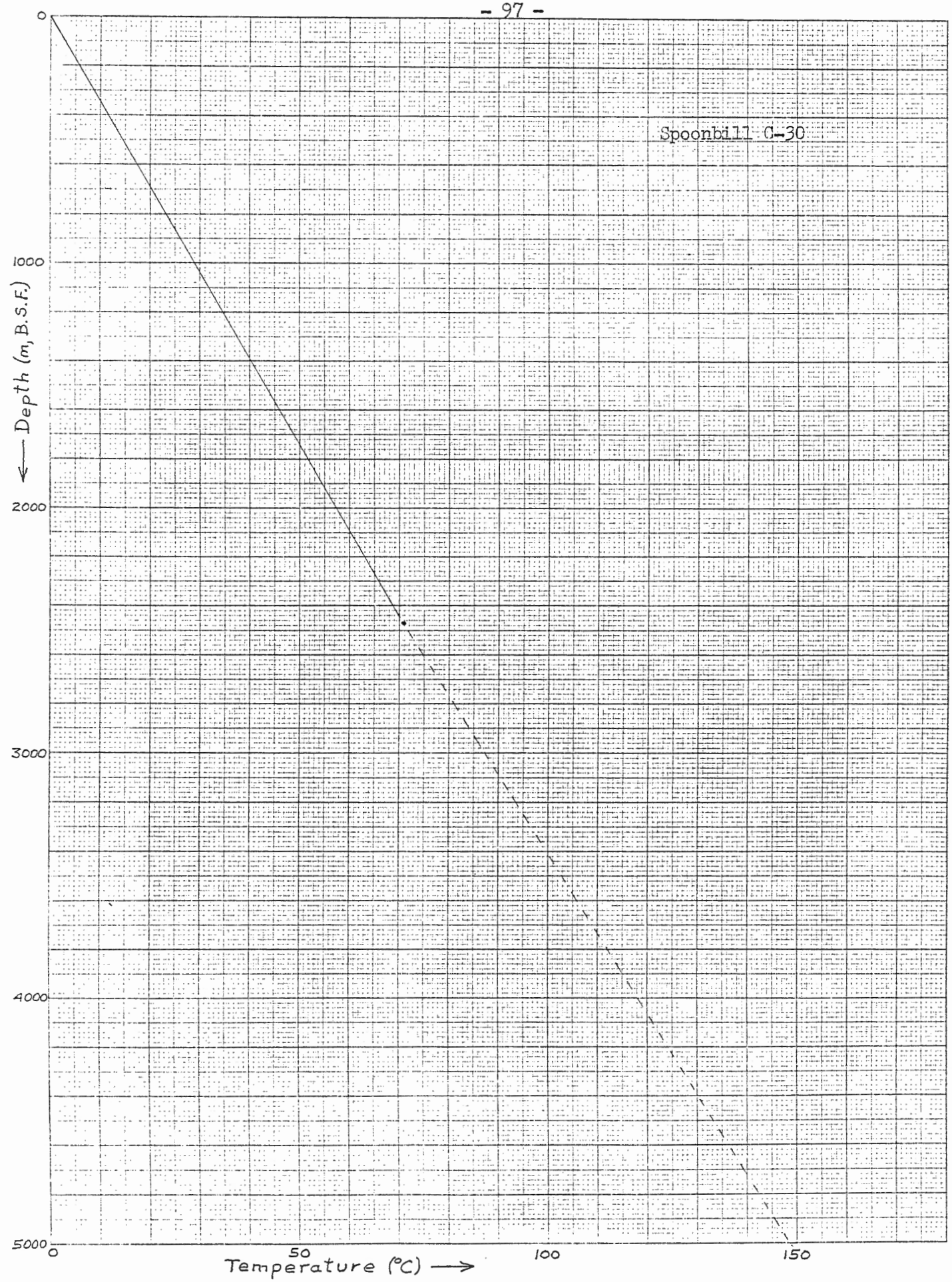
Spoonbill C-30
0
1000
2000
3000
4000
5000
Depth (m, B.S.F.)
0
50
100
150
Temperature (°C) →

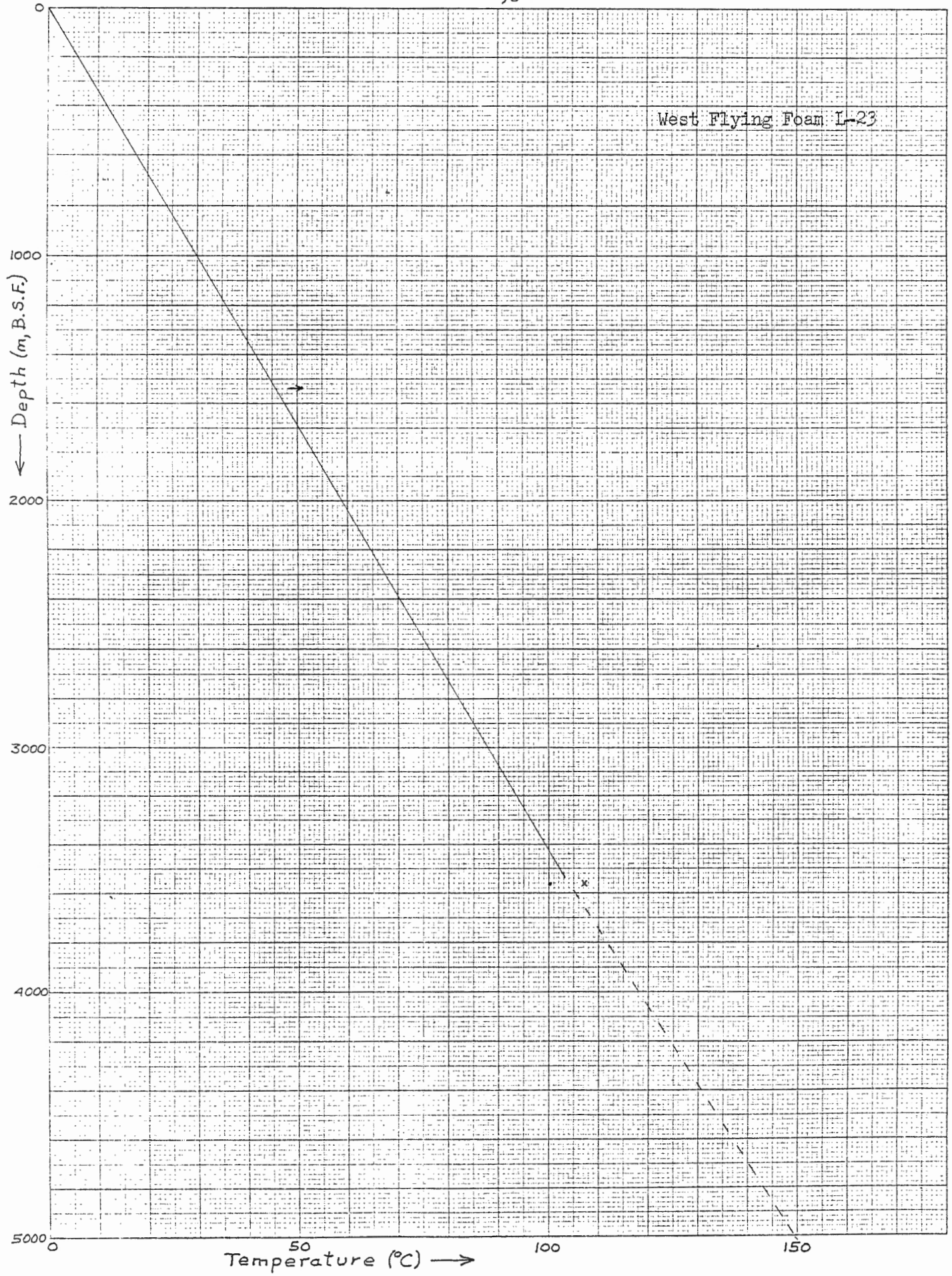
West Flying Foam L-23
0
1000
2000
3000
4000
5000
← Depth (m, B.S.F.)
0
50
100
150
Temperature (°C) →

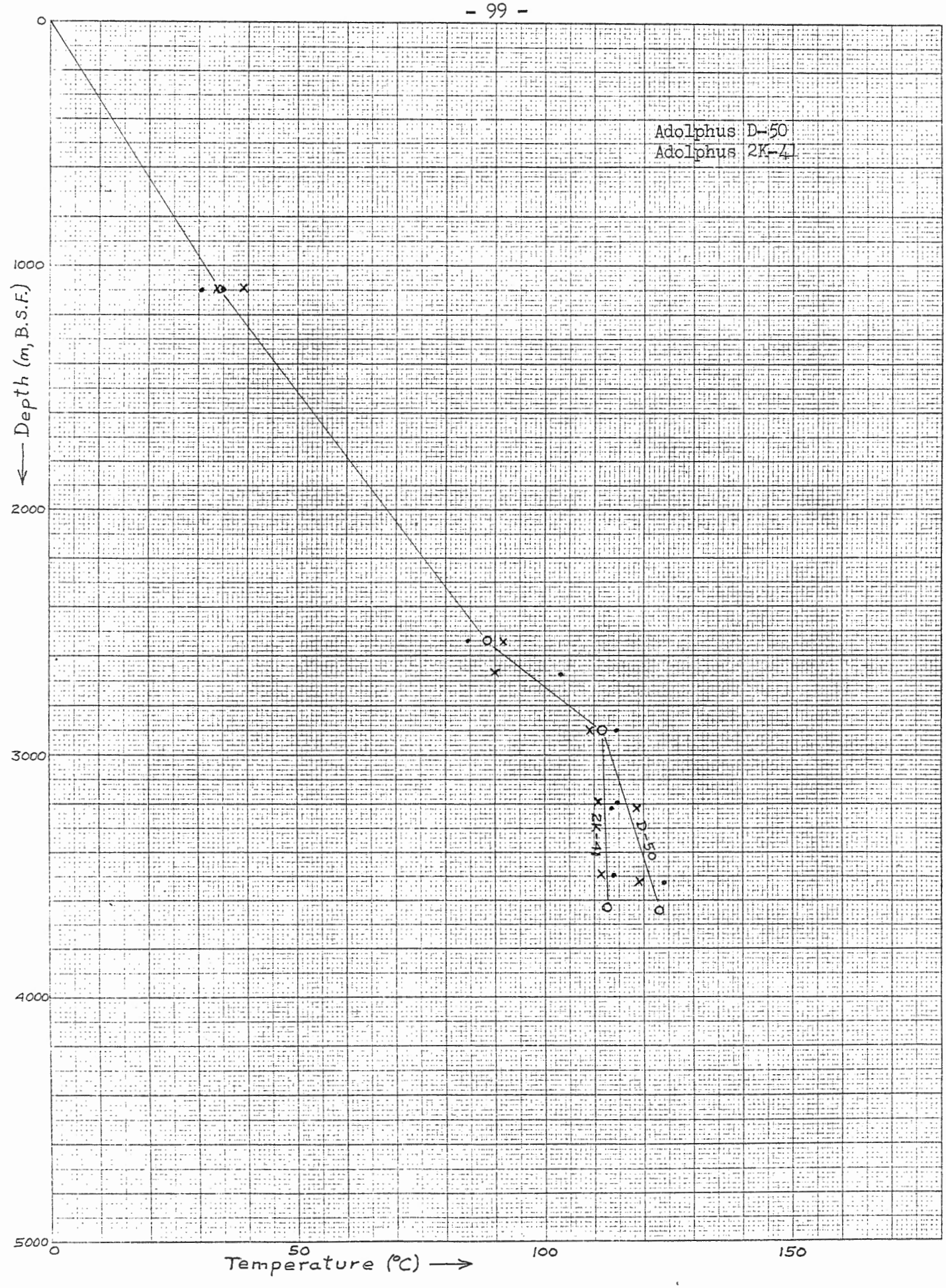
Adolphus D-50
Adolphus 2K-41
Depth (m, B.S.F.)
0
1000
2000
3000
4000
5000
0
50
100
150
Temperature (°C)
D-50
2K-41

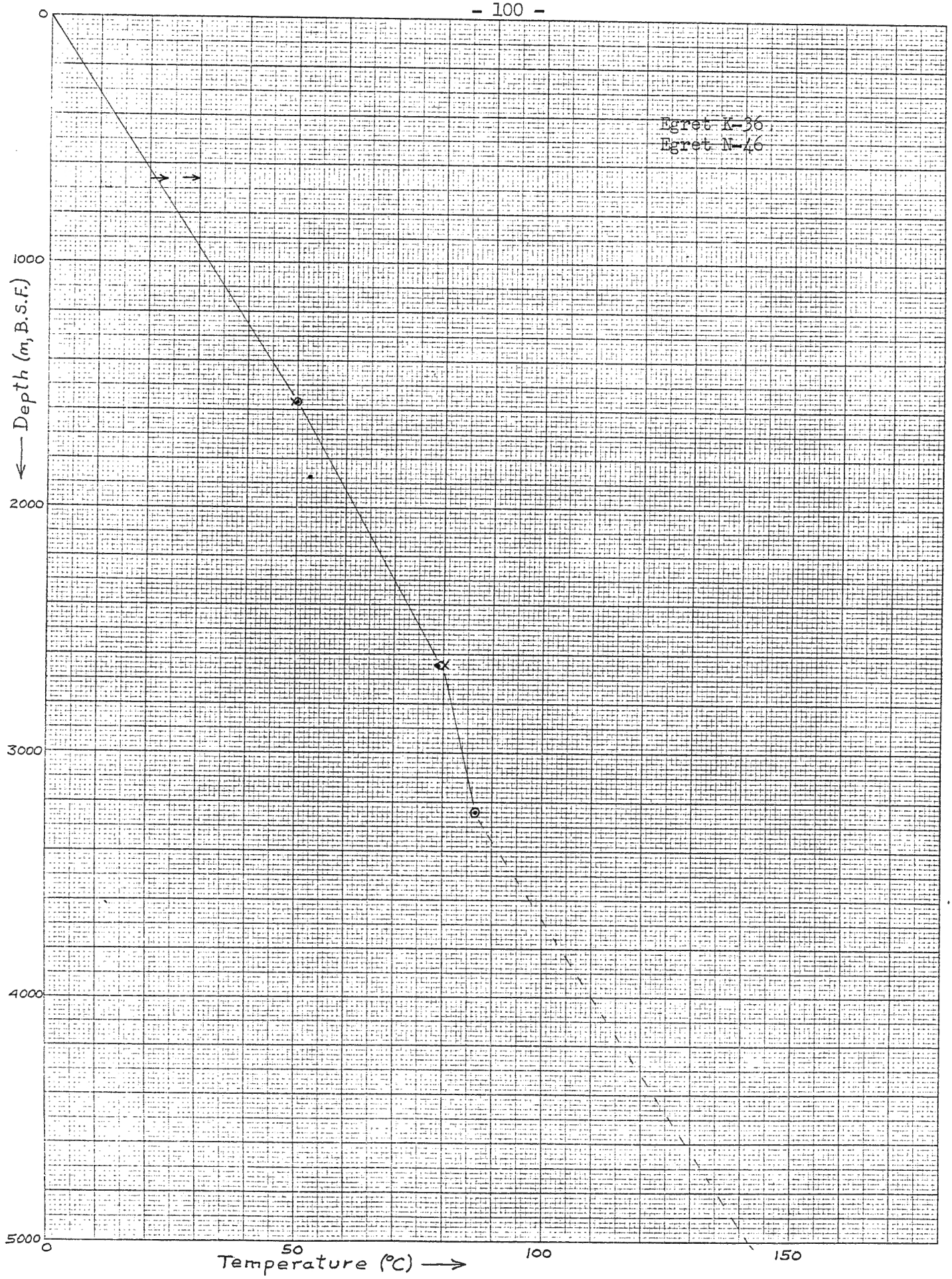
Egret K-36
Egret N-46
0
1000
2000
3000
4000
5000
← Depth (m, B.S.F.)
0
50
100
150
Temperature (°C) →

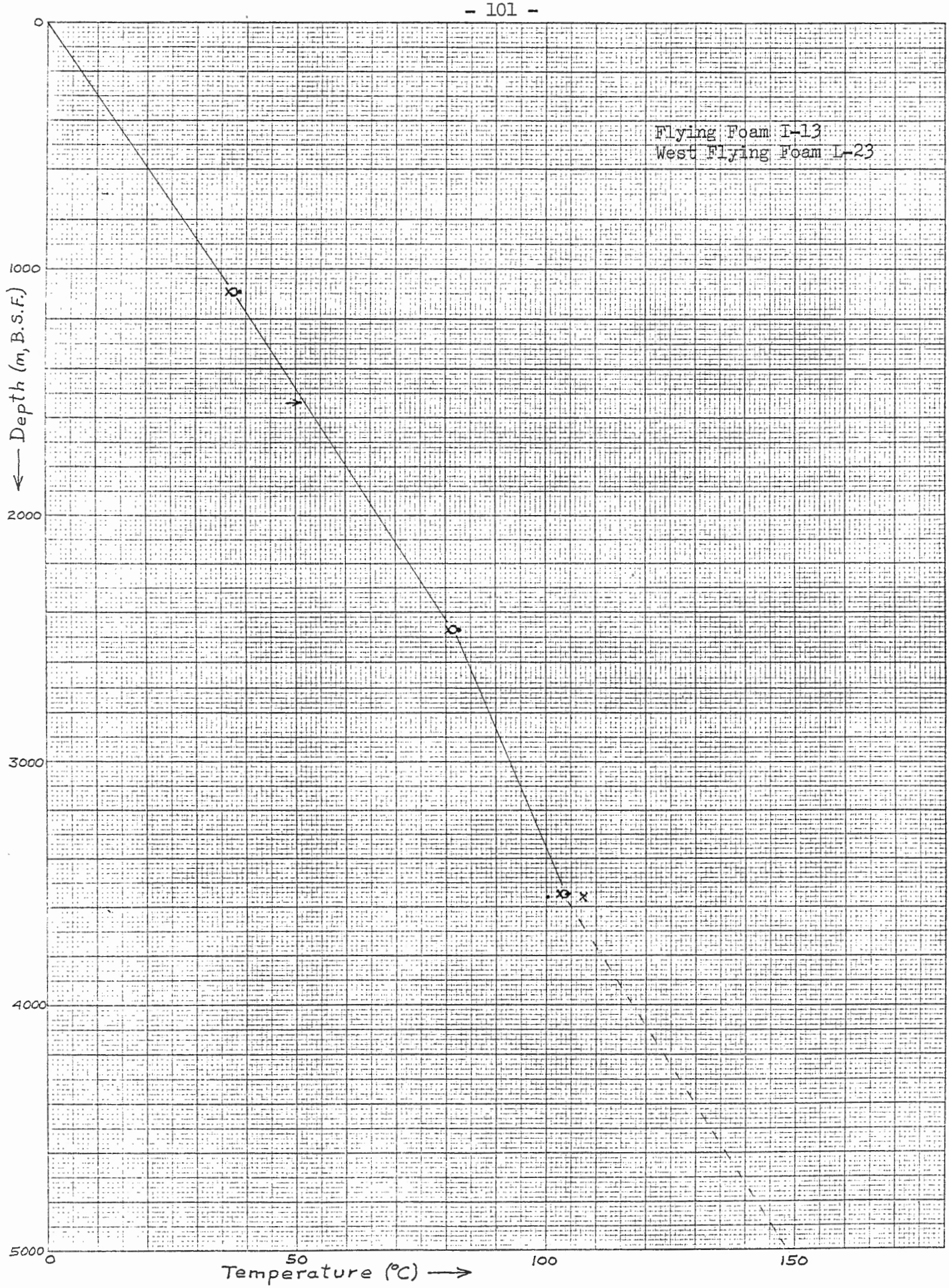
Flying Foam I-13
West Flying Foam L-23
0
1000
2000
3000
4000
5000
← Depth (m, B.S.F.)
0
50
100
150
Temperature (°C) →

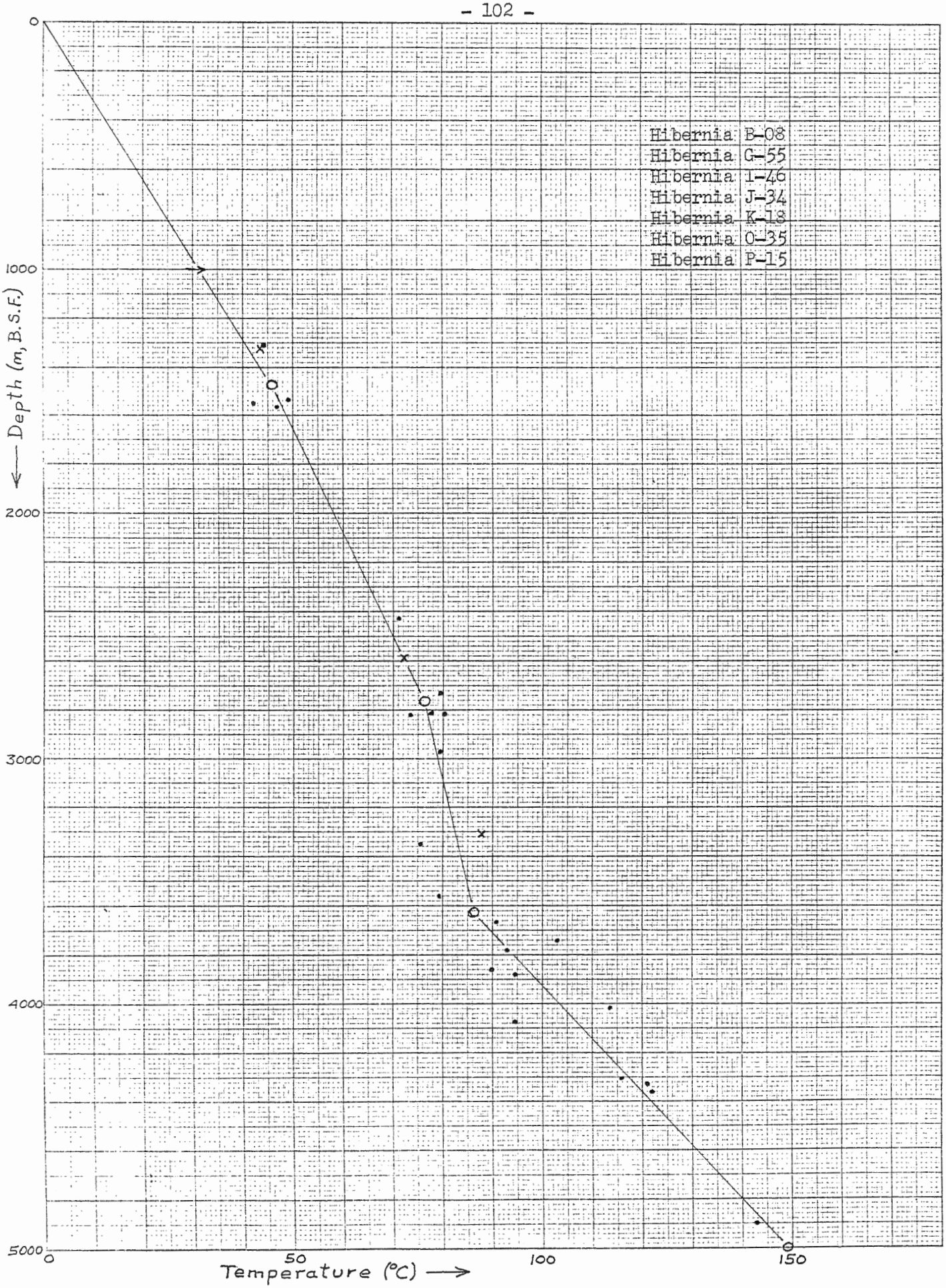
Hibernia B-08
Hibernia G-55
Hibernia I-46
Hibernia J-34
Hibernia K-18
Hibernia O-35
Hibernia P-15
0
1000
2000
3000
4000
5000
Depth (m, B.S.F.)
0
50
100
150
Temperature (°C)

FIGURE 1A

Correlation of 50 Hour and CT Projections

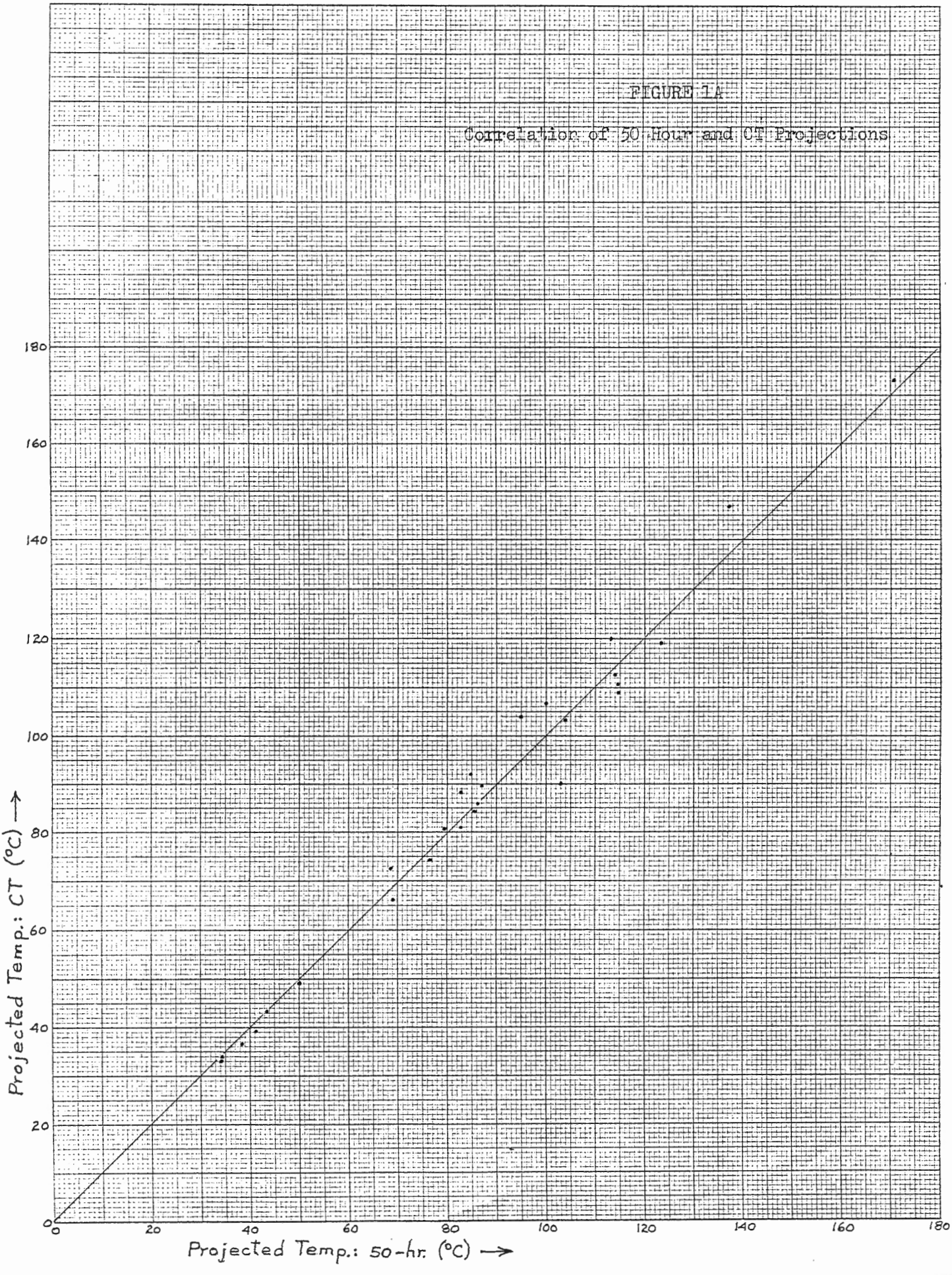

TABLE 1A

TTI Values for Specified Horizons in Each Well

Top of:	Adolphus D-50	Adolphus 2K-41	Ben Nevis I-45	Bonnition H-32	Cormorant N-83	Dominion O-23	Egret K-36	Egret N-46	Flying Foam I-13	Hebron I-13	Hibernia B-08
L. Olig.	.0441	.033		.023		.0368	.023		.0278		
L. Eoc.	.1889	.2632	.0708	.053	.0408	.1574	.0388	.0664	.1249		.1119
M. Eoc.	.9674										
E. Eoc.	2.9785	1.5553									
L. Paleo.						3.5687					
E. Paleo.			.4519								
Maast.	5.8178	2.974		.219							
Turon.	15.268	5.769			.2339		.2293	.247		.444	.801
Ceno.											
Albion	27.507	24.2469	2.1129				.297	.361	1.414	.555	
Aptian											
Barr.											
Haut.			3.291	.7404		5.0508	.619	.490	1.662	.783	.893
Val.			9.5179			7.2218			5.7669	.889	
Berr.			25.8207							2.684	1.425
Tith.			63.6082	2.0927	.287		1.682	.698		4.113	10.7808
Kimm.			91.3046	2.9248			2.646	.780	8.0218	4.321	18.3915
Oxf.											
Bath.					.590						
Aal.					1.298						
Plien.					3.5853						
Sin.					7.6698						
Nor.					12.066						

TABLE 1A

TTI Values for Specified Horizons in Each Well

Top of:	Hibernia G-55	Hibernia I-46	Hibernia J-34	Hibernia K-18	Hibernia O-35	Hibernia P-15	Murre G-67	Nautilus C-92	Skua E-41	Spoonbill C-30	W. Flying Foam L-23
L. Olig.						.023	.023		.0259		
L. Eoc.					.0769	.0994	.053		.069		
M. Eoc.											
E. Eoc.											
L. Paleo.											
E. Paleo.										.0589	
Maast.	.215		.245	.296		.2669					
Turon.				.633	.5224	.602	.176				
Ceno.								1.516		.182	
Albion	.656	.674	.609	1.023	.825	.888	.226	2.447			1.725
Aptian	1.002										2.921
Barr.			1.419		1.489						6.0279
Haut.	2.797	1.941		1.198		1.684		12.338	.319		
Val.			2.441	1.365	2.311	2.057		22.2073			
Berr.				2.791	4.571	3.152					
Tith.				7.9319	19.6748	32.9889	.288	258.5508	.481		
Kimm.				10.079	32.8407	51.3575		506.7206	.530		
Oxf.									2.2359		
Bath.							.775		3.0899		
Aal.									8.8886		
Plien.							1.992				
Sin.		5.989									
Nor.										.4079	